TEMPERATURES AND LUMINOSITIES OF M TYPE DWARFS FROM INFRARED PHOTOMETRY

Thesis by

Glenn J. Veeder, Jr.

In Partial Fulfillment of the Requirements

for the Degree of

Doctor of Philosophy

California Institute of Technology

Pasadena, California

1974

(Submitted August 21, 1973)

To

Gandalf

Acknowledgements

I am indebted to my advisor, Professor J.L. Greenstein, for suggesting this project and providing encouragement and assistance. I am especially thankful to Professor G. Neugebauer for making available his equipment and the facilities of his laboratory which made the measurements possible. I am also grateful to the powers that be for a large amount of observing time at Mt. Wilson even if most of it was over weekends during the light run. Special thanks are due to the night assistants for efficiently running the telescopes. G. Clough, S. Loer, D. Matson and many others assisted in taking the measurements. Suzan (sic) Robinson suffered through most of the typing. Finally, I am grateful to the National Science Foundation for a two year Traineeship.

Abstract

Broad-band infrared photometry at 1.65, 2.2 and 3.5μ has yielded the first accurate bolometric magnitudes for a large number of M dwarfs. The intrinsic dispersion in these stars is found to be $\sim \pm 0.4$ magnitudes in M_b vs. V-K and M_b vs. R-I magnitude-color diagrams. This dispersion in the lower main sequence may be the result of differential blanketing in the UBVRI filter bands and thus there may be no such thing as a unique main sequence for the intrinsically faint M dwarfs. Scanner observations from 4500Å to 10000Å show severe blanketing by TiO in cool M dwarfs, but analysis shows that one parameter is sufficient to describe the blanketing in all of the UBVRI bands for all types of M dwarfs. In general, late M dwarfs seem to have lower effective temperatures than are predicted by theoretical models. Stars with hydrogen lines in emission average 0.2 to 0.3 bolometric magnitudes brighter than M dwarfs without any emission lines. The existence of flare stars with old disk space motions and also the existence of some flare stars below the main sequence complicates the picture of these stars as a pre-main sequence evolutionary stage. M dwarfs that belong to the halo population on the basis of their large space motions tend to be subluminous in M_b vs. V-K and M_b vs. R-I magnitude-color diagrams although there is a large scatter among the few objects of this type.

The data for late dwarfs with known masses imply the empirical mass-luminosity relation: $L/L_{\odot} \propto (M/M_{\odot})^{2.2 \pm 0.2}$ for stars fainter than $M_b = 7.5$. In addition, the late M dwarfs are found to account for all of the "missing mass" in the plane of the galaxy.

Table of Contents

I. Introduction

With the development of photodectectors which are sensitive into the red, Kron, Eggen, and Johnson used measurements in the R and I filter bands to continue studies of the main sequence down through the K dwarfs. However, the spectral energy distributions of cool M dwarfs peak near 1μ which is still beyond the I filter band. Scanner observations from 4500Å to 10000Å show that these cool stars are heavily blanketed by conspicuous TiO bands at these wavelengths so that their bolometric corrections are large and very uncertain. The complicated temperature dependence of the opacity due to the effect of convection, atomic absorption lines, and the extensive blanketing of molecular absorption bands in cool M dwarfs makes it very difficult to construct models for them. In general, the very late M dwarfs have lower effective temperatures than the most recent models would predict. (for example, see Hoxie (1970))

Johnson (1965) and Iriarte (1970) have published infrared magnitudes for a few M dwarfs, but in order to define the faint end of the main sequence, it was decided to observe a large number of M dwarfs at 1.65, 2.2, and 3.5μ. Only stars with known trigonometric parallaxes were included in order to be able to accurately convert the observed fluxes to absolute values so that the intrinsic

dispersion of these stars could be examined. It was also important to have a sample of M dwarfs that are bright enough to measure accurately in the infrared. These considerations immediately limited the program to stars in the solar neighborhood. This sample of stars provides a chance to compare flare stars, stars with calcium or hydrogen emission lines, young disk, old disk, and halo population stars.

Infrared observations of these stars are necessary to help answer the questions of whether the intrinsic dispersion of the faint end of the main sequence is greater than that of the upper main sequence and whether in fact all of these stars have stabilized on the main sequence. In particular, there is disagreement in the literature concerning the effect of the presence of UV Ceti type activity in a late M dwarf on its position in a Hertzsprung-Russell or various color-color diagrams. Whereas Iriarte (1971) found no difference in color between a few flare stars and other M dwarfs in the solar neighborhood, the results of this program are more consistent with Haro and Chavira (1966) who found that most flare stars in clusters lie above the main sequence, but that some also lie below it. In addition, the decline in chromospheric activity from flare stars to those with hydrogen lines in emission to those with the H and K lines of calcium in emission to those without any emission lines has been suggested to

represent an evolutionary sequence.

The existence of K and earlier type subdwarfs has also been argued in the literature. Eggen (1973) finds that old disk motion K and early M dwarfs are less luminous than young disk motion stars and that stars with halo type space motions are even more subluminous. The results of this program show that this trend continues through the late M dwarfs although the population groups do overlap.

Stars for the program were taken from Gliese (1969), Woolley et al. (1970), Riddle et al. (1970, 1971), and Dahn et al. (1972). All stars taken from these sources have parallaxes larger than $0.040''$ except for four stars whose parallaxes were revised below this value after the program was started. Only stars brighter than apparent visual magnitude 15 were included in the program. All such stars that satisfied any one of the following criteria were included:

1) K and M dwarfs with well determined masses
2) M dwarfs with parallax $\geq 0.100''$
3) Spectral type dM6 or later
4) Stars classified as sdM by Joy (1947)
5) M dwarfs with |radial velocity| $\geq$ 65 km/sec
6) M dwarfs with halo type space motions
7) Known flare stars

Other stars were favored for inclusion if they had red B-V or red R-I colors, bright m_v, faint M_v, or were known to

have Ca II or Hα in emission. Additional stars were included in the final list in order to represent all spectral types from M0 to M8, in particular to represent M dwarfs of low radial velocity that have no emission lines.

Whenever possible stars are referred to by their number (GL) in Gliese's (1969) catalogue. Stars which don't appear in this catalogue are referred to by their Giclas (G) number or else their Luyten (L) number. If the common name of a star is often used in the literature, it is also given for the sake of clarity. Thus, GL699 is identical to Barnard's star. Also, R614 (=GL234) and W359 (=GL406) originally came from the lists compiled by Ross and Wolf. As listed in the appendix, many of the flare stars in this program also have variable star numbers.

For purposes of comparing the photometric colors of different population types, those stars with known radial velocities were assigned to either the young disk population, the old disk population, or the halo population on the basis of their space motion. Following Eggen (1969) stars with small space velocities in the U-V plane were assigned to the young disk population. For U defined to be positive away from the galactic center, the approximate limits of young disk velocities are:

$$-20 \leq U \leq +50 \text{ km/sec}$$

$$-40 \leq V \leq +10 \text{ km/sec}$$

Eggen derived these limits from the small space velocities

observed for young main sequence stars with early spectral types. Most of the asymmetry in these limits is due to the small peculiar motion of the sun. The remaining stars were assigned to the old disk if the eccentricity of their galactic orbits is less than 0.5 or to the halo population if the eccentricity is greater than 0.5. In addition, stars with a large space velocity component perpendicular to the galactic plane were assigned to the halo population, i.e. if $|W| > 75$ km/sec. These stars reach distances $\gtrsim$ 1kpc from the galactic plane. Stars with high radial velocities ($|RV| \geq 65$ km/sec) that otherwise have been assigned to the old disk population are so indicated.

II. Procedure

A. Observations

The observations for this program were carried out during 80 nights from Sept. 1970 to Jan. 1973 on the 60" and 100" telescopes at Mt. Wilson. Every star was observed in the 1.65μ and 2.2μ bands and about half of the program stars were bright enough to give good results in the 3.5μ band also. The infrared photometer used has been described by Becklin and Neugebauer (1968). The photometer was mounted at the f/16 cassegrain station of the telescope. It makes use of a mirrored rotating chopper wheel to alternately sample a field containing the object and a nearby out of focus reference ("sky") field. The chopper throw was usually set to 50" on the 60" telescope (or 30" on the 100" telescope). The chopper was run at 5 Hz for the 1.65μ and 2.2μ measurements and at 15 Hz for the 3.5μ measurements. A phase-lock amplifier was used to increase the signal to noise of the system. The field observed by the detector is determined by a circular aperture in the focal plane of the telescope. In general, the aperture used was equivalent to 15" on the 60" telescope (10" on the 100" telescope) unless the seeing was bad. The aperture used was always much larger than the seeing disk.

The IR detectors consist of 1/2mmx1/2mm PbS cells

mounted behind an 8mm f/1 field lens and cooled by liquid nitrogen. Two different detectors were used. "D-15" was used for the 1.65μ and 2.2μ measurements and "D-20" was used for the 3.5μ measurements. The bandpass was selected by a set of interference filters such that the 1.65μ (=H) band extends from 1.5μ to 1.8μ, the 2.2μ (=K) band extends from 2.0μ to 2.4μ, and the 3.5μ (=L) band extends from 3.1μ to 3.8μ. The 3.5μ filter was cooled by liquid nitrogen, but the 1.65μ and 2.2μ filters were at the ambient temperature.

Most observations were made using an offset guide star. Two or four ten-second integrations were taken in one beam of the photometer and then the star was moved into the other beam. This process was repeated until a sufficient signal to noise was achieved. In general a standard star was measured at the beginning and end of an observing night and also after every other object star, that is, about every hour during the night.

The integrations were recorded on a printed tape or punched directly on cards and were also monitored on a strip chart. A standard data reduction computer program was used to convert the measured signals to equivalent magnitudes. The extinction corrections applied were 0.10 mag/air mass at 1.65μ and 2.2μ and 0.15 mag/air mass at 3.5μ. Almost all observations were made at an air mass of

less than two. The system of standard star magnitudes which was used for this program was set up by Becklin (1972) and Neugebauer. In this system α Lyrae is used to define magnitude 0.00 in each IR band. The absolute calibration of the flux of α Lyrae in these bands is given by Wilson et al. (1972).

The data for 144 program stars are listed in the appendix. The values for GL551 (=Proxima Centauri) are taken from Frogel et al. (1972).

B. Errors

Thirty-two stars in the present program had been previously measured by Johnson (1965) at 2.2μ and 3.5μ (but not at 1.6μ). The differences between Johnson's values for the 2.2μ magnitudes and those reported here are plotted versus V-K in figure 2-1. These differences are relatively large, but there appears to be no systematic displacement from zero. Figure 2-2 is a similar plot of the differences between Iriarte's values for the 2.2μ magnitudes and those reported here for twenty common stars. The spread is somewhat smaller than in figure 2-1, but there appears to be a systematic displacement in the sense that Iriarte's magnitudes seem to be about ∿ 0.05 magnitudes too faint. Figure 2-3 is a plot of the difference between Iriarte's (1.65μ - 2.2μ) colors and the values from this study for eighteen common stars. (Iriarte did not

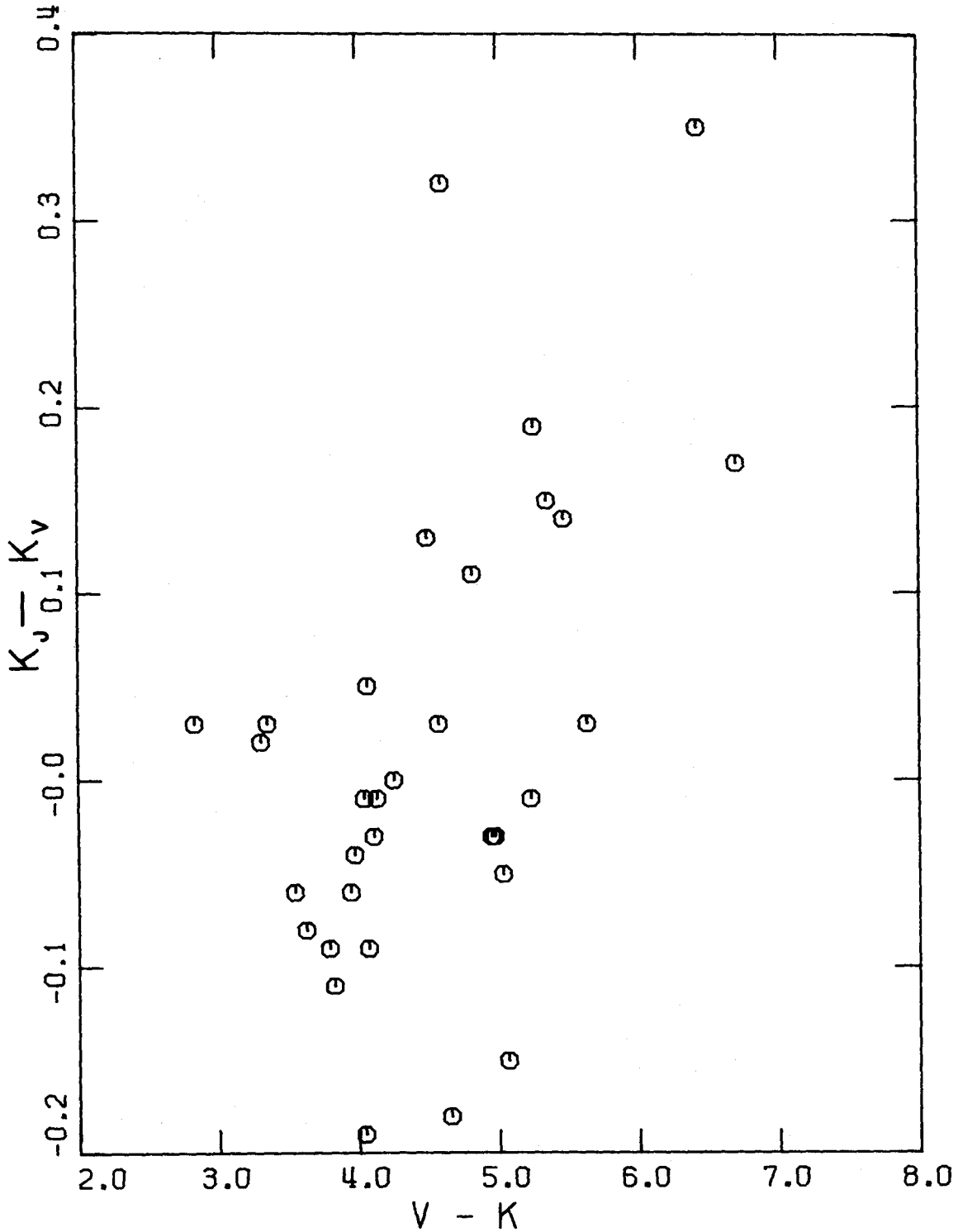

Fig.2-1.--Difference between Johnson's (1965) values and Veeder's values at 2.2μ vs. V-K for 32 common stars.

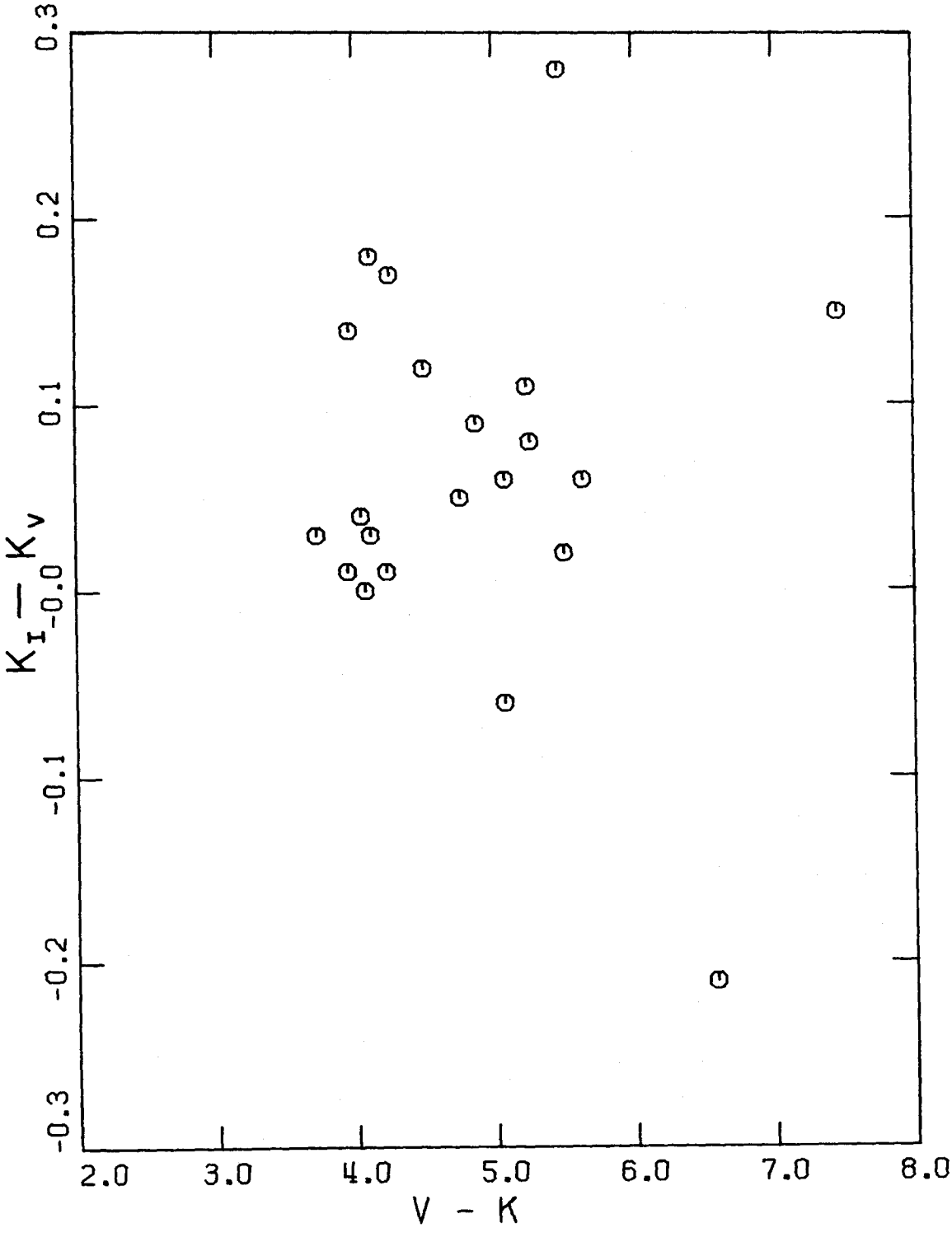

Fig.2.2--Difference between Iriarte's (1970) values and Veeder's values at 2.2μ vs. V-K for 20 common stars.

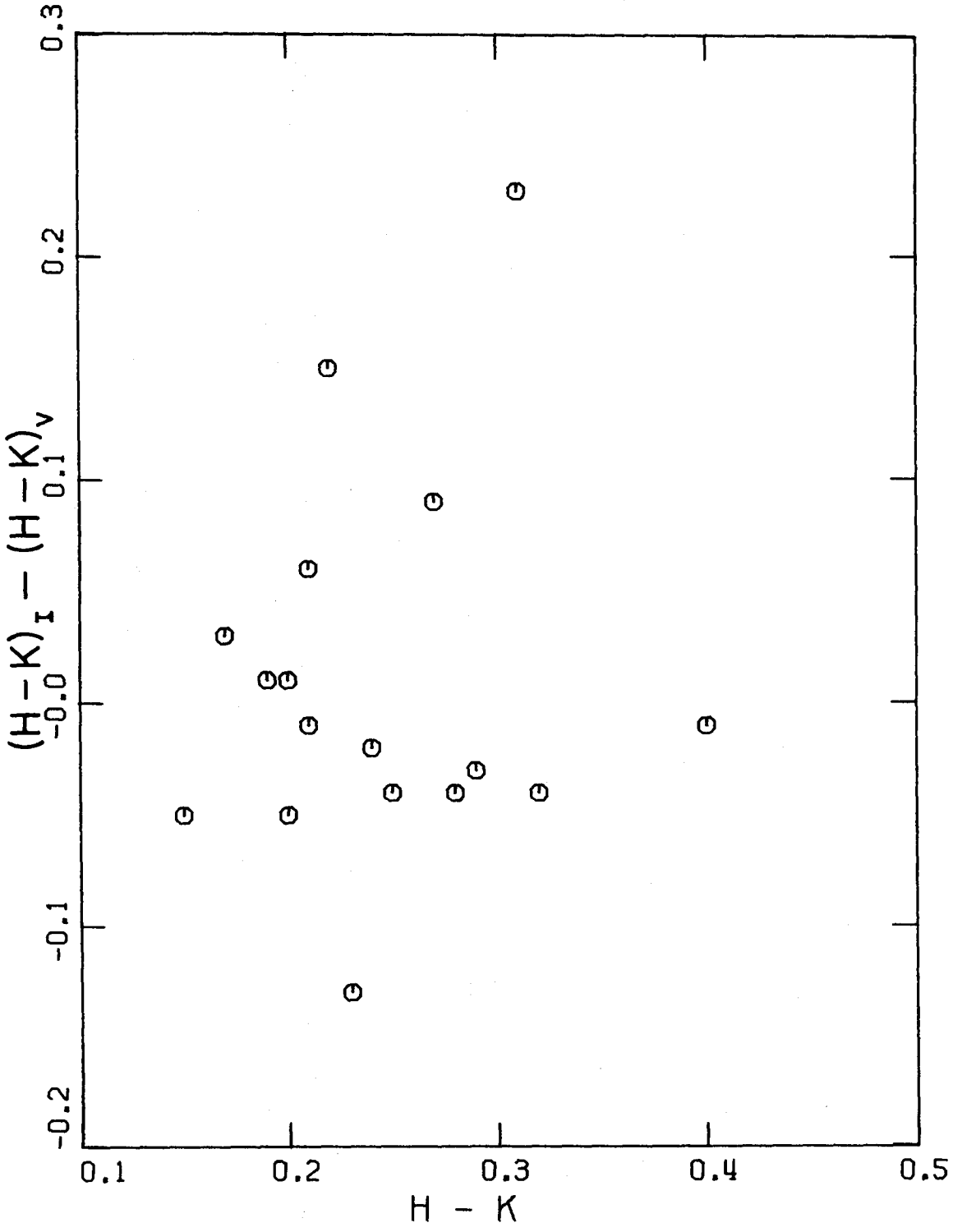

Fig.2-3.--Difference between Iriarte's (1970) values and Veeder's values for the (1.65μ-2.2μ) color vs. Veeder's (1.65μ-2.2μ) color for 18 common stars.

measure GL654 at 1.65μ and his value of H-K = 0.68 for EV Lac is much too large for an M dwarf.) There appears to be no systematic shift in the differences of this color, so the displacement in figure 2-2 is probably due to a difference in calibration of standards. Iriarte claims a "probable error of a single observation" of 0.05 magnitudes at 2.2μ, but he does not describe the calibration of his system of standards.

Most of the stars in the present program were observed during several different observing runs. The internal repeatability was good enough to determine the mean value of the 2.2μ magnitude to within ∿ ±0.03 magnitudes (1 s.d.). Similarly, the mean value of the (1.65μ - 2.2μ) color is also determined to within ∿ ±0.03 magnitudes. The stability of the system of measurement and the calibration of the system of standard stars probably introduces an additional error of ∿ ±0.07 magnitudes. That is, for a star that was observed more than once, the value of the 2.2μ magnitude is probably reliable to ±0.1 magnitudes, whereas the (1.65μ - 2.2μ) color is probably reliable to ±0.03 magnitudes. The values given for 3.5μ are not as accurate as those at the shorter wavelengths. The internal repeatability was found to be only ∿ ±0.1 magnitudes(1 s.d.). Revision of the magnitudes assigned to the standard stars by Becklin (1972) and Neugebauer

improved the internal consistency of the 3.5μ measurements substantially, but the residual errors in calibration are probably still of the order of ±0.1 magnitudes. Therefore, any given value at 3.5μ may be in error by ±0.2 magnitudes. The values quoted by Greenstein et al. (1970) for W359 agree to within these errors with the values obtained during this program.

Table 2-1 is a résumé of the calibration and probable errors of the infrared measurements. Column 1 is the effective wavelength in microns for each band. Column 2 lists the bandpass, that is, the points at which the response of the system falls to one-half of the peak response within the band. Column 3 is the log of the apparent flux from a zero magnitude star in watts/m^2/Hz. Column 4 lists the probable errors in magnitudes for the values measured in each band.

Table 2-1

Absolute Calibration of the IR bands

	λ_{eff}(μ)	Bandpass (μ)	log flux watts/m^2/Hz	Δm
H	1.65	1.5 - 1.8	-23.01	±.1
K	2.2	2.0 - 2.4	-23.21	±.1
L	3.5	3.1 - 3.8	-23.55	±.2

C. Bolometric Magnitudes

The bolometric magnitudes for the program stars with R and I magnitudes were calculated directly by integrating the flux under the spectral energy curve. For this purpose the solar bolometric magnitude was taken as 4.69 and the solar luminosity as 3.9×10^{26} watts. The effective temperature of the sun is taken as $5760^{\circ}K$. In general, the flux longward of the last infrared band is between 10 and 15% of the total flux of a given star. This unobserved flux was estimated by smoothly extrapolating a blackbody curve of the approximate effective temperature of the star. A more serious error in the determination of the total flux of a star is the uncertainty in the shape of the spectral energy distribution near its maximum between 1μ and 1.65μ. The linear interpolation used may underestimate the total flux by up to 10% for stars with measured R and I magnitudes. Auman (1966) suggests that straight interpolation between observed bands may tend to overestimate the total flux by 10% at an effective temperature of $2520^{\circ}K$ because the infrared bands are restricted to terrestrial H_2O windows. Therefore, we estimate the error in the determination of M_b due to deficiencies in the observational technique as ±0.1 magnitudes. The error for a given star is compounded by the error in the determination of its parallax. We have:

$$\Delta M_b \simeq 5 \cdot \log_{10}(e) \cdot \frac{\Delta\pi}{\pi}$$

$$\simeq 2.17 \frac{\Delta\pi}{\pi} \qquad (2\text{-}1)$$

Typically, this additional error may range from ± 0.1 magnitudes up to ± 0.4 magnitudes for those stars with small parallaxes ($\pi \sim 0.05''$). Then, the total error in determination of the bolometric magnitudes is : $0.14 \lesssim |\Delta M_b| \lesssim 0.4$.

D. Bolometric Corrections

The bolometric corrections for all single program stars with R and I magnitudes are plotted against M_v in figure 2-4. The trend of the stars follows the values tabulated by Johnson (1965) for mean stars of a given spectral type and gives support to the large bolometric corrections found by Greenstein et al. (1970) for W359 (≡GL406) and VB10, but the stars obviously scatter badly. It is clearly impossible to infer the bolometric magnitude of a cool M dwarf to better than $\sim \pm 0.3$ magnitudes from its visual magnitude.

In order to obtain a better estimate of the bolometric magnitudes of those stars for which R and I magnitudes are unavailable, those stars which do have these magnitudes were replotted in figure 2-5. This diagram shows a strong correlation between the absolute bolometric magnitude and the absolute 2.2μ magnitude. (M_k is also strongly correlated with M_I which has been used by Eggen and others to

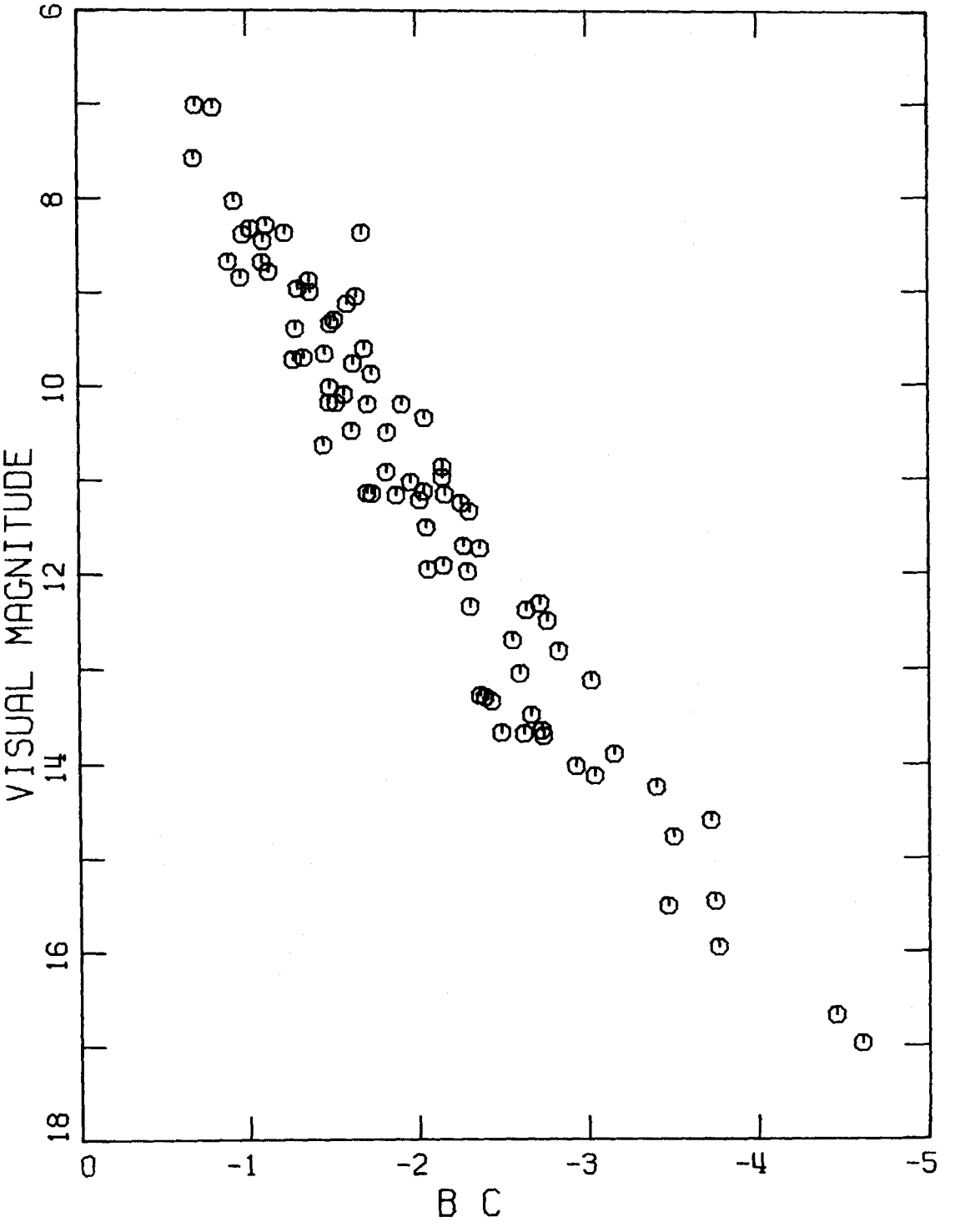

Fig.2-4.--Absolute visual magnitude vs. bolometric correction for all single program stars which have been observed at R and I.

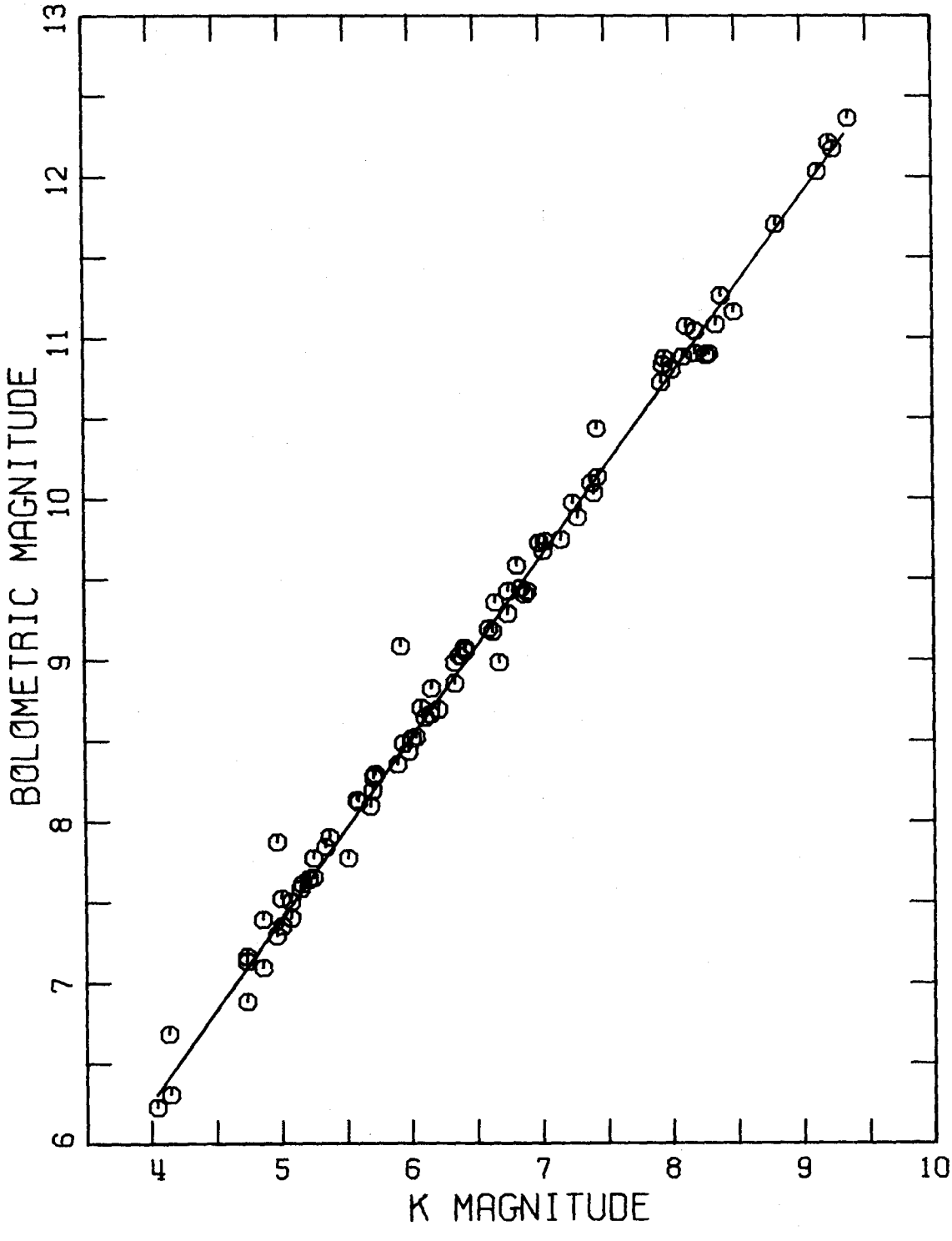

Fig.2-5.--Absolute bolometric magnitude vs. absolute 2.2μ magnitude for all single program stars which have also been observed at R and I. The mean relation $M_b = 1.13M_k + 1.76$ is indicated.

estimate M_b for those stars that have been observed at I.) The straight line in this diagram represents the mean relation

$$M_b = 1.13\ M_k + 1.76$$

which was obtained by a least-squares fit to the data points. This relation was then used to estimate the bolometric magnitudes of the remaining stars. This procedure probably introduces an additional uncertainty of $\sim\pm 0.15$ into the values adopted for these stars. Thus, the total error in the determination of the bolometric magnitude for a star that has not been observed at R and I is approximately

$$0.2 \lesssim |\Delta M_b| \lesssim 0.5$$

depending upon how well the value for its parallax is determined.

III. Discussion

A. Intrinsic Dispersion in the Lower Main Sequence

A diagram of M_b vs. V-K for all single program stars with parallaxes larger than $0.100''$ is plotted in figure 3-1. Only those stars which also have observed R and I magnitudes are included so that the stars in this group have well determined luminosities. The line drawn in this figure represents the mean relation:

$$M_b = 1.39(V-K) + 2.74 \qquad (3\text{-}1)$$

which was obtained by a least-squares fit to the data points for all single low velocity (i.e. $|RV| < 65$ km/sec and either an old disk or young disk total space motion as defined in the Appendix) stars which also have observed R and I magnitudes but are not known to have emission lines. The observed dispersion of the stars in figure 3-1 is $\sim\pm0.5$ magnitudes in M_b.

The largest error quoted for the parallax of any star plotted in this diagram is $\pm0.014''$. From equation 2-1 this results in an error in the absolute bolometric magnitude of this star of:

$$\Delta M_b \simeq 2.17 \cdot \frac{.014}{.109} \simeq \pm0.28$$

For all other stars:

$$\Delta M_b \lesssim \pm0.2$$

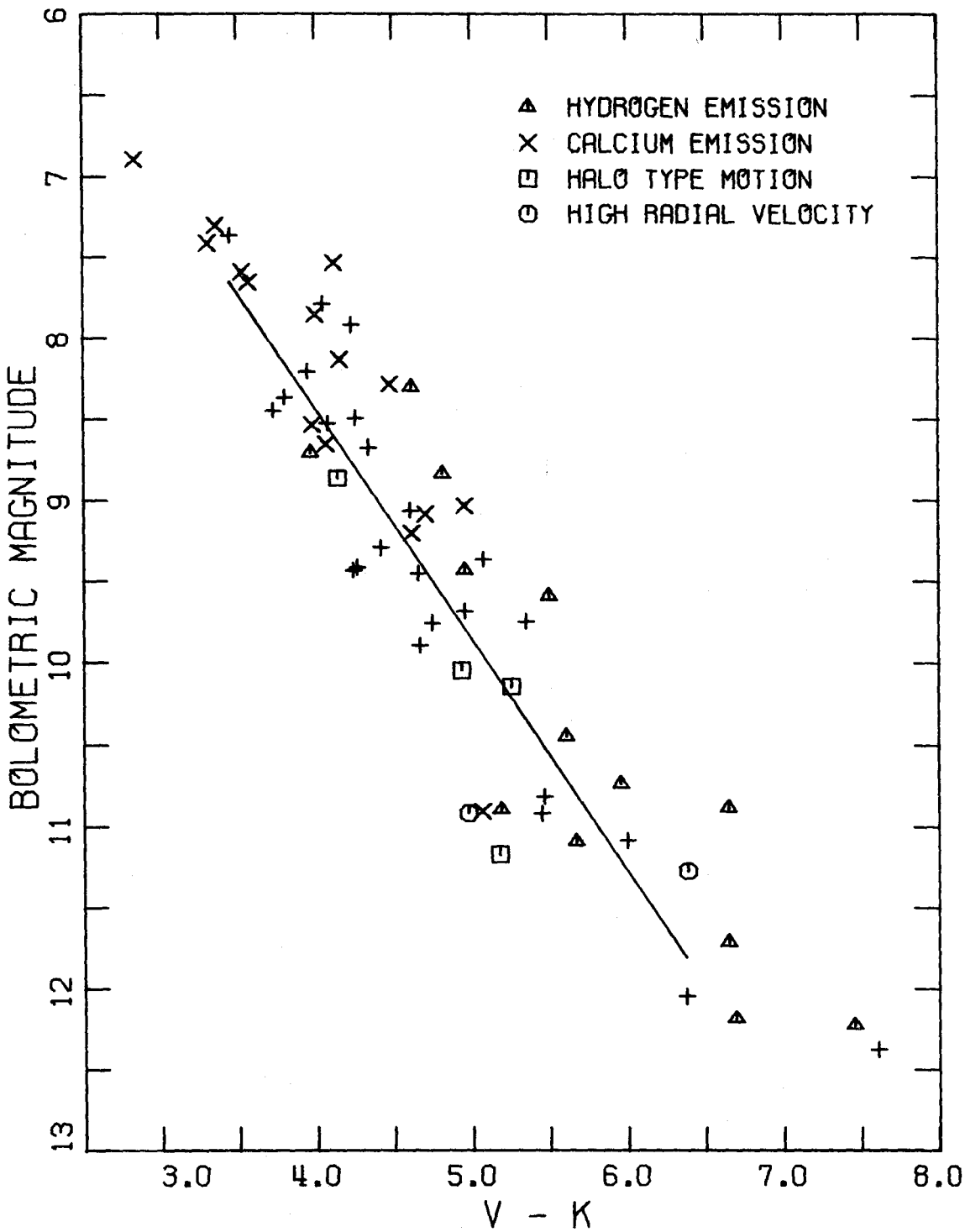

Fig.3-1.--Absolute bolometric magnitude vs. (V-2.2μ) color for all single program stars with trigonometric parallaxes $\geq 0.100''$ and which have also been observed at R and I. The mean relation $M_b = 1.39(V-K) + 2.74$ is indicated.

This error from the uncertainty in the parallax combined with the uncertainty of ±0.1 magnitudes in the photometric bolometric magnitude gives a combined uncertainty in the vertical position of a star in figure 3-1 of:

$$\Delta M_b \lesssim \pm 0.22$$

However, here we are concerned with the displacement of a star relative to the mean relation (3-1). An additional consideration is that the 2.2μ magnitude may be in error by ±0.1. The resulting error in the V-K color could change the apparent vertical displacement of a star from the mean relation by ∿ ±0.14 bolometric magnitudes.

The possible sources of error discussed above are sufficient to account for at most only about ±0.26 magnitudes when they are combined together. To change the vertical position of a typical star by 0.5 magnitudes requires either a change in the parallax of the star by more than $0.025\hat{}$" or else a change in the V-K color of 0.35 magnitudes. Several stars in figure 3-1 would require a change in their parallax of more than $0.100\hat{}$" in the proper direction in order to place them back on the mean relation. It is extremely unlikely that the errors in the parallaxes or the colors of these stars could be this large.

Therefore, it is necessary to conclude that the intrinsic dispersion in the bolometric magnitudes for stars of a

given color in an H-R diagram appears to be $\Delta M_b \sim \pm 0.4$ magnitudes. This is consistent with an intrinsic dispersion in visual magnitudes of $\Delta M_v = \pm 0.4$ found by Upgren (1973) in an analysis of the errors in parallax determinations for stars from K3 to M2. Spinrad (1972) has also observed a scatter of $\Delta M_v \simeq \pm 0.5$ magnitudes in the main sequence and concludes that it is real. Other observers have found a similar dispersion for the earlier main sequence in M_v vs. B-V diagrams. (e.g. see Johnson and Mitchell (1958), Eggen and Sandage (1962), and Eggen (1968)).

It is not clear what the physical reasons are for the observed intrinsic dispersion. Copeland et al. (1970) find that changing the mixing length from 1.0 to 2.0 times the pressure scale height only changes the bolometric magnitude by at most 0.1 magnitude. This is insufficient by itself to explain the dispersion in figure 3-1. Differences in composition are a more likely cause of the dispersion. Differences in composition might not only affect the bolometric magnitudes predicted for stars from models of stellar interiors, but also affect the observed colors and effective temperatures by differential blanketing in the relatively cool atmospheres of these stars.

Copeland's models differ by about 0.5 bolometric magnitudes between population I and II compositions for models with masses $M/M_\odot \sim 0.4$. This could explain part of the displacement of high velocity objects such as GL699

(Barnard's star) and GL299 (R619). Both of these stars lie $\sim$ 1.0 magnitudes below the mean relation of equation 3-1. This is somewhat more than can be comfortably explained by the models. GL299 and the other high velocity stars plotted in figure 3-1 are presumably halo, population II, objects; but they only make up a small fraction of the sample of stars considered in this program. Most of the program stars are disk population objects. Some are young disk objects with very low space velocities and the majority are probably "old disk" objects with intermediate space velocities. These are presumed to be population I objects and therefore the compositional differences within this group are expected to be less than the compositional differences between population I and II.

B. Hertzsprung-Russell Diagrams

Various H-R diagrams were constructed in order to examine whether or not there were systematic displacements between the different types of M dwarfs. Such systematic displacements might be expected to account for some of the observed intrinsic dispersion in the main sequence. For this purpose the program stars were separated into five groups according to the following criteria:

1) Presence of hydrogen lines in emission
2) Presence of H and K calcium lines in emission (but not hydrogen)
3) Halo type space motion (i.e. either a galactic orbit with $e \geq 0.5$ or $|W| > 75$ km/sec)
4) $|\text{Radial Velocity}| \geq 65$ km/sec (but not halo type motion)
5) Others

The absolute bolometric magnitudes of the single program stars in these groups are plotted against the V-K, R-I, and H-K colors in figures 3-2a, 3-3a, and 3-4. The straight lines drawn in these figures represent the average main sequence for low velocity (i.e. $|RV| < 65$km/sec and either

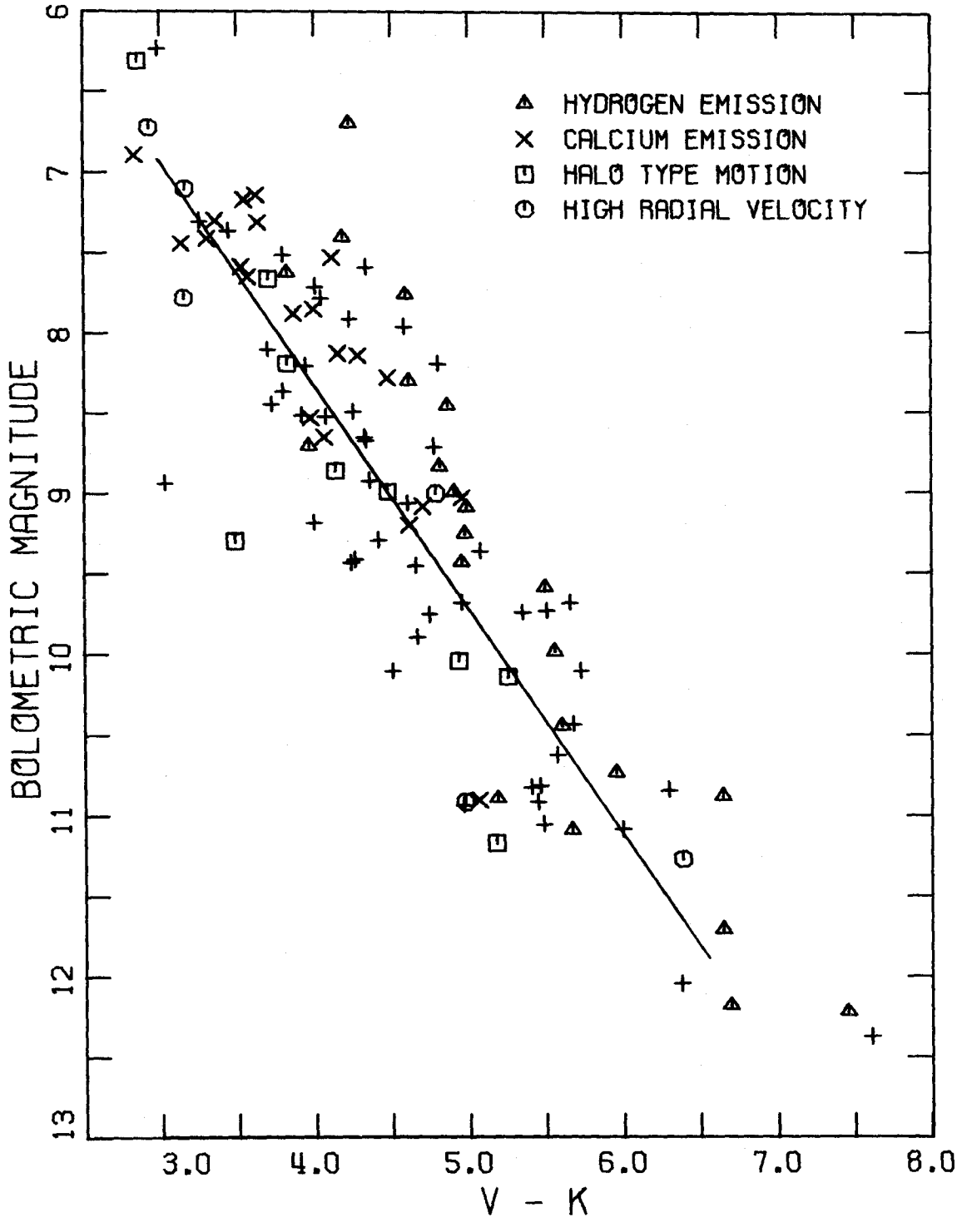

Fig.3-2a.--Absolute bolometric magnitude vs. (V-2.2μ) color for all single program stars. The mean relation indicated is $M_b = 1.39(V-K) + 2.74$.

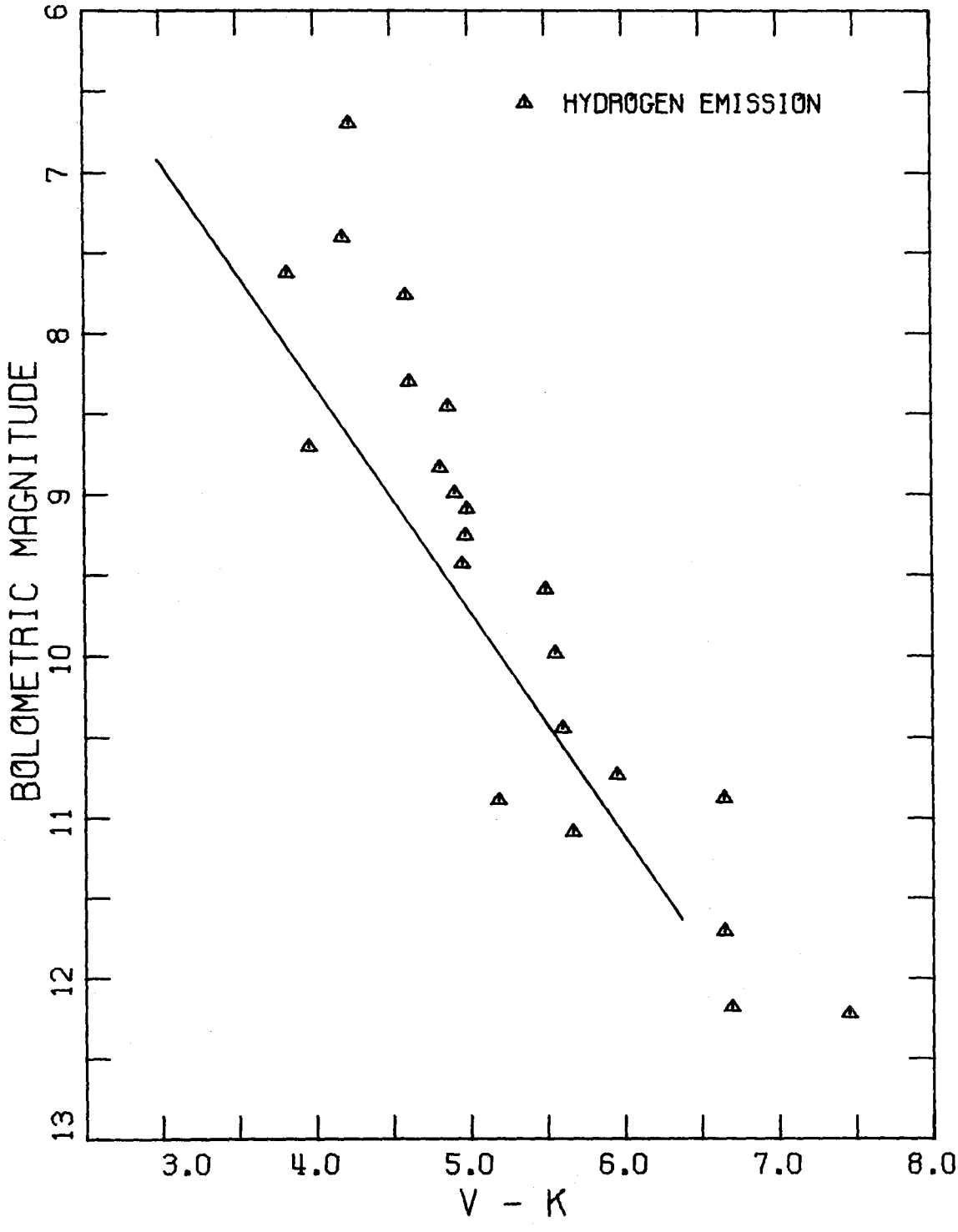

Fig.3-2b.--Absolute bolometric magnitude vs. (V-2.2μ) color for the M dwarfs from figure 3-2a which show hydrogen lines in emission. The mean relation $M_b = 1.39(V-K) + 2.74$ is indicated.

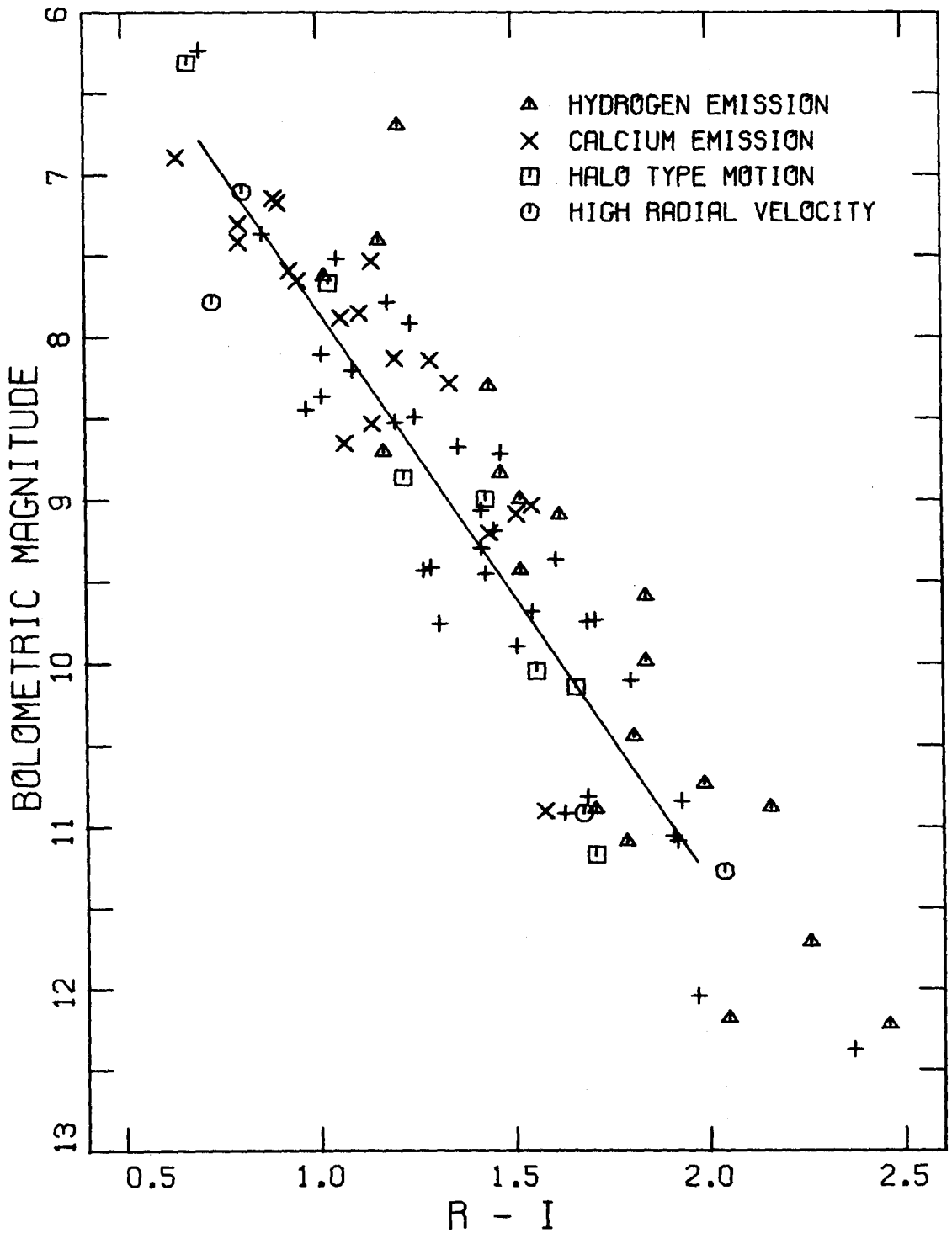

Fig.3-3a.--Absolute bolometric magnitude vs. R-I color for all single program stars. The mean relation $M_b = 3.49(R-I) + 4.34$ is indicated.

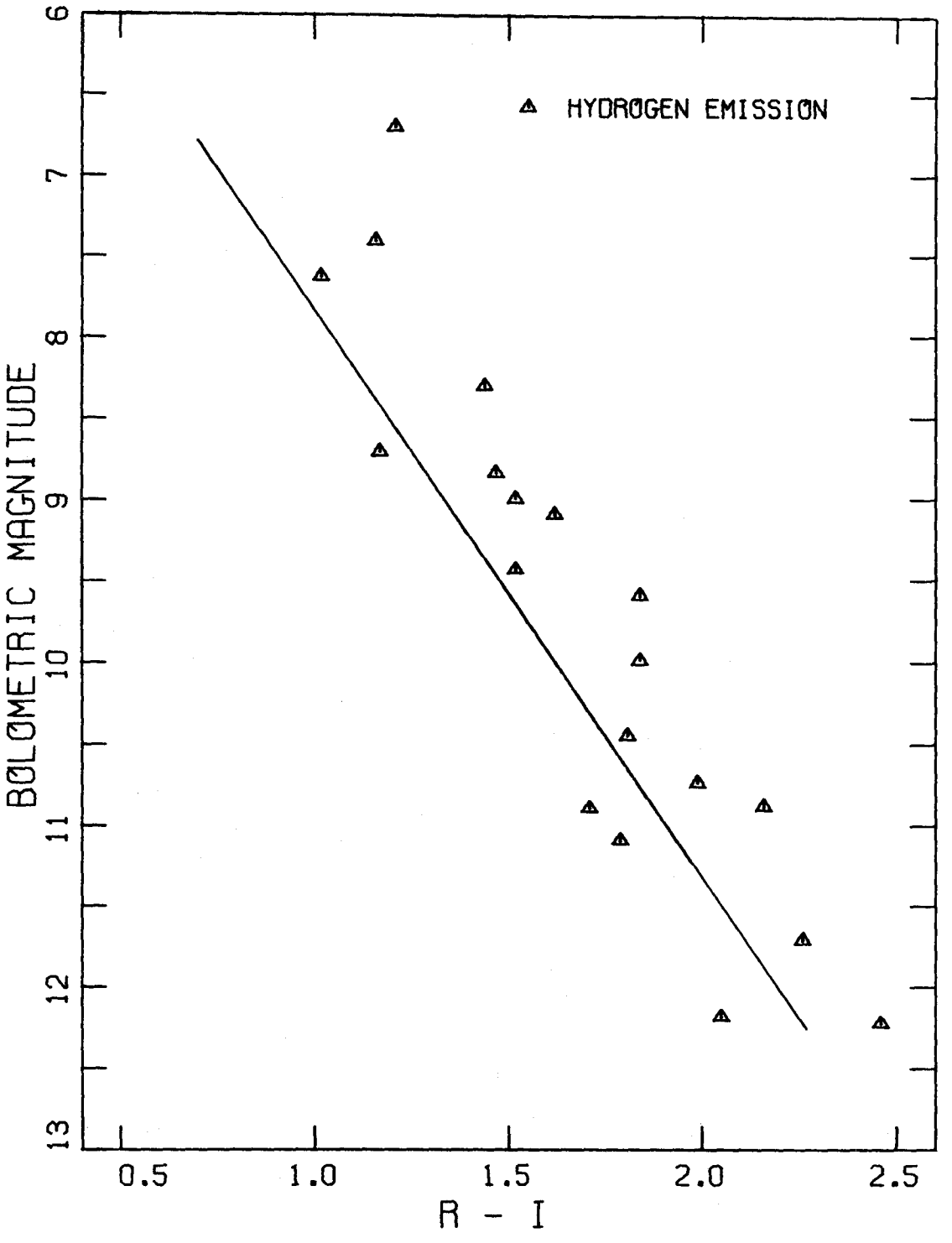

Fig.3-3b.--Absolute bolometric magnitude vs. R-I color for the M dwarfs from figure 3-3a which show hydrogen lines in emission. The mean relation $M_b = 3.49(R-I) + 4.34$ is indicated.

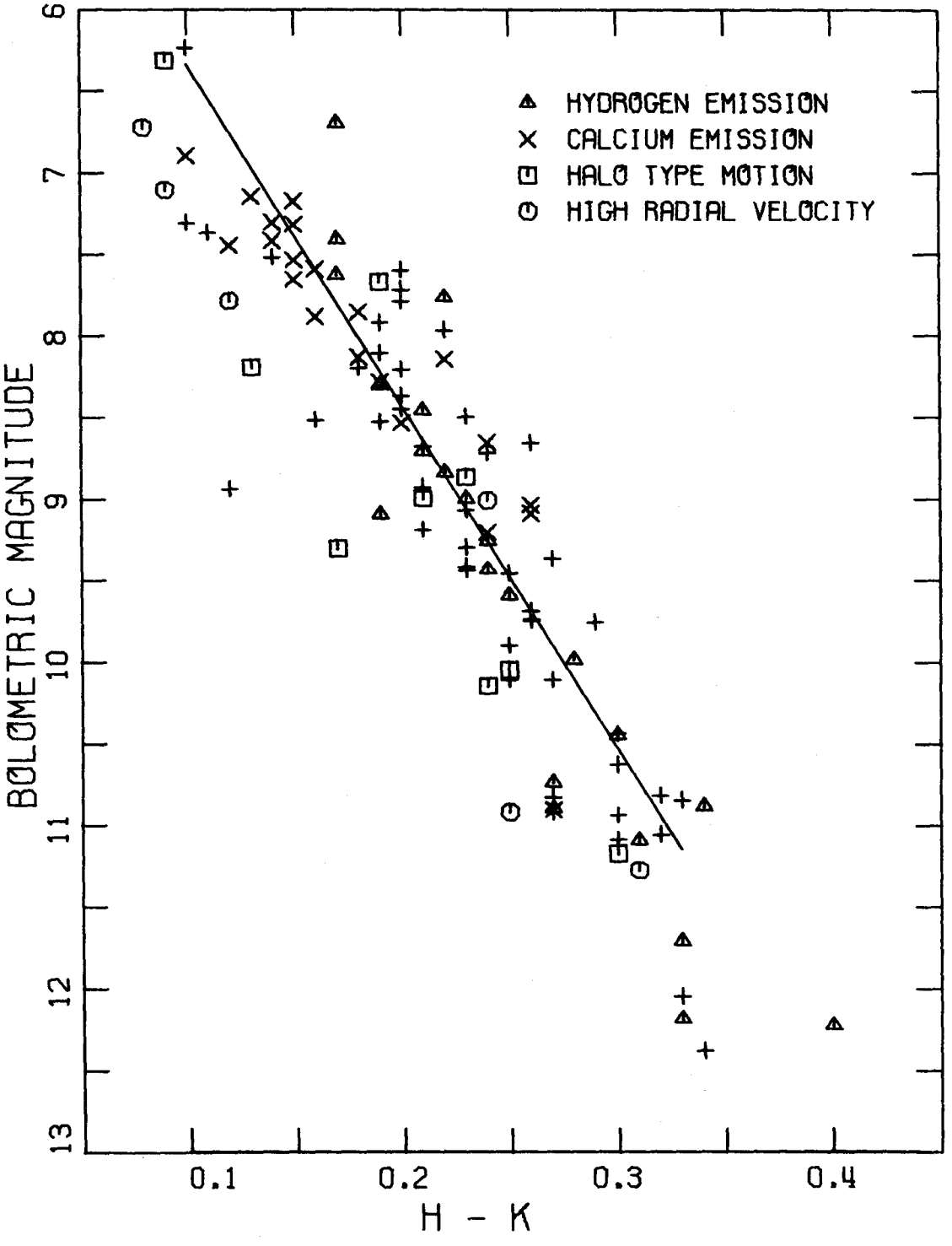

Fig.3-4.--Absolute bolometric magnitude vs. (1.65μ-2.2μ) color for all single program stars. The mean relation indicated is M_b = 20.9(H-K) + 4.2.

old disk or young disk space motion as defined in the Appendix) stars which also have observed R and I magnitudes but are not known to have emission lines. Stars which are not known to have high velocities or emission lines are plotted as plus signs in the diagrams. The three linear relations derived from least-squares fits to the data for these stars are:

$$M_b = 1.39(V-K) + 2.74 \qquad (3\text{-}1)$$

$$M_b = 3.49(R-I) + 4.34 \qquad (3\text{-}2)$$

$$M_b = 20.9(H-K) + 4.2 \qquad (3\text{-}3)$$

In these diagrams there does not appear to be a significant difference between the UV Ceti type flare stars and the other stars that show hydrogen lines in emission, so for the following discussion these were all combined into one group in an effort to improve the statistics. Table 3-1 lists the 34 flare and hydrogen emission line program stars that are either single or corrected for a visible companion. Column 5 is the difference between the bolometric magnitude observed for a star and the value calculated from equation (3-1) from the V-K color of the star. Similarly, column 7 is the difference between the bolometric magnitude of the star and the value calculated from equation (3-2) from the R-I color. The other columns are self explanatory. If we omit the stars GL616.2 and GL735 because their values are too extreme, the average displacements of these stars in

Table 3-1

Flare Stars and Stars with Hydrogen Emission Lines

GL	Type	Pop.	M_b	V-K	ΔM_b (V-K)	R-I	ΔM_b (R-I)
*15A	M1	OD	8.8	4.05	-.43	1.16	-.46
*15B	M6	OD	10.9	5.07	-1.11	1.58	-1.10
48	M3.5E	OD	8.3	4.62	.86	1.44	1.01
51	M7E	--	10.7	5.96	.29	1.99	.49
*65A	M5.5E	YD	11.7	6.60	.20	2.18	.16
83.1	M8E	--	11.2	5.67	-.53	--	--
*207.1	M3E	--	8.5	4.87	1.06	--	--
234	M7E	YD	10.2	5.61	.33	1.81	.38
277B	M4.5E	YD	9.1	4.99	.59	1.62	.85
278:	M0.5E	YD	7.6	3.83	.44	1.02	.24
*285	M4.5E	YD	9.6	5.50	.79	1.84	1.11
*388	M4.5E	YD	8.8	4.82	.61	1.47	.59
*406	M8E	OD	12.2	7.46	.89	2.46	.62
*412B	M8E	OD	12.2	6.70	-.13	2.05	-.76
424	M1	OD	8.4	3.80	-.34	1.01	-.54
*447	M5	YD	10.8	5.47	-.47	1.69	-.63
473:	M5.5E	YD	11.5	6.43	.17	2.08	.02
494	M2E	YD	7.3	4.19	1.25	1.16	1.03
516A	M4E	OD	9.1	4.60	.05	1.32	-.18
551	M5E	YD	11.7	6.65	.27	2.26	.44
*616.2	M1E	OD	6.7	4.23	(1.93)	1.21	(1.83)

Table 3-1 (Continued)

GL	Type	Pop.	M_b	V-K	ΔM_b (V-K)	R-I	ΔM_b (R-I)
644:	M4.5E	OD	8.8	4.58	.35	1.40	.41
669A	M4E	YD	9.0	4.91	.57	1.52	.60
669B	M5E	YD	10.0	5.56	.49	1.84	.72
729	M4.5E	YD	10.9	5.19	-.94	1.71	-.64
735	M2E	YD	7.4	4.60	(1.73)	--	--
766A	M4.5E	--	10.2	5.09	-.41	1.66	-.16
815A	M3E	OD	8.1	4.05	.29	1.16	.26
866	M7E	OD	10.9	6.65	1.10	2.16	.92
867B	M4E	YD	9.3	4.98	.41	--	--
*873	M4.5E	YD	9.4	4.96	.20	1.52	.16
*896A	M4E	YD	9.0	5.08	.84	1.58	.84
905	M6E	OD	11.3	6.39	.35	2.04	.12
908	M2E	OD	8.7	3.97	-.44	1.17	-.32

* measured by Iriarte also

: mean component

the M_b vs. R-I and M_b vs. V-K diagrams are $\sim$0.21 and 0.24, respectively, in the sense that these stars tend to lie above the average main sequence. This displacement can be seen more clearly in figures 3-2b and 3-3b where all the stars except for those with hydrogen in emission have been omitted. If we omit GL15A, 15B, 424, and 447 because they don't show hydrogen in emission in the quiescent state, the average displacements become $\sim$0.36 magnitudes in both diagrams. There does not appear to be a significant displacement of this group of stars in the M_b vs. H-K plane.

A similar treatment of the 24 single program stars which show Ca II emission lines but don't show any hydrogen emission lines give average displacements of $\sim$0.10 and 0.19 in the M_b vs. R-I and the M_b vs. V-K diagrams. Again, there does not appear to be a significant displacement of this group of stars in the M_b vs. H-K plane. Apparently, the behavior of this group of dwarfs with Ca II in emission is similar to, but not as marked as, the displacement of the dwarfs that have hydrogen emission lines.

These results are consistent with the comments of Haro and Chavira (1966) who find that most flare stars in clusters lie above the main sequence but some do lie below it. However, these results are contrary to Iriarte's (1971) conclusions. He compared 11 flare stars with 14 other M dwarfs from the solar neighborhood in R-I vs. R-J, R-K, and R-L color-color diagrams. He concluded that there

was no systematic difference between the flare stars and the others. Figure 3-5 is a color-color plot of R-I vs. R-K for all the single program stars with available R and I magnitudes. The line drawn indicates the average main sequence. There is apparently no significant deviation of the emission line stars in this diagram which is consistent with Iriarte's interpretation of a similar diagram for his stars. Figure 3-6a is another color-color plot of the same stars in the R-I vs. H-K plane. The average main sequence is also indicated. There is an obvious shift of the stars with hydrogen emission lines from the mean of the stars without any emission lines in the sense that for a given H-K color the flare stars have a redder R-I color than the stars without emission lines. This shift is even more clearly seen in figure 3-6b where only the stars with hydrogen in emission are compared with the average main sequence. If we take the flare stars from table 3-1 which Iriarte also measured, but omit GL616.2 because it is too extreme and also omit GL15A, 15B, and 447 because they don't have hydrogen emission lines in the quiescent state, we calculate an average displacement of 0.4 magnitudes in the M_b vs. R-I plane for seven common stars. Iriarte seems to have based his conclusions on a set of color-color diagrams where the two colors are too well correlated with each other to show any of the systematic differences between different groups of stars that appear in other diagrams.

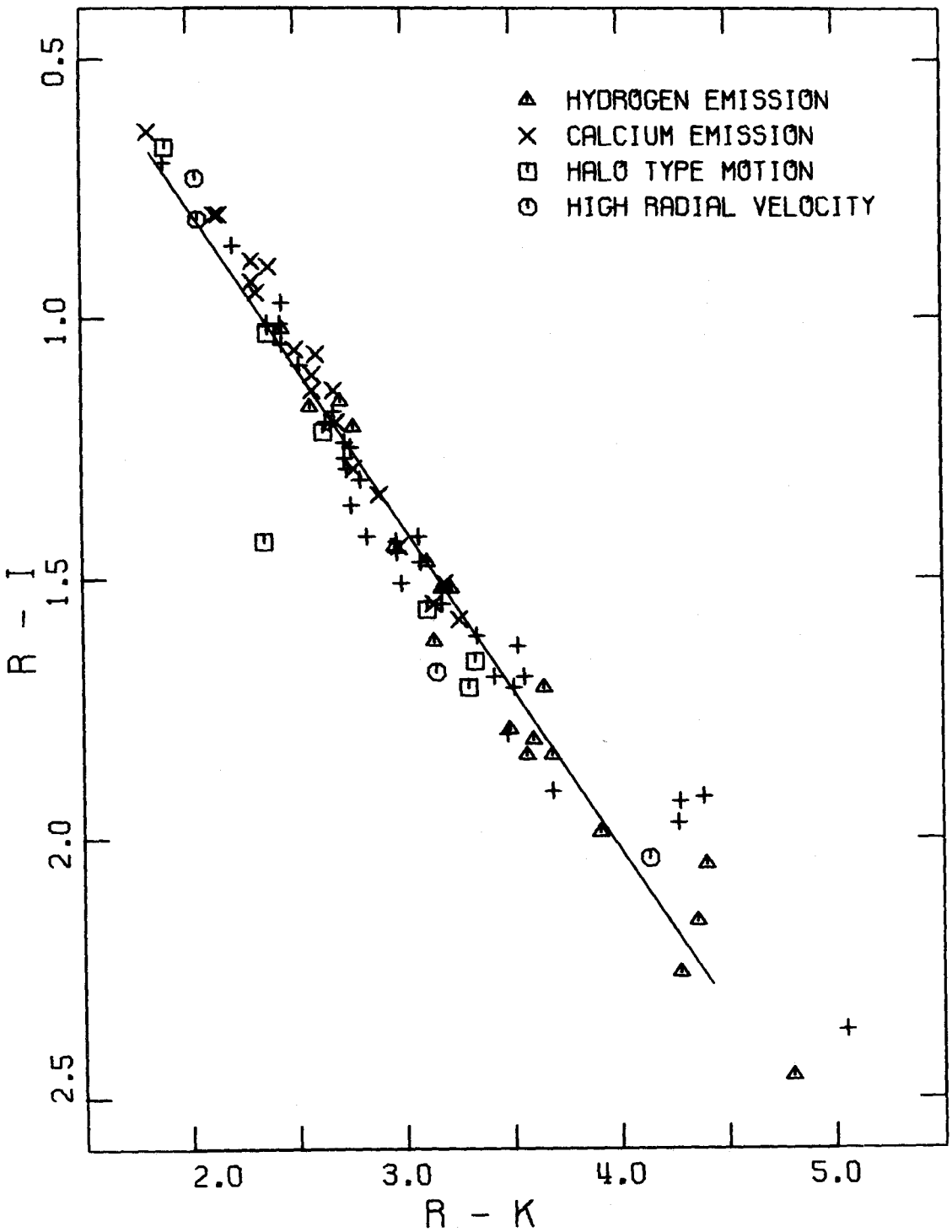

Fig.3-5.-(R-I) color vs. (R-2.2μ) color for all single program stars. The average main sequence is indicated.

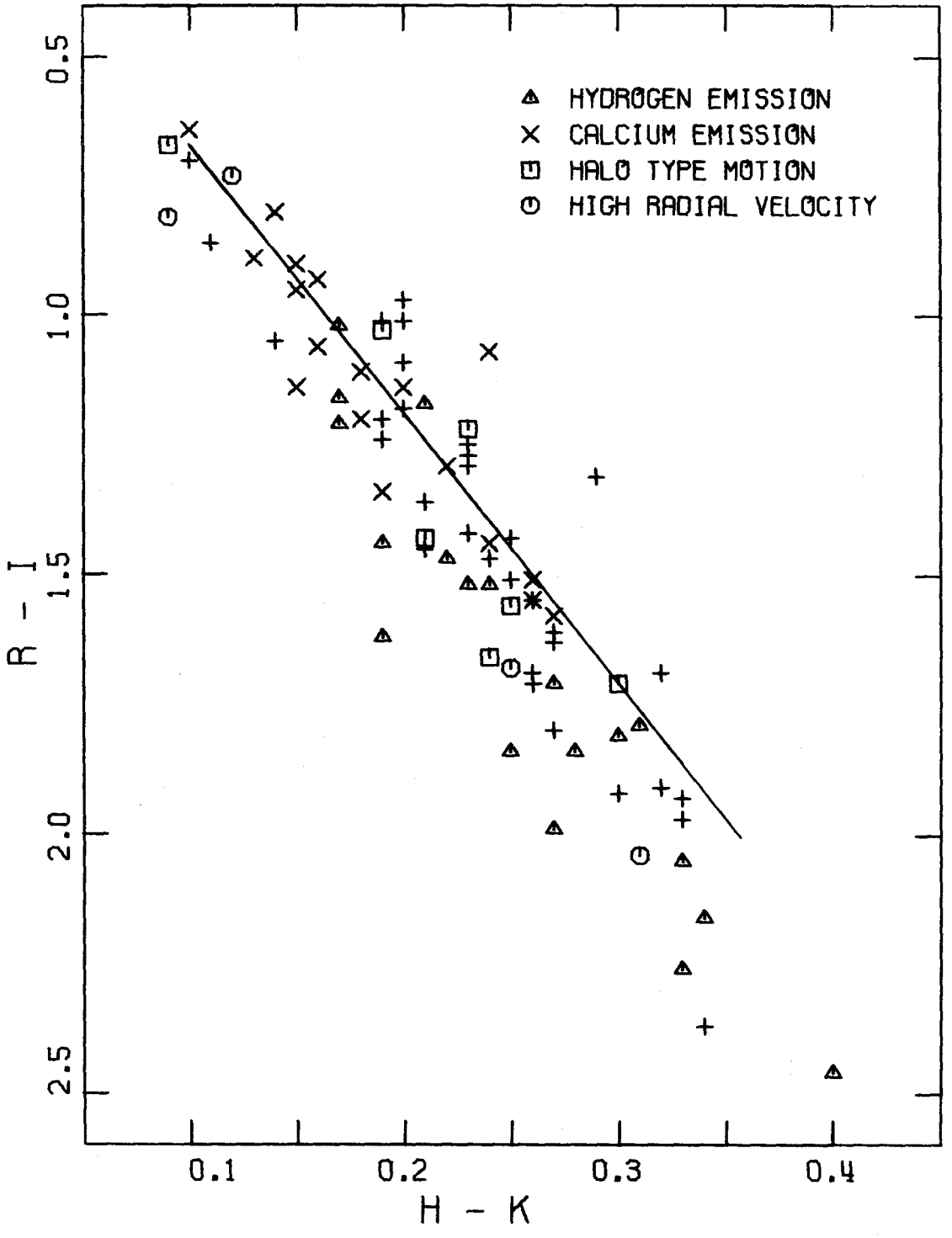

Fig.3-6a.--(R-I) color vs. (1.65μ-2.2μ) color for all single program stars. The average main sequence is indicated.

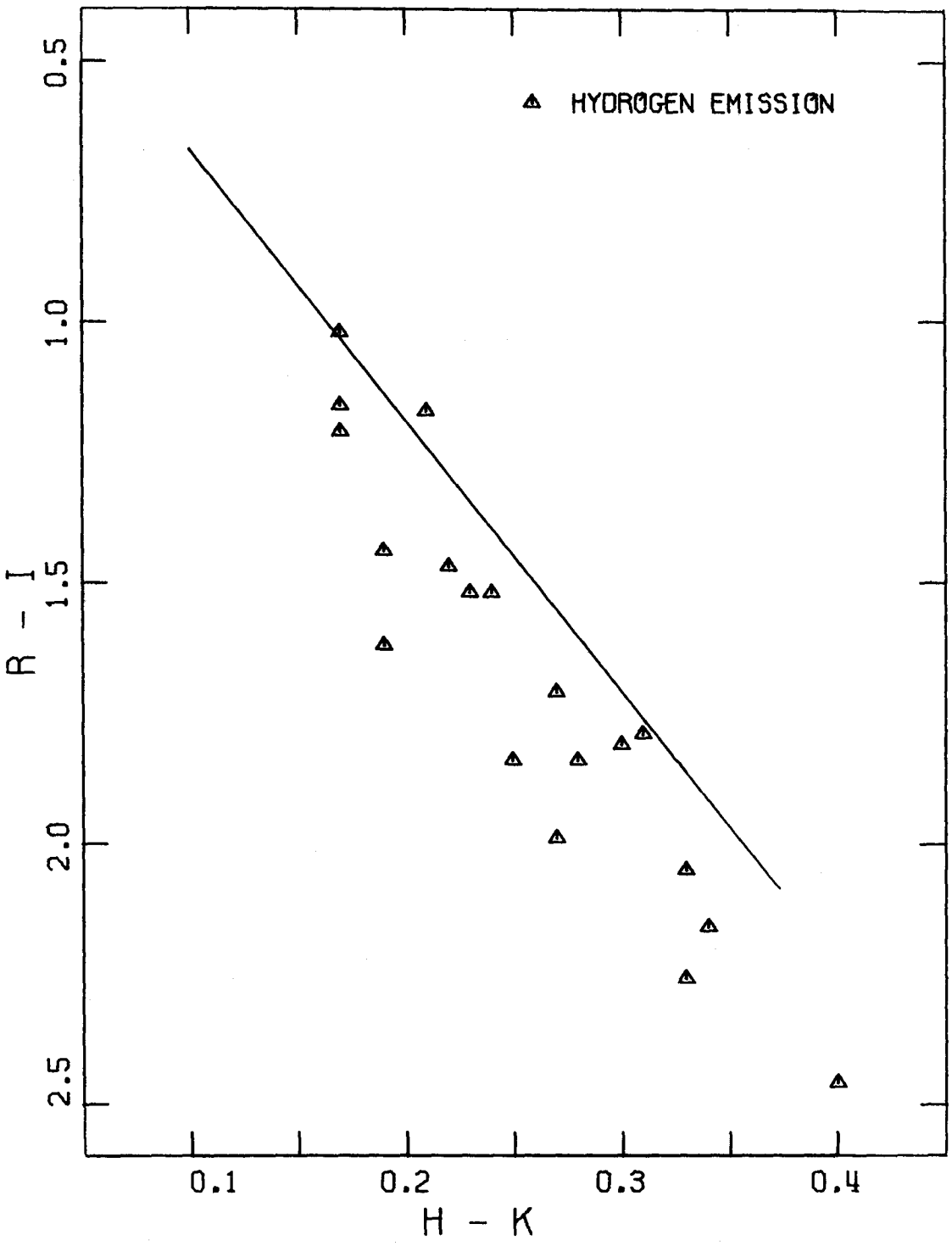

Fig.3-6b.--(R-I) color vs. (1.65μ-2.2μ) color for the M dwarfs from figure 3-6a which show hydrogen lines in emission. The average main sequence is indicated.

The average displacement of the stars in table 3-1 assigned to the old disk population in the M_b vs. V-K plane is $\sim$0.12 for twelve stars. Similarly, the average displacement for the sixteen young disk stars in table 3-1 is $\sim$0.36. These numbers are not well determined because of the small number of stars left in these groupings and can only suggest that stars selected for both hydrogen emission lines and young disk space motions may have the largest average displacement above the main sequence.

Figures 3-7a and 3-7b are plots of M_b vs. V-K and M_b vs. R-I for all single program stars divided into the three population groups on the basis of their space motions. The mean of the young disk stars lies about 0.2 magnitudes above the mean of the old disk stars in the M_b vs. V-K plane and about 0.3 magnitudes above in the M_b vs. R-I plane. The two mean sequences are indicated by the lines drawn in the figures. There is considerable overlap in the scatter of the stars in each group such that the displacements in these figures is not as dramatic as those seen when the stars are divided on the basis of hydrogen line emission.

M dwarfs with halo type space motions or high radial velocities tend to be subluminous in all three M_b vs. R-I, V-K, and H-K diagrams. The seventeen program stars with halo type space motions and/or high radial velocities are listed in table 3-2 along with their displacements in these

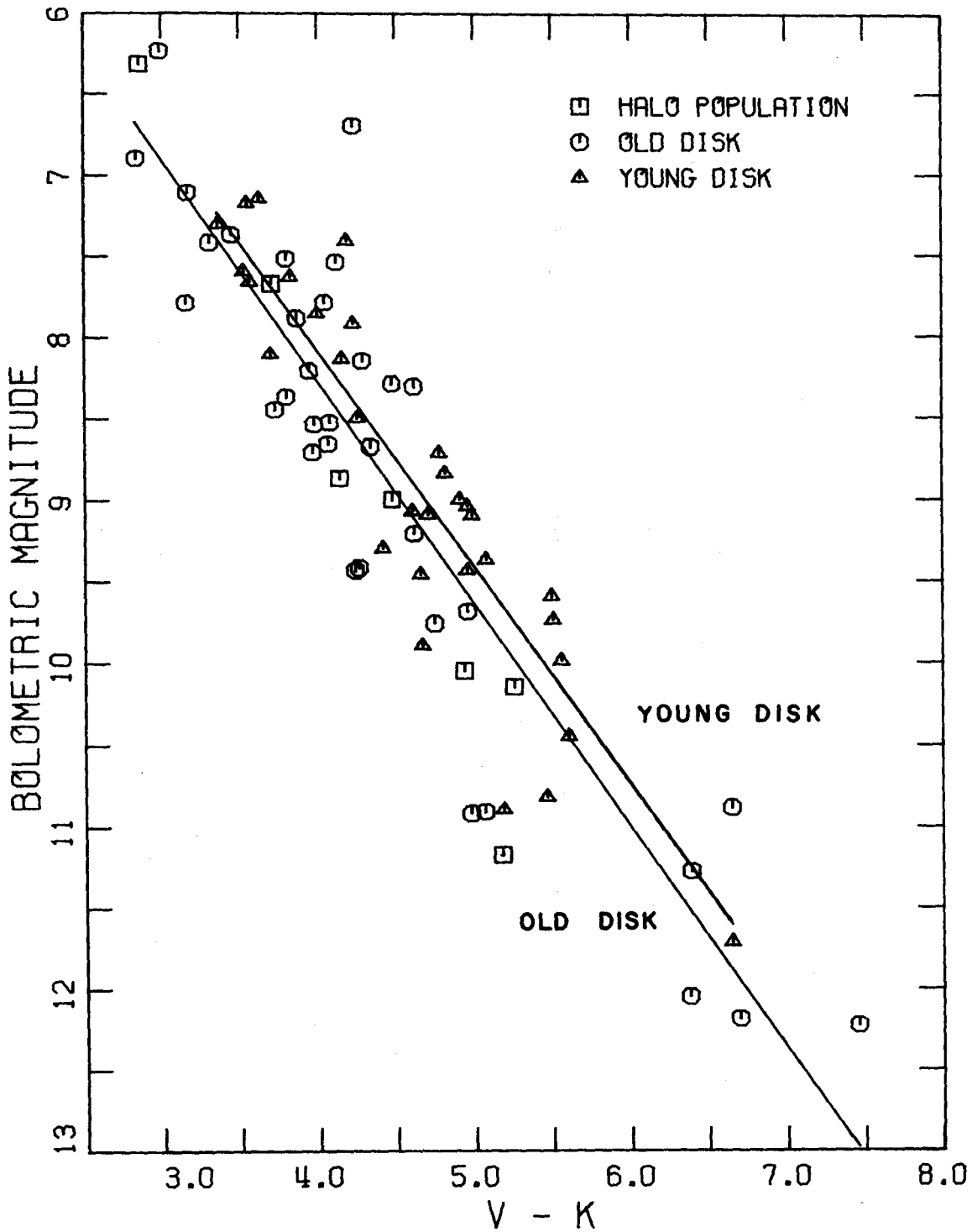

Fig.3-7a.--Absolute bolometric magnitude vs. (V-2.2μ) color for all single program stars which have also been observed at R and I. The three population types are defined in the text. Mean relations for the young disk motion dwarfs and the old disk motion dwarfs are indicated.

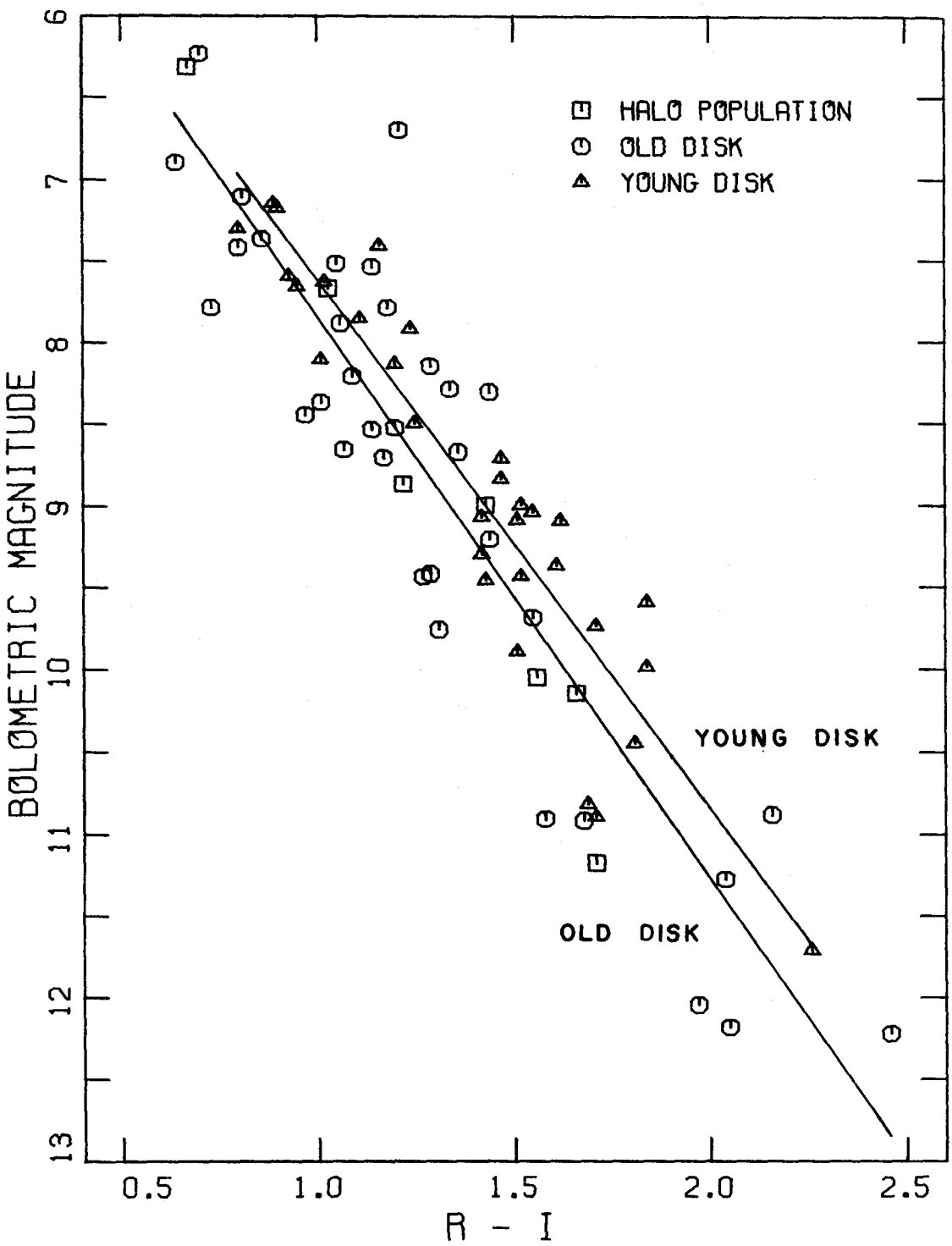

Fig.3-7b.--Absolute bolometric magnitude vs. R-I color for all single program stars. The three population types are defined in the text. Mean relations for the young disk motion dwarfs and the old disk motion dwarfs are indicated.

Table 3-2

Halo Stars and High Radial Velocity Stars

GL	Type	Pop.	M_b	ΔM_b (R-I)	ΔM_b (V-K)	ΔM_b (H-K)
105.5	M0p	OD	6.7	--	.09	-.82
G95-59	Mp	Halo	9.3	--	(-1.71)	(-1.51)
129	sdM0	Halo	10.5	--	(-2.71)	(-.82)
157.1	M4	OD	9.0	--	.40	.26
184	M0	Halo	7.7	.23	.24	.55
213	sdM5.5	Halo	10.1	-.07	-.09	-.88
299	M5	Halo	11.2	-.92	-1.23	-.64
369	M2	Halo	8.2	--	-.13	-1.24
411	M2	Halo	8.9	-.31	-.37	.19
413	M0p	Halo	6.3	(.34)	(.41)	(-.20)
445	sdM4	Halo	10.0	-.31	-.43	-.57
699	sdM5	OD	10.9	-.77	-1.25	-1.44
717	M0	OD	7.8	-.92	-.65	-1.04
748	M4	Halo	9.3	.06	-.30	-.64
G231-27	sdM1	Halo	10.0	(-2.05)	(-2.03)	(-2.19)
830	M0	OD	7.1	.03	.05	-.99
905	M6E	OD	11.3	.12	.35	-.53

three diagrams. The displacements are relative to equations 3-1, 3-2, and 3-3. If we omit GL129 and G231-27 as too extreme (the parallax of GL129 was recently decreased from $0.068''$ to $0.030''$ but is still probably too large) and also GL413 because of its poor parallax, the average displacements of these stars are $\sim$-0.3, -0.3, and -0.6. For the best seven halo stars (only six of which have R-I colors), the average displacements become $\sim$-0.2, -0.3, and -0.5 magnitudes in the M_b vs. R-I, V-K, and H-K planes. Apparently, these high velocity stars are subluminous by at least 0.2 magnitudes on the average, although there is a large scatter among the few objects available.

Table 3-3 lists three additional stars classified as subdwarfs by Joy (1947). Together with the halo stars and GL699 from table 3-2, these stars average displacements of $\sim$-0.4, -0.6, and -0.5 magnitudes in the M_b vs. R-I, V-K, and H-K planes. The criteria used by Joy to assign a subdwarf spectral type to M stars included a general weakening of the absorption spectrum and a strengthening of the Lindblad depression at λ 4226Å. Of course, it is unknown what additional stars would meet the criteria used by Joy. It is not even certain that subdwarfs can be reliably recognized spectroscopically. The seven sdM dwarfs are certainly subluminous, but there are other subluminous dwarfs such as GL299 or G95-59 which may be similar to Joy's subdwarfs. It would be extremely helpful to have a consis-

Table 3-3

Additional Joy Subdwarfs

GL	Type	Pop.	M_b	ΔM_b (R-I)	ΔM_b (V-K)	ΔM_b (H-K)
643	sdM4	OD	10.6	-.69	-1.04	-.48
745A	sdM2	OD	9.4	-.62	-.73	-.36
745B	sdM2	OD	9.4	-.71	-.80	-.38

tent classification of the spectra of all of the stars that appear to be significantly subluminous in the H-R diagrams discussed here.

The average upward displacement of the stars with hydrogen emission by $\sim$0.3 bolometric magnitudes and the average downward displacement of the halo stars of between 0.2 and 0.6 magnitudes do not imply that there is a well defined sequence for flare stars above the main sequence and a sequence for halo stars below the main sequence. As discussed in section 3-A, the intrinsic dispersion in the low velocity stars is $\pm$0.5 magnitudes. As can be seen in the magnitude-color diagrams, all the sub-groupings of stars overlap. The average displacements of these groups are nonetheless reasonably well determined. The small number of stars available in each group does limit the accuracy with which the average displacements can be determined. Arbitrarily throwing out one of the stars with the largest individual displacement can affect the average displacement of the emission line stars by at most $\sim$0.04 magnitudes in the M_b vs. V-K diagram. Similarly, the average displacement of the halo stars is uncertain by $\sim$0.13. These estimates of the possible errors are smaller than the average displacements of these groups. The average displacement of the halo stars in the M_b vs. H-K plane is probably not significant because the main sequence is so steep in this

plane. The error in the color of $\sim \pm 0.03$ can cause an apparent vertical displacement of a star from the main sequence of $\sim \pm 0.6$. This is comparable with the average displacement of this group of stars in this case, but in the M_b vs. R-I and M_b vs. V-K diagrams the main sequences are much less steep and the displacements are probably not a result of errors in the color.

Further support for the significance of these average displacements is that the three groups of stars (hydrogen emission line, calcium emission line, and halo population) each have similar displacements in both the M_b vs. R-I and the M_b vs. V-K diagrams. In addition, there definitely appears to be a progression from hydrogen emission line stars to calcium emission line stars to "normal" dwarfs to halo type dwarfs which is consistent with the traditional ordering of the ages of these types of stars.

There are several possible physical explanations for the displacements observed. Unresolved binaries could cause an apparent upward displacement of a star's bolometric magnitude by up to 0.75 magnitudes. It is possible that young disk or emission line stars contain a larger percentage of binaries than old disk or stars without any emission lines. An attempt has been made to eliminate this problem by excluding all known doubles from the previous calculations. Few of the stars left should still be doubles. In particular, most of the superluminous stars are flare

stars and it is unlikely that a companion bright enough to affect the photometry would be missed on all the spectra taken of these flare stars. It turns out that some of the stars known to be double are apparently subluminous (e.g. GL15A, GL643, or GL781).

Another possible explanation for the average upward displacement of the emission line stars is that they are still evolving downward and have not yet settled on the main sequence. This explanation would be consistent with a very young age for these stars. Unfortunately, some of these superluminous stars do have old disk motions and therefore must be relatively old objects with ages of $\sim 10^9$ years. (cf. the section (3-G) on old disk flare stars) These stars have had more than sufficient time to reach the main sequence since the evolutionary time scale for an early M dwarf to reach the main sequence is only a few times 10^8 years. In addition, some of the superluminous stars don't have any emission lines and some flare stars are subluminous. (e.g. GL83.1 and 729, which have large parallaxes, lie ~ 0.5 and ~ 0.9 magnitudes below the main sequence in the M_b vs. V-K plane.) A simple evolutionary scheme cannot explain why some old stars still have emission lines and why some superluminous stars don't have any emission lines.

Traditionally, subluminous dwarfs have been assumed to

be metal poor. Late M dwarfs suffer from extreme blocking by atomic lines and molecular bands in absorption in their spectra and differences in blocking might explain relative displacements of the different groups of stars. In M dwarfs, TiO absorption bands extend across the V, R, and I band-passes and the U and B bands are heavily blanketed by low excitation metal lines. The H and K infrared bands are probably relatively unblanketed in the temperature range covered by M dwarfs. The apparent upward displacement of the flare stars by $\sim$0.3 bolometric magnitudes could be produced by a systematic color differences of $\Delta(V-K) \sim 0.2$ and $\Delta(R-I) \sim 0.1$.

The following attempt was made to test whether the blocking in different wavelength bands is related: All the program stars were plotted in a M_k vs. V-K diagram. A smooth curve was drawn by eye to represent a reasonably tight left hand envelope of the main body of stars. Only the subluminous stars G95-59, G231-27, and GL129 and also the star GL550.1 (which has an uncertain parallax) lie significantly to the left of the adopted smooth curve. This curve was taken to represent a relatively unblanketed sequence in the sample of stars available. The difference in V-K between this curve and the position of each star in the M_k vs. V-K plane was taken as a blanketing index for each star. The stars which happen to lie close to this curve and which therefore have a small blanketing index may

still in fact be somewhat blanketed. This is especially true toward the faint end of the sequence where there are only a few stars. Corrections to the U, B, R, and I magnitudes were made for each star by multiplying its blanketing index by a constant factor for each magnitude. This factor was taken equal to 1.0 for U and B, 0.65 for R, and 0.3 for the I magnitude. The largest percentage of flux redistributed by this procedure was $\sim$20% for GL866. The corrected stars were then replotted in M_k vs. U-K, B-K, R-K, and I-K diagrams. The results of this procedure can be seen by comparing figures 3-8a to 3-11a with 3-8b to 3-11b. The uncorrected average main sequence is indicated in each of these diagrams for comparison. This procedure reduced the scatter in all of these diagrams to within the observational error in the color determination.

An attempt was also made to reduce the scatter in the M_k vs. H-K plane by correcting the H magnitude in a similar manner. However, no constant factor was found which significantly reduced this scatter. That is, the above blanketing index does not seem to be correlated with the displacement of a star from the main sequence in the M_k vs. H-K plane. This suggests that the H and K bands do not suffer from blanketing as much as the shorter wavelength bandpasses and therefore the H-K color is a simple temperature indicator for M dwarfs in the sense that these bands sample the

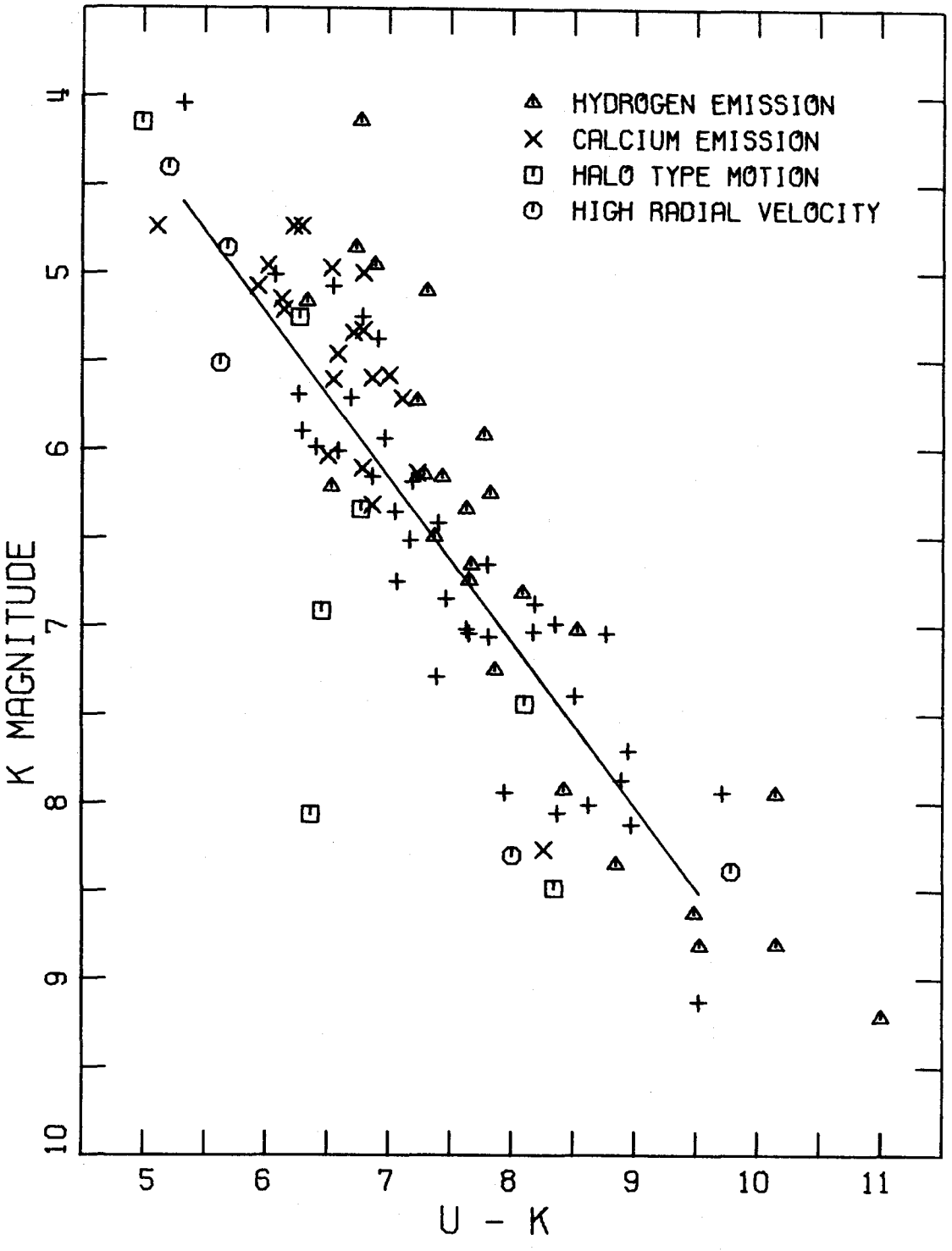

Fig.3-8a.--Absolute 2.2μ magnitude vs. (U-2.2μ) color for all program stars. The average main sequence is indicated.

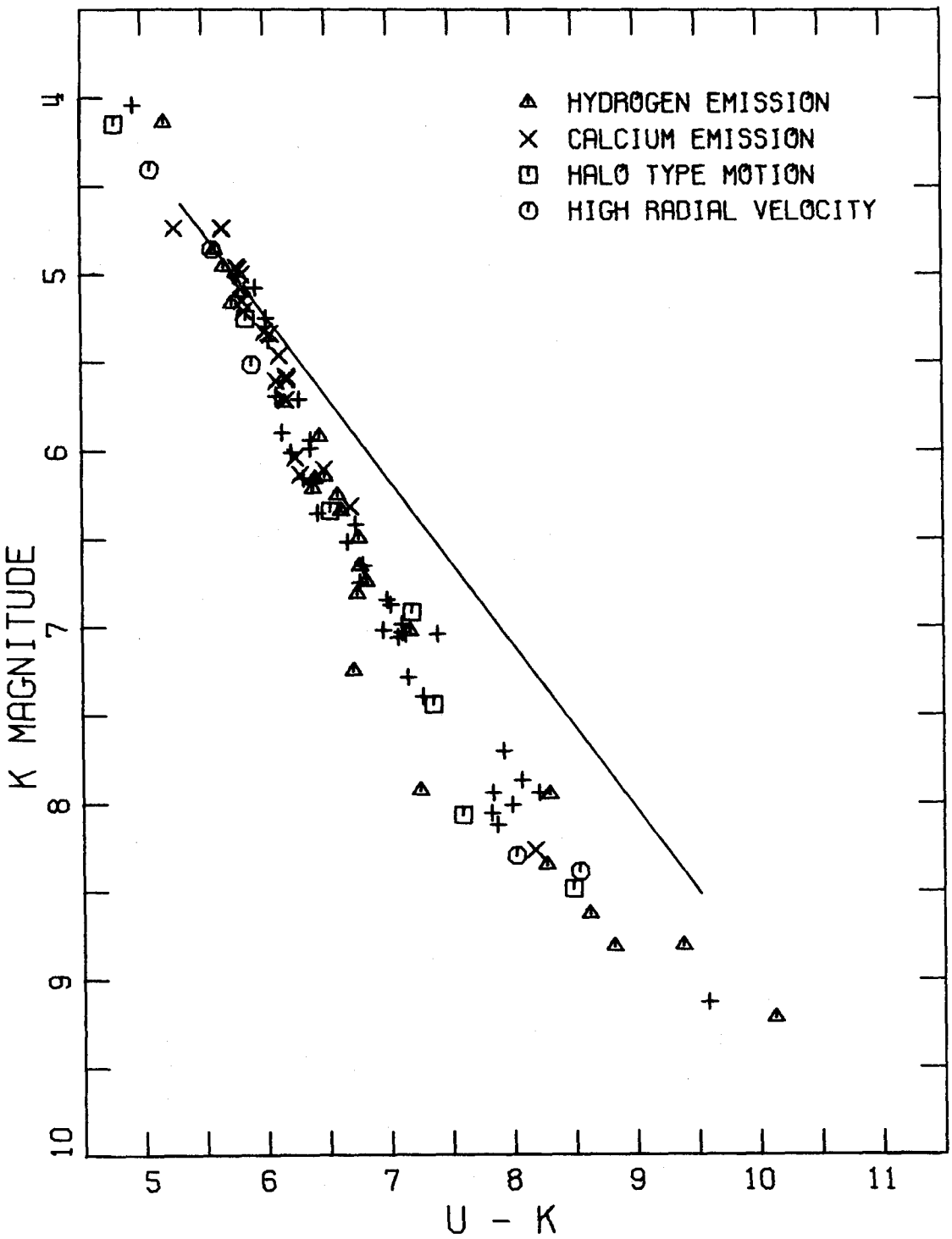

Fig.3-8b.--Absolute 2.2μ magnitude vs. (U-2.2μ) color corrected for blanketing as explained in the text for all program stars. The uncorrected average main sequence is indicated.

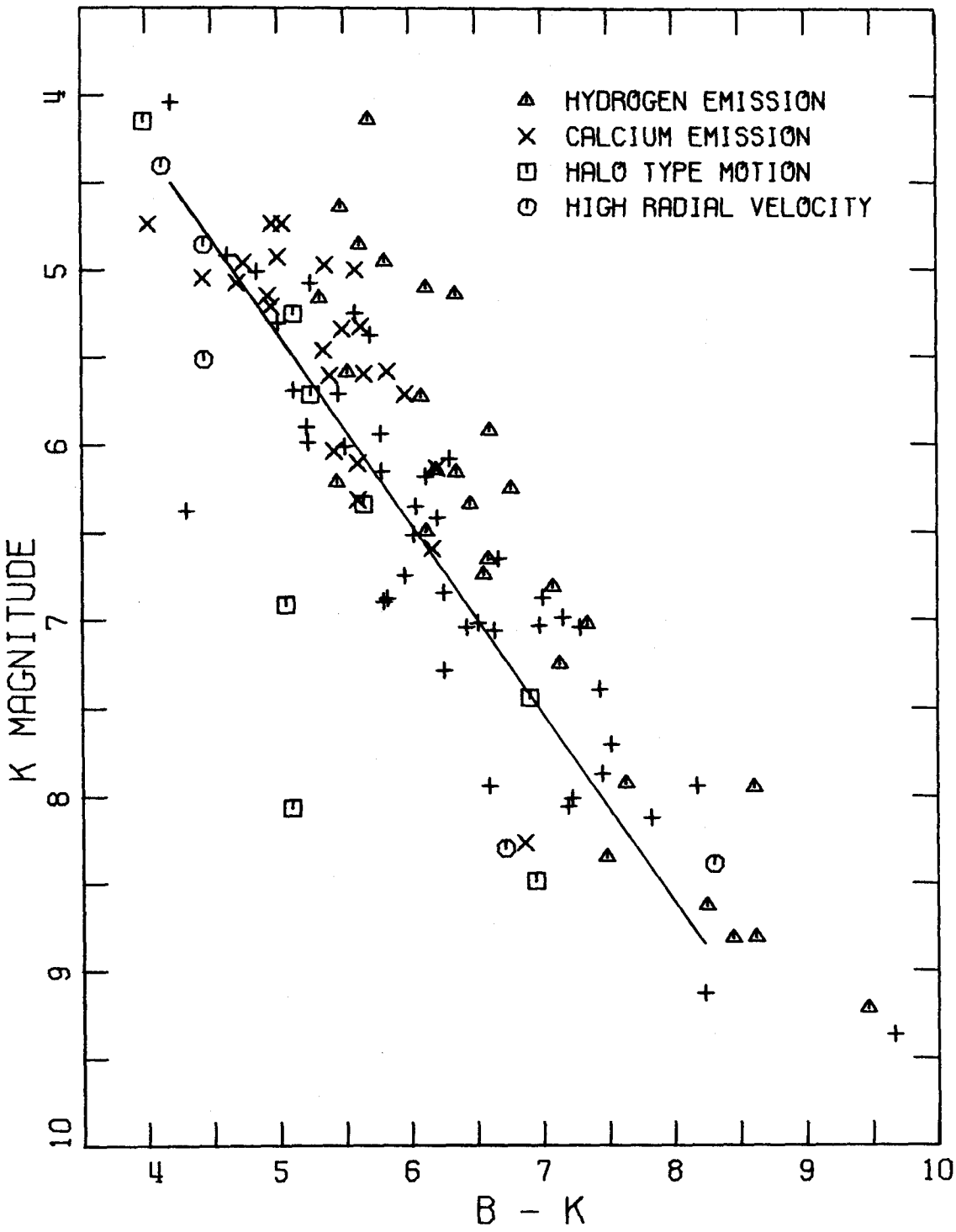

Fig.3-9a.--Absolute 2.2μ magnitude vs. (B-2.2μ) color for all program stars. The average main sequence is indicated.

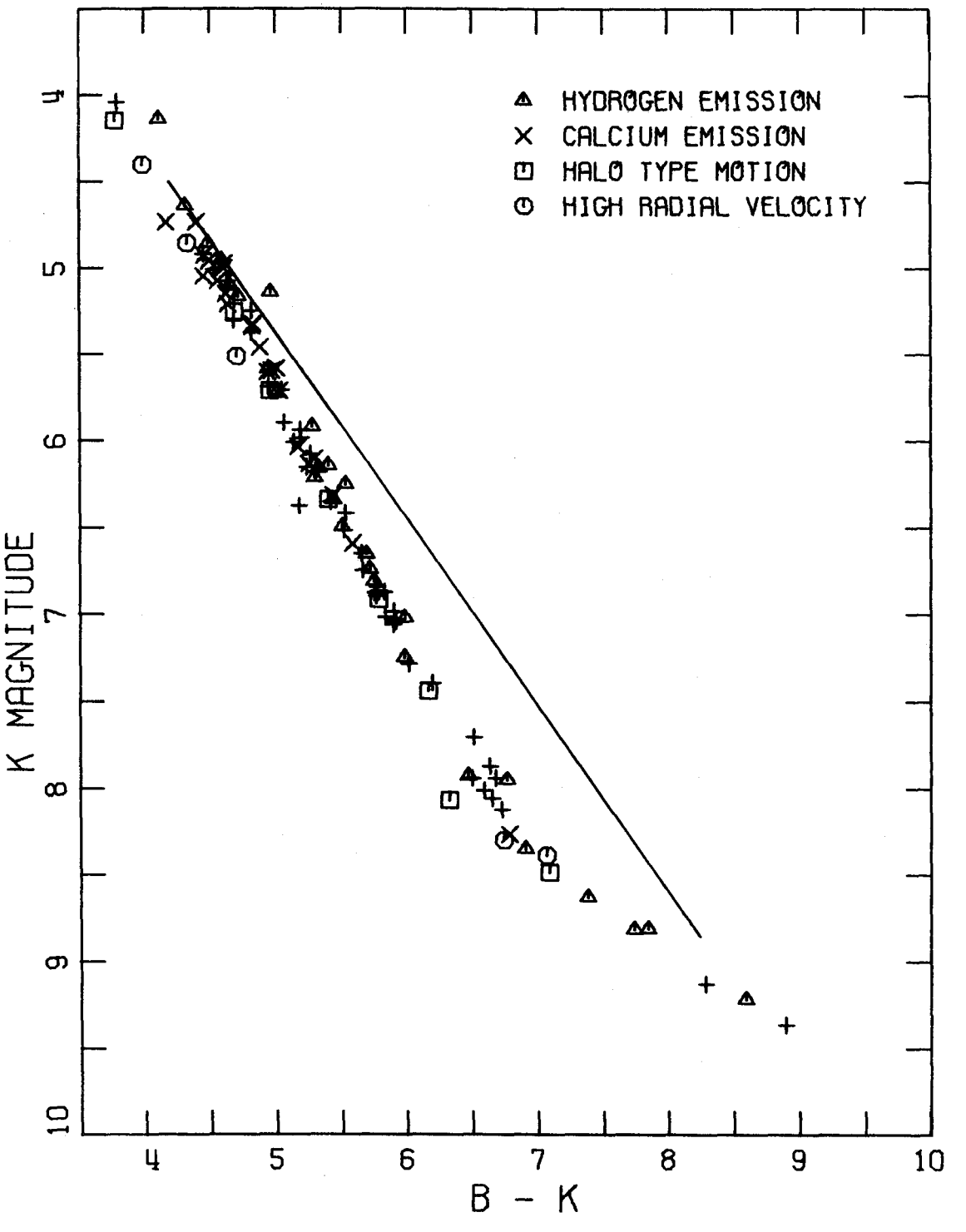

Fig.3-9b.--Absolute 2.2μ magnitude vs. (B-2.2μ) color corrected for blanketing as explained in the text for all program stars. The uncorrected main sequence is indicated.

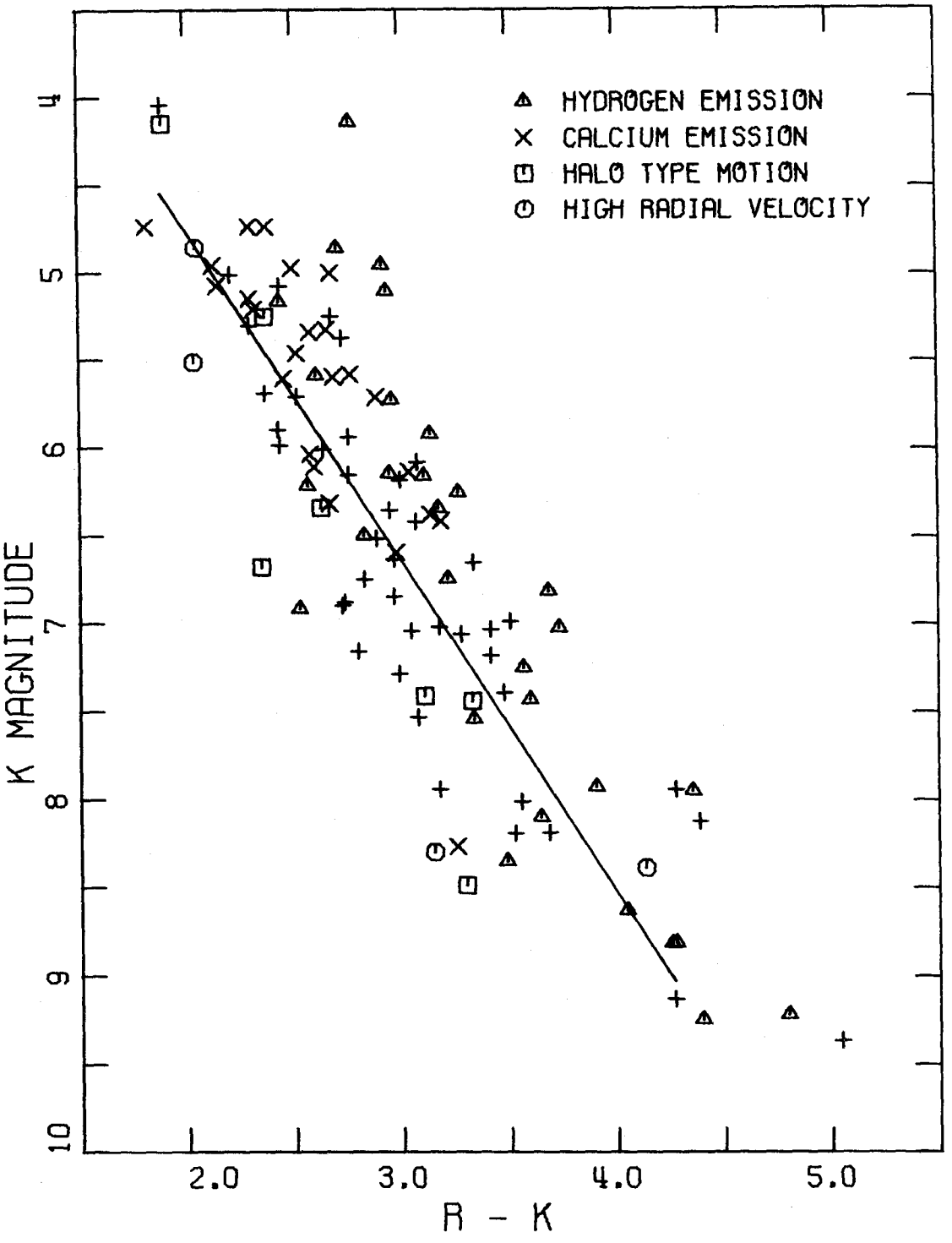

Fig.3-10a.--Absolute 2.2μ magnitude vs. (R-2.2μ) color for all program stars. The average main sequence is indicated.

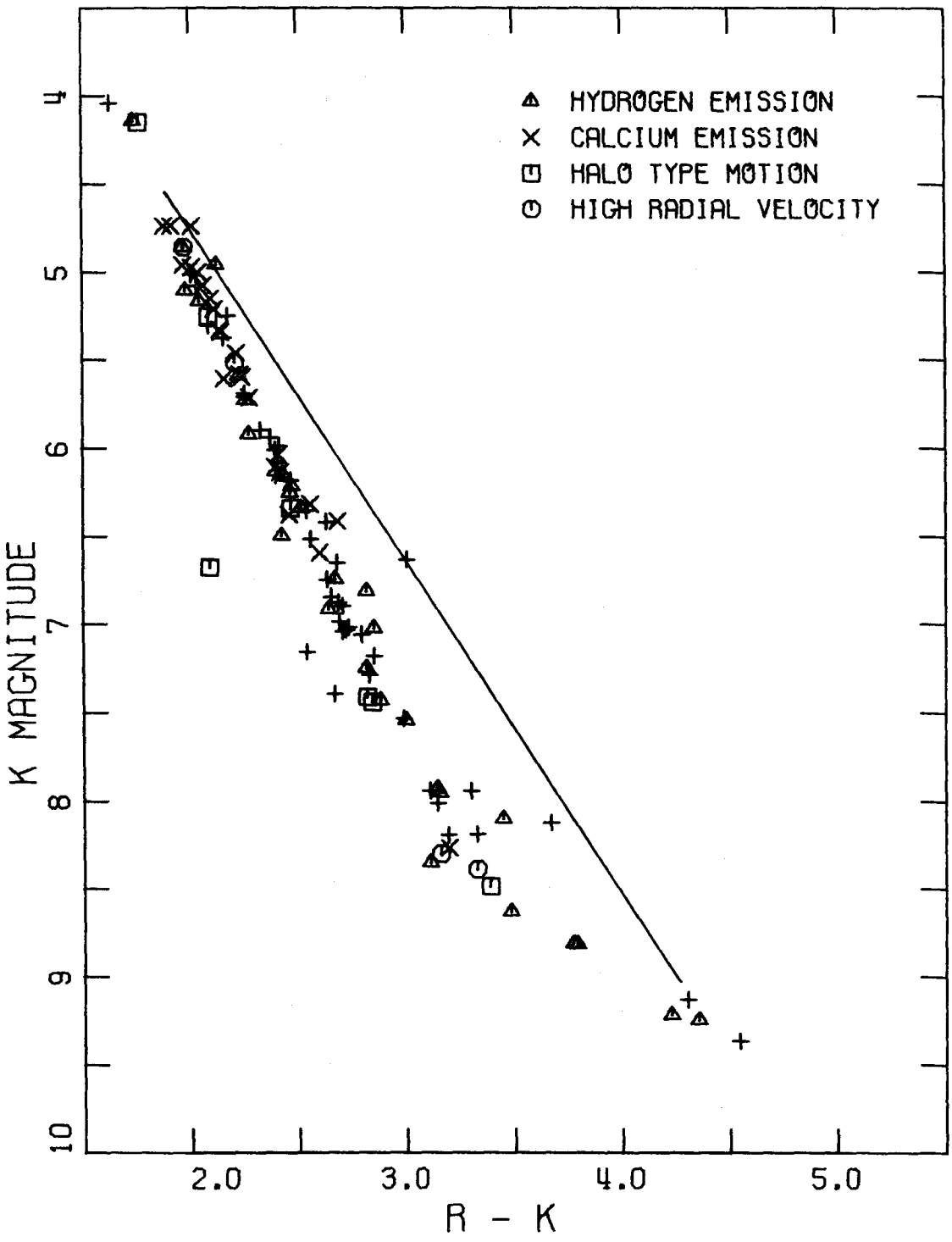

Fig.3-10b.--Absolute 2.2μ magnitude vs. (R-2.2μ) color corrected for blanketing as explained in the text for all program stars. The uncorrected average main sequence is indicated.

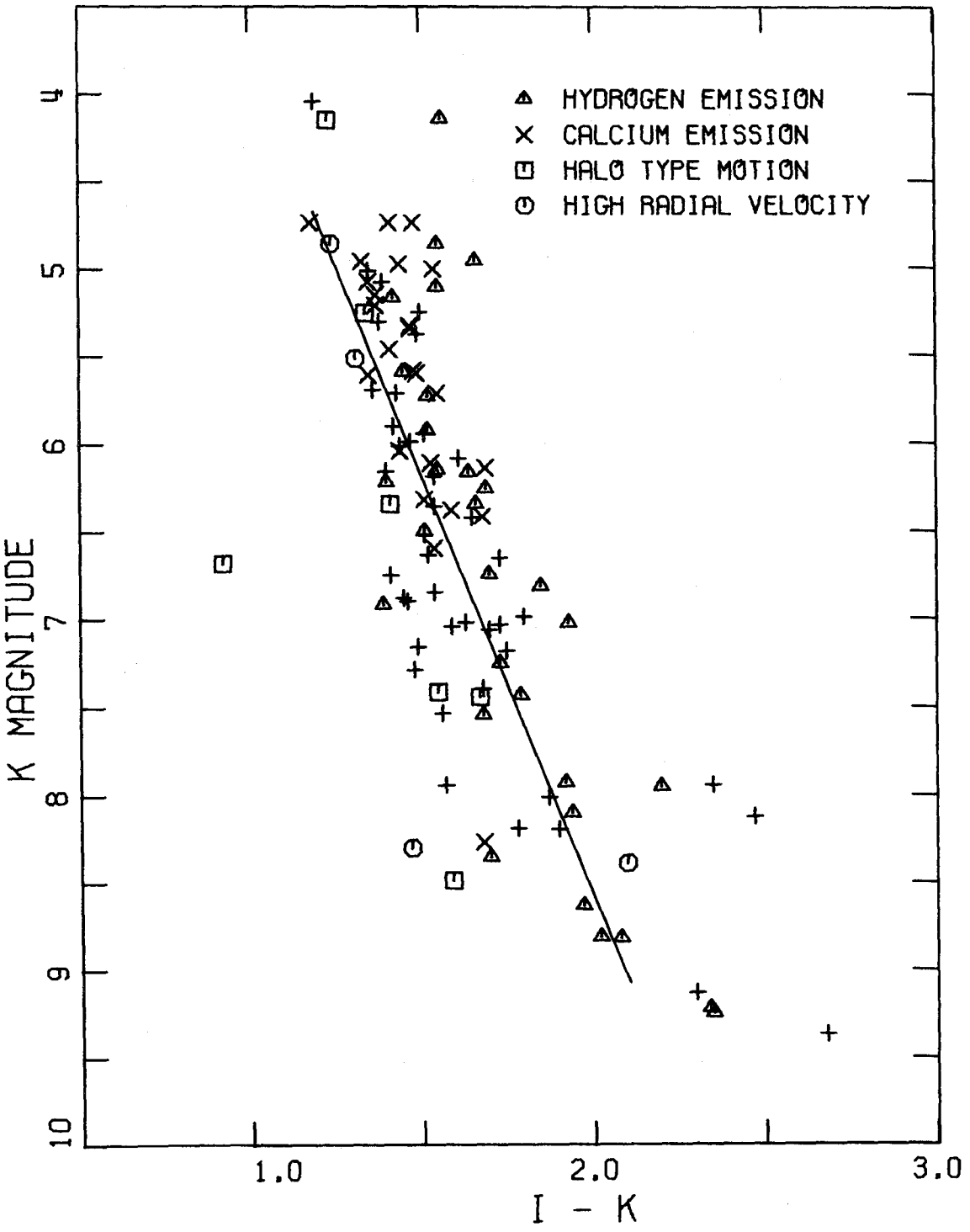

Fig.3-11a.--Absolute 2.2μ magnitude vs. (I-2.2μ) color for all program stars. The average main sequence is indicated.

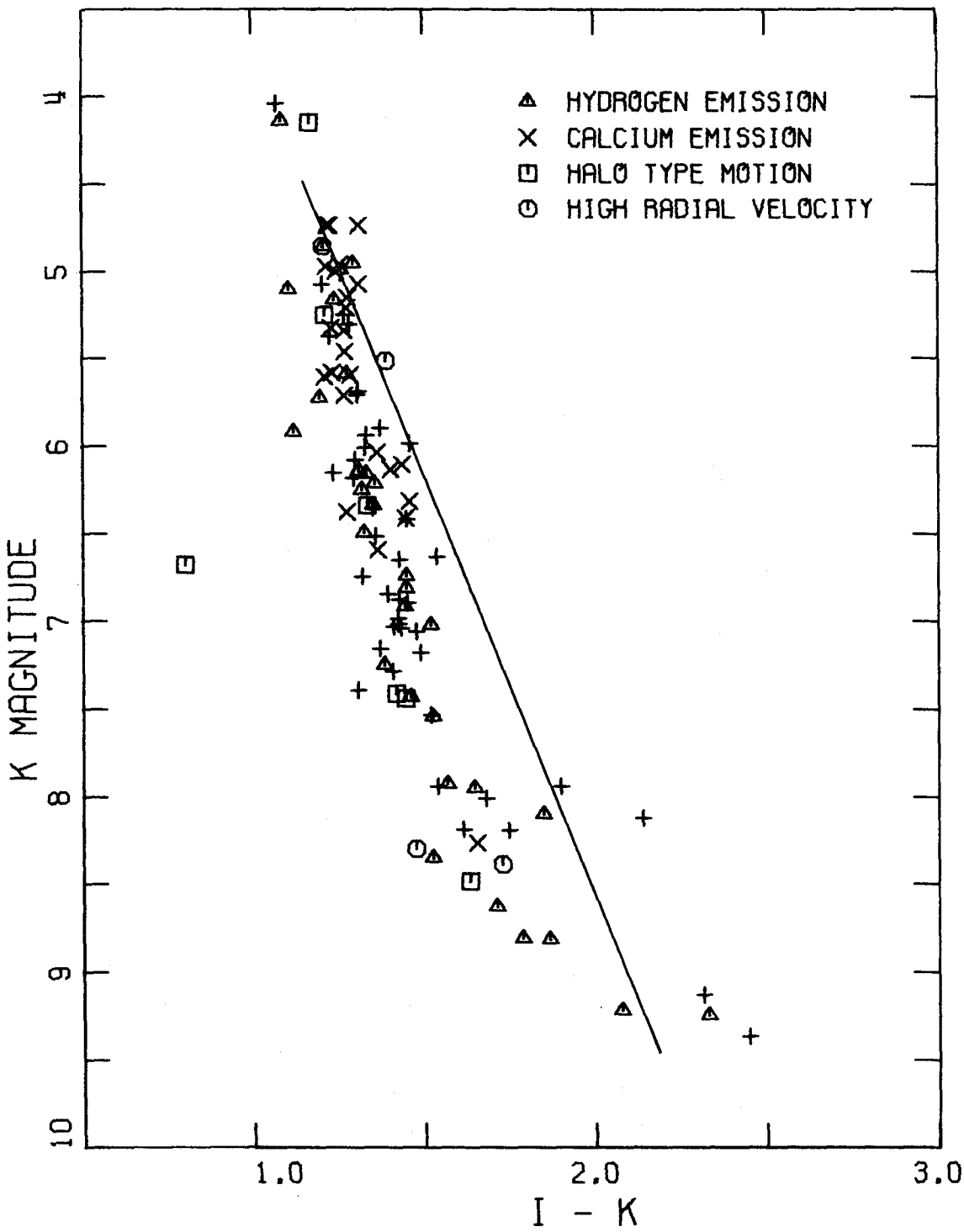

Fig.3-11b.--Absolute 2.2μ magnitude vs. (I-2.2μ) color corrected for blanketing as explained in the text for all program stars. The uncorrected average main sequence is indicated.

continuum of these stars near the peak of the spectral energy distribution. Unfortunately, the H-K color is not a very precise indicator because its dynamic range is only $\lesssim$0.4 magnitudes from spectral class M0 to M8 while the uncertainty in its measurement is $\sim\pm$0.03 magnitudes.

The procedure described above strongly implies that the broad-band blanketing in M dwarfs can be described by one parameter. This is a little surprising because the blanketing in the U and B bands is due to low-excitation metal lines while the blanketing in the V, R, and I bands is due to TiO. There is no a priori reason why the blocking due to atomic lines at short wavelengths should be closely correlated to the blocking due to molecular bands at longer wavelengths. In addition, there does not appear to be any systematic residual differences between the different kinds of M dwarfs. This would suggest that the same blanketing function applies to all M dwarfs (including flare stars as well as stars with halo type space motions). The success of reducing the scatter in all of the diagrams by this procedure argues strongly that the scatter in the original diagrams is due to scatter in blanketing rather than scatter in absolute magnitudes. An additional implication is that the "superluminosity" of the emission line stars is not directly related to the fact that they have emission lines, but rather is more directly related to the fact that they are apparently more heavily blanketed on the

average than stars without emission lines.

It is tempting to speculate on the role of convection as a possible link between the chromospheric activity of the emission line M dwarfs and the increase of the average blanketing in these stars. It is well established that chromospheres of the stars are heated by acoustical noise which is generated by convective turbulence in the photosphere and then propagates upward through the atmosphere. The line emission and flare activity of the UV Ceti type stars must be driven by the convection in these stars. It is possible that increased convective turbulence may increase the blocking by TiO and H_2O absorption bands by doppler broadening the closely spaced rotational lines. These lines are sufficiently closely spaced that velocities of a few km/sec should begin to smear them together. TiO bands extend across most of the V, R, and I filter bandpasses. An increase by a factor of $\sim$2 in the blocking would explain the dispersion in the colors across the main sequence. However, Tsuji's (1971) discussion of sources of opacity in cool stars indicates that these rotational lines may already be smeared together at temperatures $\gtrsim$ 2800°K. Thus, it is still not clear whether increased convective turbulence is responsible for both increased chromospheric activity and increased molecular blanketing.

C. Scanner Observations

Multi-channel scans for the wavelength interval from ∿4500Å to ∿10000Å were obtained by Greenstein (1973) at the 200" telescope for several of the program stars. These scans give a more detailed picture of the nature of the absorption bands of M dwarfs than is possible with broad-band photometry. Oke (1969) has described the 32 channel scanner. Scans of two of these stars obtained in September 1972 and January 1973 are plotted in figures 3-12 and 3-13 together with the data points at 1.65μ and 2.2μ which have been taken from the broad-band infrared photometry. Blackbody curves of the approximate effective temperatures of these stars have been drawn in these figures for comparison with the data. Those features which have been identified in the scans are listed in table 3-4. Column 1 is the frequency in inverse microns, column 2 is the equivalent wavelength in angstroms, and column 3 is the identification.

In the late M dwarfs G51-15 and G158-27 it is clear that a large part of the spectrum from ∿5000Å to ∿9000Å is severely blanketed by TiO bands. The nine bands listed in table 3-4 can be easily recognized in the scans, but there are probably others that contribute to the blanketing, but cannot be identified with the 80Å resolution of the 32 channel scanner. It is impossible to pick out any part of

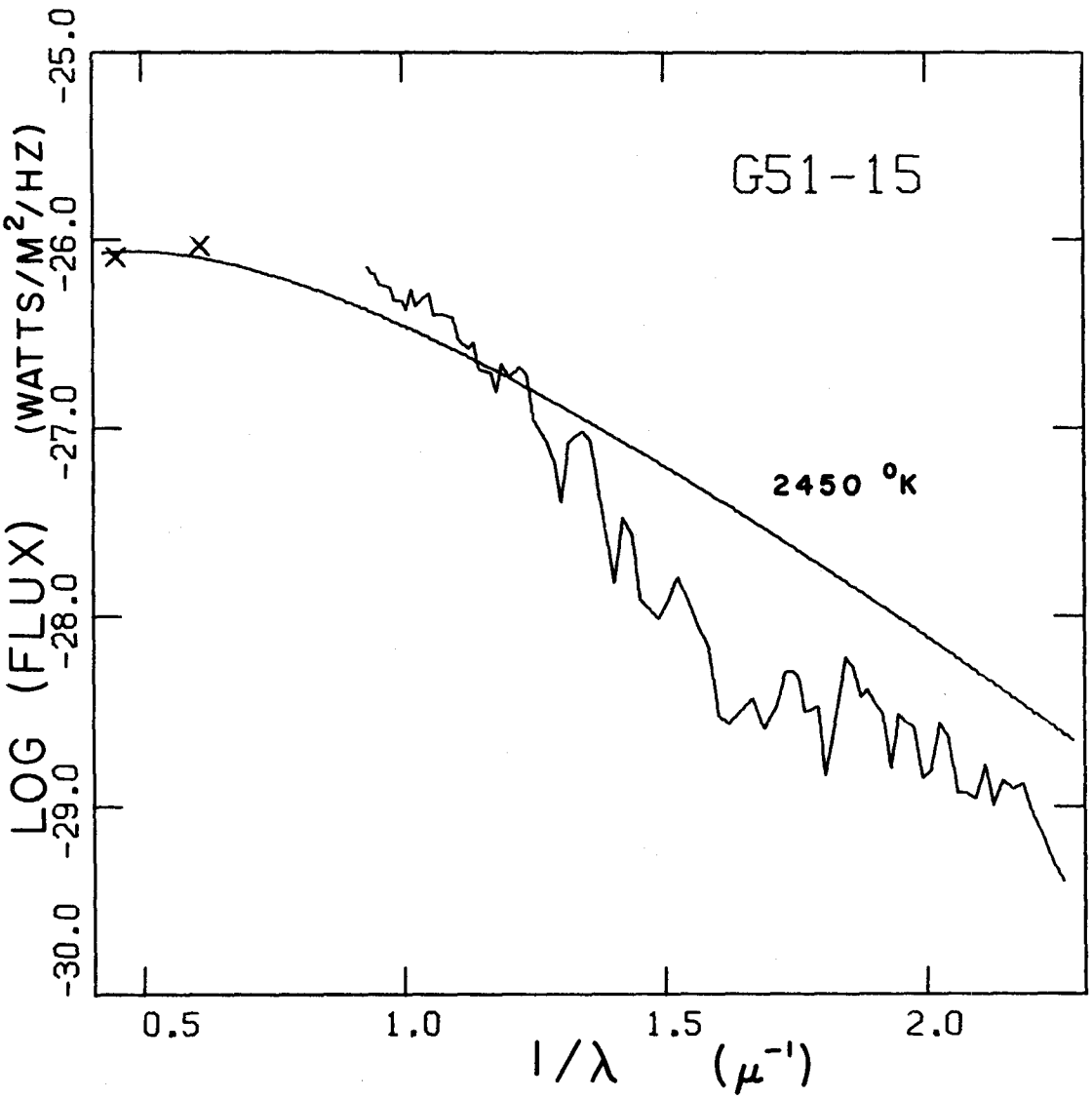

Fig.3-12.--Apparent flux vs. frequency for the late M dwarf G51-15. The frequency scale is in inverse microns. The two points are the values from broad-band photometry at 1.65μ and 2.2μ. The data curve is from a scan obtained by Greenstein (1973). A blackbody curve is indicated for comparison.

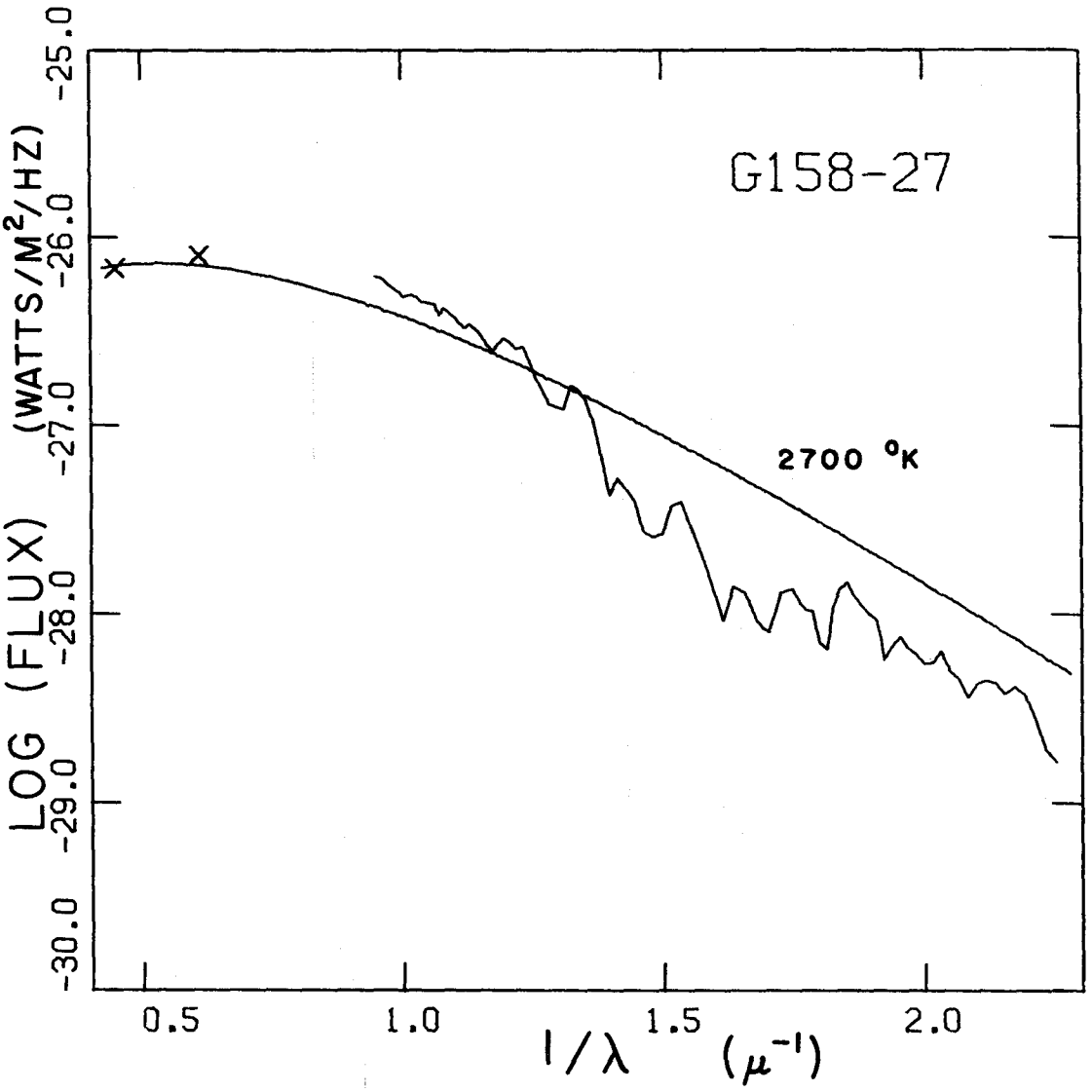

Fig.3-13.--Apparent flux vs. frequency for the late M dwarf G158-27. The frequency scale is in inverse microns. The two points are the values from broad-band photometry at 1.65μ and 2.2μ. The data curve is from a scan obtained by Greenstein (1973). A blackbody curve is indicated for comparison.

Table 3-4

Identified Features in M Dwarf Scans

μ^{-1}	A	Identification
1.06	9441	H_2O
1.13	8860	TiO
1.17	8538	VO
1.30	7672	TiO
1.41	7054	TiO
1.49	6714	TiO
1.62	6159	TiO
1.70	5896 5890	Na
1.79	5598	TiO
1.84	5448	TiO
1.93	5186 5167	MgH TiO
2.02	4955	TiO
2.06	4845	MgH
2.10	4761	TiO

this portion of the spectrum that is unaffected by the blanketing.

G51-15 and G158-27 happen to have comparable bolometric magnitudes, but the comparison of the scans for these two stars shows that on the average G51-15 has a much redder spectrum and also has much stronger TiO bands than G158-27. G51-15 is 0.4 magnitudes redder than G158-27 in R-I and 1.2 magnitudes redder in V-K. The blanketing index discussed in the previous section (3-B) is $\sim$0 for G158-27 and $\gtrsim$0.8 for G51-15. That is, the "blanketing corrections" for G51-15 are approximately : $\Delta B \sim 0.8$, $\Delta V \sim 0.8$, $\Delta R \sim 0.5$, and $\Delta I \sim 0.2$. Thus, its position corrected for blanketing is very close to the position of G158-27. These two stars represent the extremes in blanketing observed for late M dwarfs. Out of a total of seven late M dwarfs which have been scanned in this program, G51-15 shows the strongest TiO absorption bands while G158-27 shows the weakest bands. The essential point here is that not only are the bands stronger in G51-15, but also its <u>entire</u> spectrum between $\sim$5000Å and $\sim$9000Å has been depressed relative to its infrared flux. This extensive blanketing results in a lower effective temperature and redder R-I and V-K colors for G51-15. These scans thus add additional support to the conclusion drawn in the previous section that differential TiO blanketing can decrease the effective temperatures of

late M dwarfs and move them to the right in M_b vs. R-I and M_b vs. V-K diagrams and can account for the width of the lower main sequence.

D. Effective Temperatures

The effective temperatures for the stars in this program were calculated according to the procedure outlined by Greenstein et al. (1970). This essentially involves fitting a blackbody curve by eye to the broad-band magnitudes while allowing for a reasonable amount of blocking toward the short wavelengths and also keeping the total flux under the blackbody curve equal to the total flux actually observed from the star. This is a very crude procedure, but it does provide a reasonable estimate of the effective temperature without detailed calculations. Figures 3-14 and 3-15 show how three blackbody curves near the effective temperature compare with the flux measured in each band for a hot M dwarf (GL278 = YY Gem) and a cool M dwarf (GL473 = W424). Both of these stars happen to be binaries with equal components. Inspection of the curves for different temperatures allows one to estimate the best effective temperature for each star to within $\sim\pm150^{\circ}K$. The best effective temperature by this procedure for W424 is $2800^{\circ}K$, and for YY Gem is $3750^{\circ}K$. Because YY Gem happens to be an eclipsing binary, its temperature is known to be about $3740^{\circ}K$ independent of this procedure. Table 3-5 lists the residuals (in magnitudes) at each bandpass for these stars

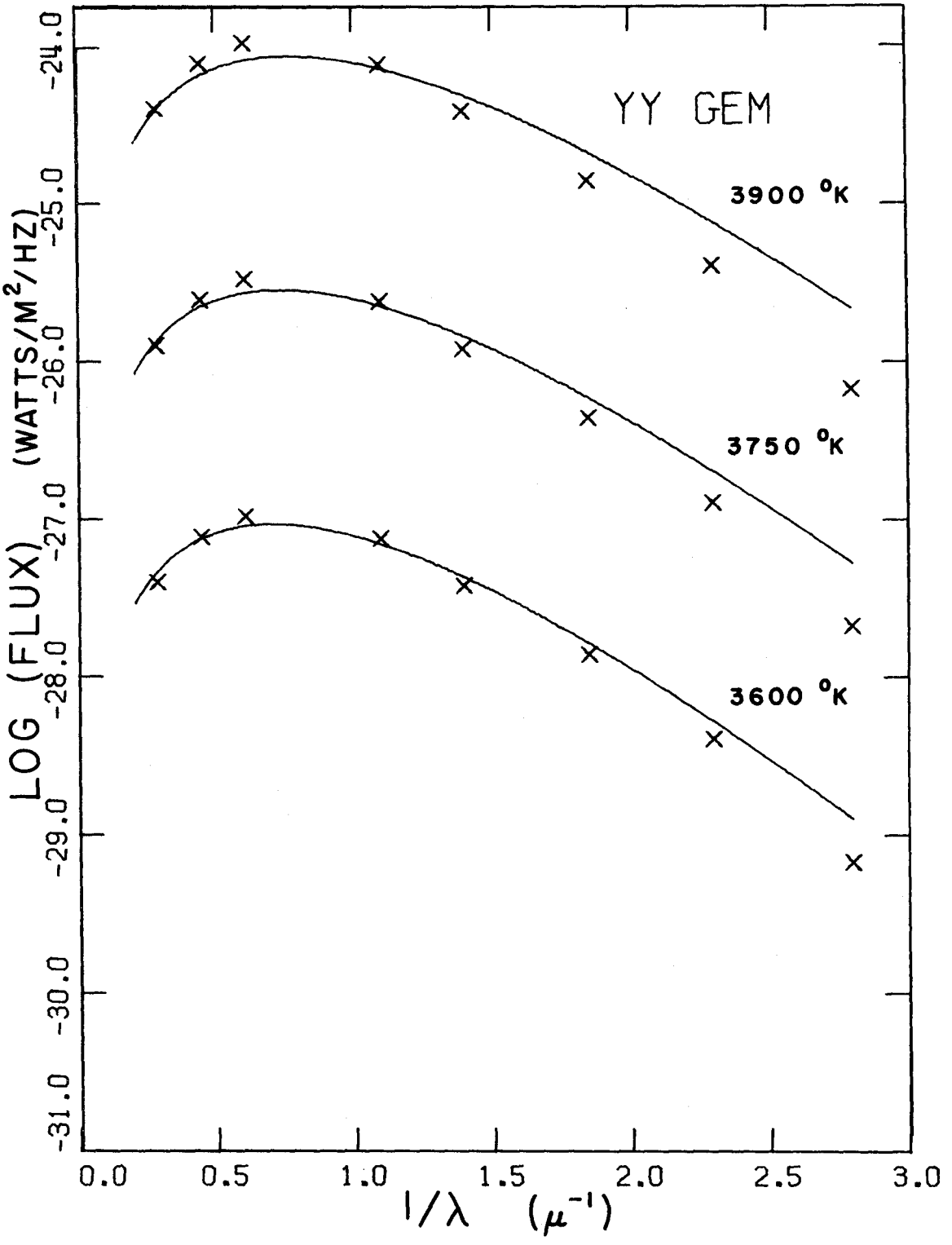

Fig.3-14.--Energy distribution in the early M dwarf YY Gem (=GL278) with three fitted blackbody curves. The frequency scale is in inverse microns. The upper and lower curves have been displaced by 1.5 in the log to avoid overlap. The best fitted T_e = 3750°K.

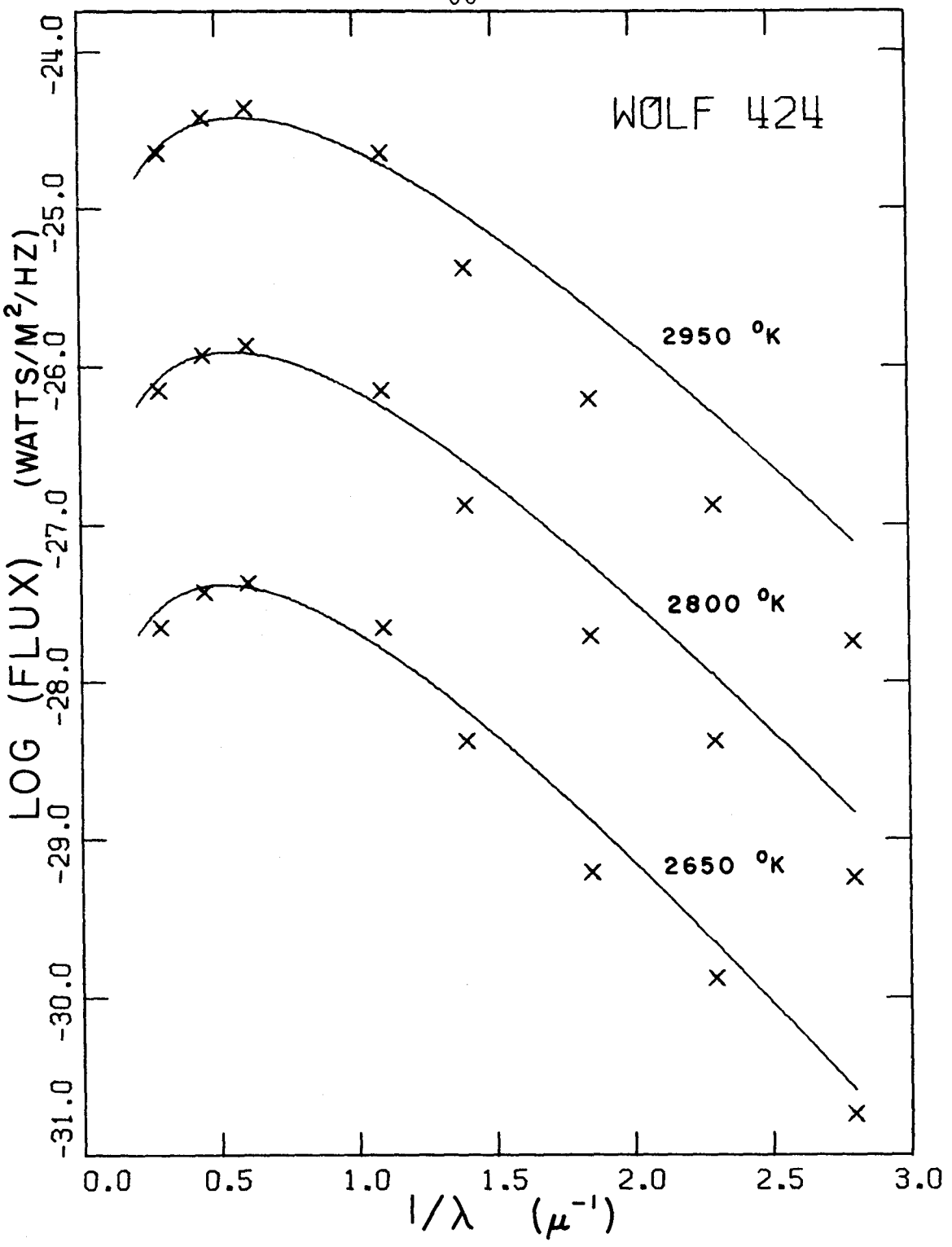

Fig.3-15.--Energy distribution in the late M dwarf W424 (=GL473) with three fitted blackbody curves. The frequency scale is in inverse microns. The upper and lower curves have been displaced by 1.5 in the log to avoid overlap. The best fitted T_e = 2800°K.

when compared to the best fit blackbody curve. The flux from each star is deficient at U, B, V, R, and L and each star has excess flux at the H and I bands. The blocking at V and R is due to TiO absorption bands and the blocking at U and B is due to blanketing by metal lines. L is probably slightly depressed by H_2O bands. As expected, the fainter star is more heavily blanketed than the brighter star. The total amount of flux energy redistributed by blanketing in these stars is comparable to the unobserved flux beyond 3.5μ, i.e. $\lesssim$15% for stars as cool as W424 ($T_e \sim 2800^oK$) to $\lesssim$5% for stars hotter than YY Gem ($T_e \sim 3740^oK$).

Table 3-5

Residuals for YY Gem and W424

	U	B	V	R	I	H	K	L
YY Gem	-1.0	- .5	- .3	-.2	+.1	+.2	+.1	-.1
W424	-1.0	-1.0	-1.1	-.7	+.2	+.1	0	-.2

The effective temperatures derived by this procedure are well correlated with both the R-I and V-K color indices. Table 3-6 lists the bolometric magnitudes, colors, and effective temperatures of some representative stars from the program. These stars are either single stars or stars that have been corrected for a faint companion. They were chosen to cover the scatter in the lower main sequence.

Table 3-6

Thirty-two Program Stars

GL	M_b	V-K	R-I	$\log(T_e)$
G158-27	12.0	6.38	1.97	3.431
15B	10.9	5.07	1.58	3.498
48	8.3	4.62	1.44	3.532
G69-47	10.8	6.30	1.93	3.431
51	10.7	5.96	1.99	3.470
65A	11.7	6.58	2.18	3.431
205	7.5	4.12	1.14	3.556
234A	10.4	5.61	1.81	3.484
239	8.4	3.73	0.97	3.562
278*	7.6	3.83	1.02	3.573
285	9.6	5.50	1.84	3.491
299	11.2	5.18	1.71	3.505
G51-15	12.4	7.61	2.37	3.389
406	12.2	7.46	2.46	3.398
473*	11.5	6.43	2.08	3.447
551	11.7	6.65	2.26	3.431
644*	8.8	4.58	1.40	3.538
661A	9.0	4.53	1.41	3.538
669A	9.0	4.91	1.52	3.518
669B	10.0	5.56	1.84	3.491
699	10.9	4.98	1.68	3.512

Table 3-6 (Continued)

GL	M_b	V-K	R-I	$\log(T_e)$
717	7.8	3.16	0.73	3.602
725A	9.3	4.42	1.42	3.538
725B	9.9	4.67	1.51	3.519
729	10.9	5.19	1.71	3.477
745A	9.4	4.27	1.29	3.544
820A	6.9	2.84	0.64	3.633
820B	7.4	3.31	0.80	3.591
829	9.0	4.96	1.55	3.518
860	9.7	4.81	1.46	3.525
866	10.9	6.65	2.16	3.439
905	11.3	6.39	2.04	3.447

* mean component

Figures 3-16 and 3-17 show V-K and R-I colors vs. log (T_e) for these stars. Both of these colors seem equally capable of being calibrated in order to give estimates of the temperature of any star whose colors are known. The following linear relations which are indicated in the figures seem to be adequate for estimating the temperature of a star from its color to within the error of estimating it by fitting a blackbody curve to all of its magnitudes, i.e. to within $\pm 150^{\circ}K$ for effective temperatures from $\sim 4500^{\circ}K$ to $\sim 2500^{\circ}K$.

$$\log T_e = -0.052(V-K) + 3.77$$

$$\log T_e = -0.13(R-I) + 3.71$$

These relations agree with the calibration of Greenstein et al. (1970) to within $\pm 100^{\circ}K$. Johnson's (1966) calibrations of the V-K and R-I color indices which are also plotted in figures 3-16 and 3-17 for comparison seem to be systematically too low by $\sim 100^{\circ}K$ in the region of interest. Johnson extrapolated beyond YY Gem by using the colors of giants with known radii. One major problem with extrapolating from this point is that this is about where TiO blanketing begins to become important. There is no reason to expect that this blanketing would have identically the same effect in the atmospheres of giants and dwarfs.

Figure 3-18 is a plot of M_b vs. log (T_e) for the stars from table 3-6. Johnson's (1965) calibration curve and the

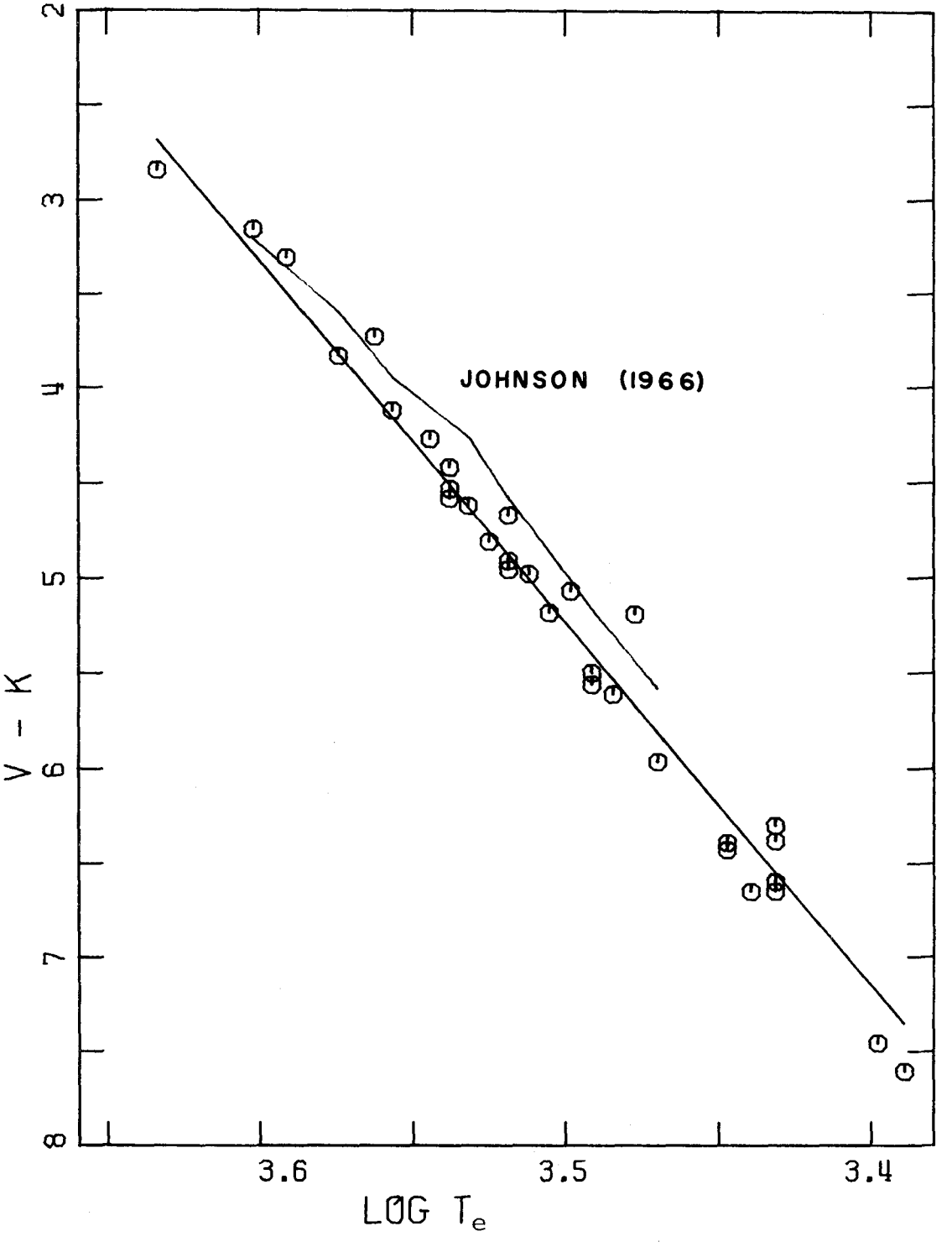

Fig.3-16.--(V-2.2μ) color vs. the fitted temperature for the stars from table 3-6. The mean relation indicated is $\log(T_e) = -0.052(V-K) + 3.77$. Johnson's (1966) calibration of his average main sequence is shown for comparison.

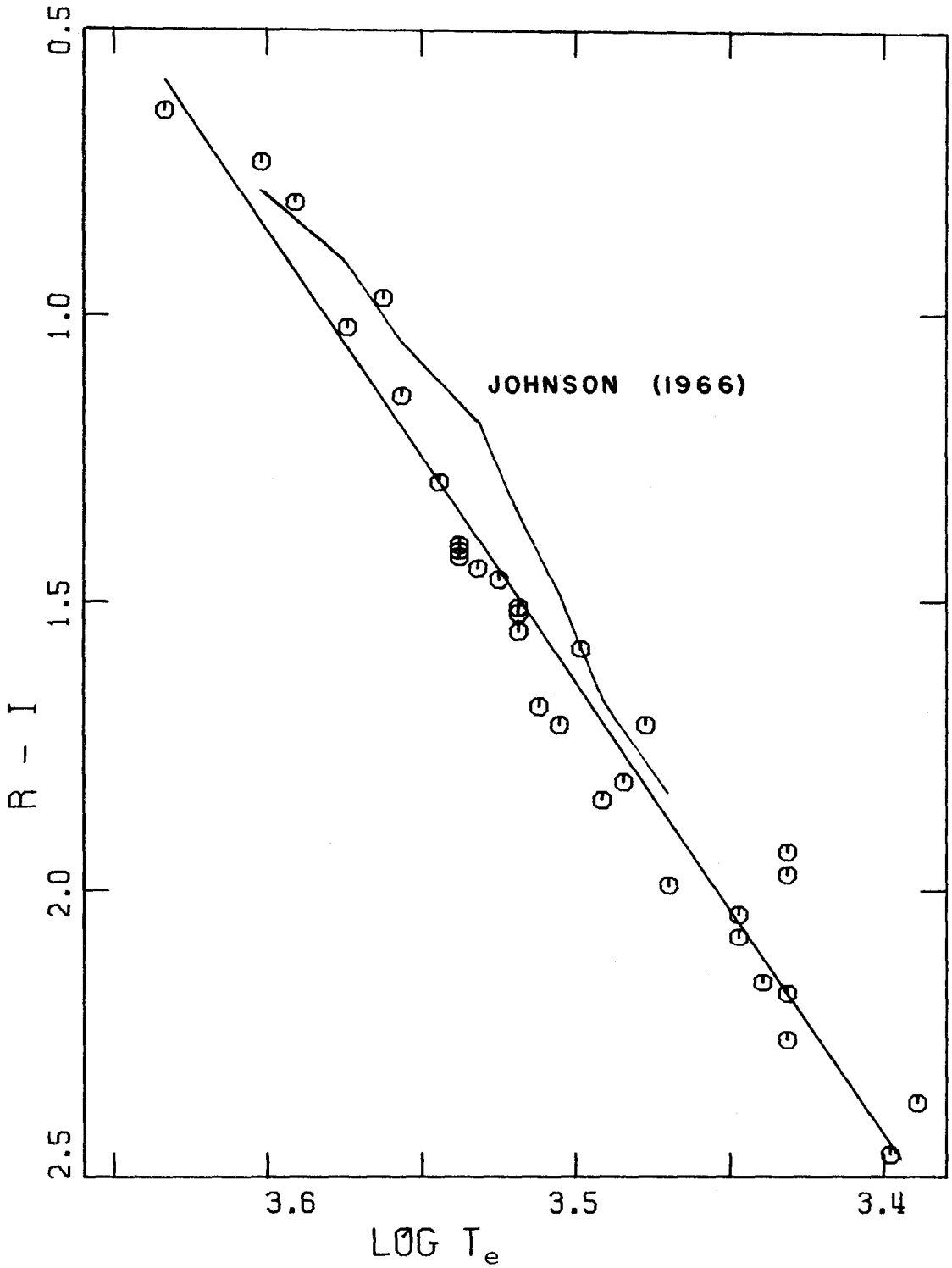

Fig.3-17.--R-I color vs. the fitted temperature for the stars from table 3-6. The mean relation indicated is $\text{Log}(T_e) = -0.13(R-I) + 3.71$. Johnson's (1966) calibration of his average main sequence is shown for comparison.

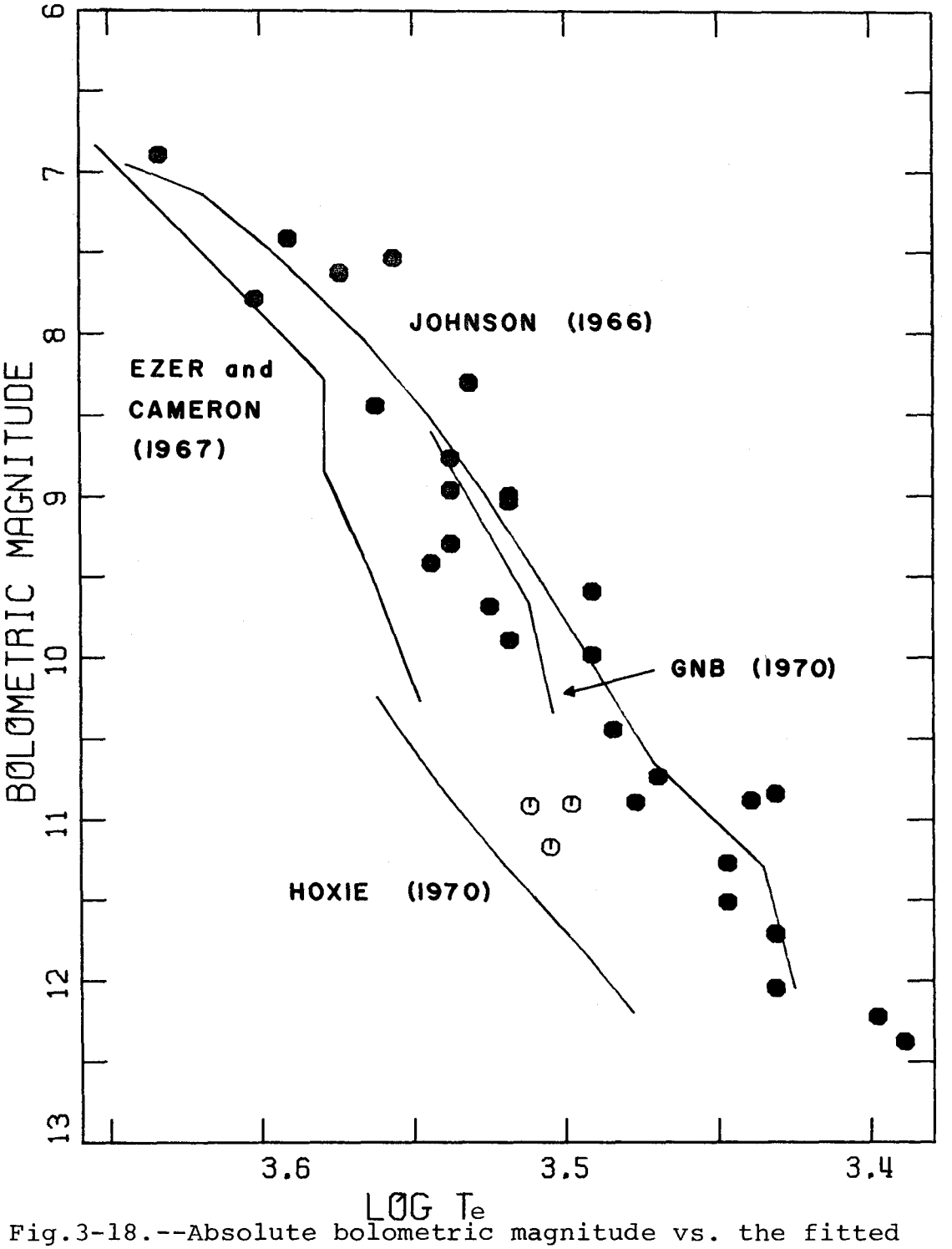

Fig.3-18.--Absolute bolometric magnitude vs. the fitted temperature for the stars from table 3-6. Theoretical curves from Ezer and Cameron (1967) and Hoxie (1970) and the average main sequences from Johnson (1966) and Greenstein et al. (1970) are shown for comparison. The open circles represent GL15B, GL299, and GL699 which may be subluminous.

calibration of Greenstein et al. (1970) are plotted for comparison. The subluminous stars GL15B, GL299, and GL699 (= Barnard's star) are plotted as open circles. The theoretical curves of Ezer and Cameron (1967) and Hoxie (1970) are also indicated. Johnson's calibration of $\log(T_e)$ with respect to M_b seems to be somewhat better than his calibration with respect to his color indices. His average sequence seems to lie within the scatter of the data. The calibration of Greenstein et al. seems to be almost equivalent to that of Johnson for $8.6 < M_b < 9.6$, but then falls off too rapidly at $M_b = 10.35$. This is probably because they average only four stars in their last group, one of which is the subluminous star GL15B (= Gr-34B = Yale 49B). The abrupt change in slope at the end of Johnson's curve suggests that his calibration is also affected by the small number of stars he had available to calibrate the faint end of the main sequence. Again, there is a large, real scatter in the lower main sequence and it is not clear that it is a meaningful exercise to average small groups of stars to obtain an "average sequence."

The theoretical models of Ezer and Cameron (1967) and Hoxie (1970) have effective temperatures which are systematically too high for their luminosities. Cool M dwarfs have deep convection zones which extend all the way to the center for $M/M_\odot < 0.3$. Models for these stars are somewhat sensitive to the stellar atmosphere calculations which are

used to establish the outer boundary conditions to which models of the interiors are fitted. These atmosphere calculations are dependent on the effects of atmospheric convection and also the complicated temperature dependence of the opacities of molecular bands such as TiO and H_2O as well as sources of continuous opacity such as H^- and H_2^-. Ezer and Cameron used very crude models for their atmospheres which included no molecular bands. Hoxie included convection and H_2O but not TiO. Tsuji (1971) emphasizes that TiO is more important than H_2O in these models, but he does not include convection in his atmosphere calculations. The TiO bands blanket the portion of the spectral energy curve just shortward of its maximum. This means that the strengths of the bands can influence the location of the maximum.

The scanner observations of G51-15 and G158-27 discussed in section 3-C show that TiO blanketing can decrease the apparent effective temperature of a late M dwarf by up to at least $250^{\circ}K$. Of course, G158-27 is already somewhat blanketed. Inclusion of TiO opacity would eliminate most of the discrepancy between the theoretical curves and the observations evident in figure 3-18.

E. Mass-Luminosity Relation for Faint Dwarfs

The mass-luminosity diagram for those late dwarfs with well determined masses is plotted in figure 3-19. The data for these stars are listed in table 3-7. Columns 1-7 are self-explanatory. The references for the adopted values of the masses are given in column 8. The components of the systems L726-8, $+45^{\circ}2505$, 70 Oph, and Kruger-60 were de-convolved in the same way as the other binaries with visible companions (see the Appendix). The mean components of the systems YY Gem, W424, and W630 were taken to be one-half of the measured flux. The bolometric magnitudes adopted for the stars in the systems which have been de-convolved are probably at best only accurate to ± 0.2 magnitudes (plus an additional amount due to uncertainty in the parallaxes). It is not clear how accurate the values for the masses are. The total mass of the system L726-8 was recently revised from $0.08M_{\odot}$ to $0.3M_{\odot}$ according to van de Kamp (1971) who quotes a private communication from Luyten. Worley and Behall (1973) have published a detailed orbit of this system and estimate the masses of the components to be $0.12M_{\odot}$ and $0.10M_{\odot}$. The parallax of $0.379''$ adopted here for this system is slightly smaller than the one they used. This change increases the value of the total mass of the system to $0.23M_{\odot}$.

The line drawn through the data points in figure 3-19

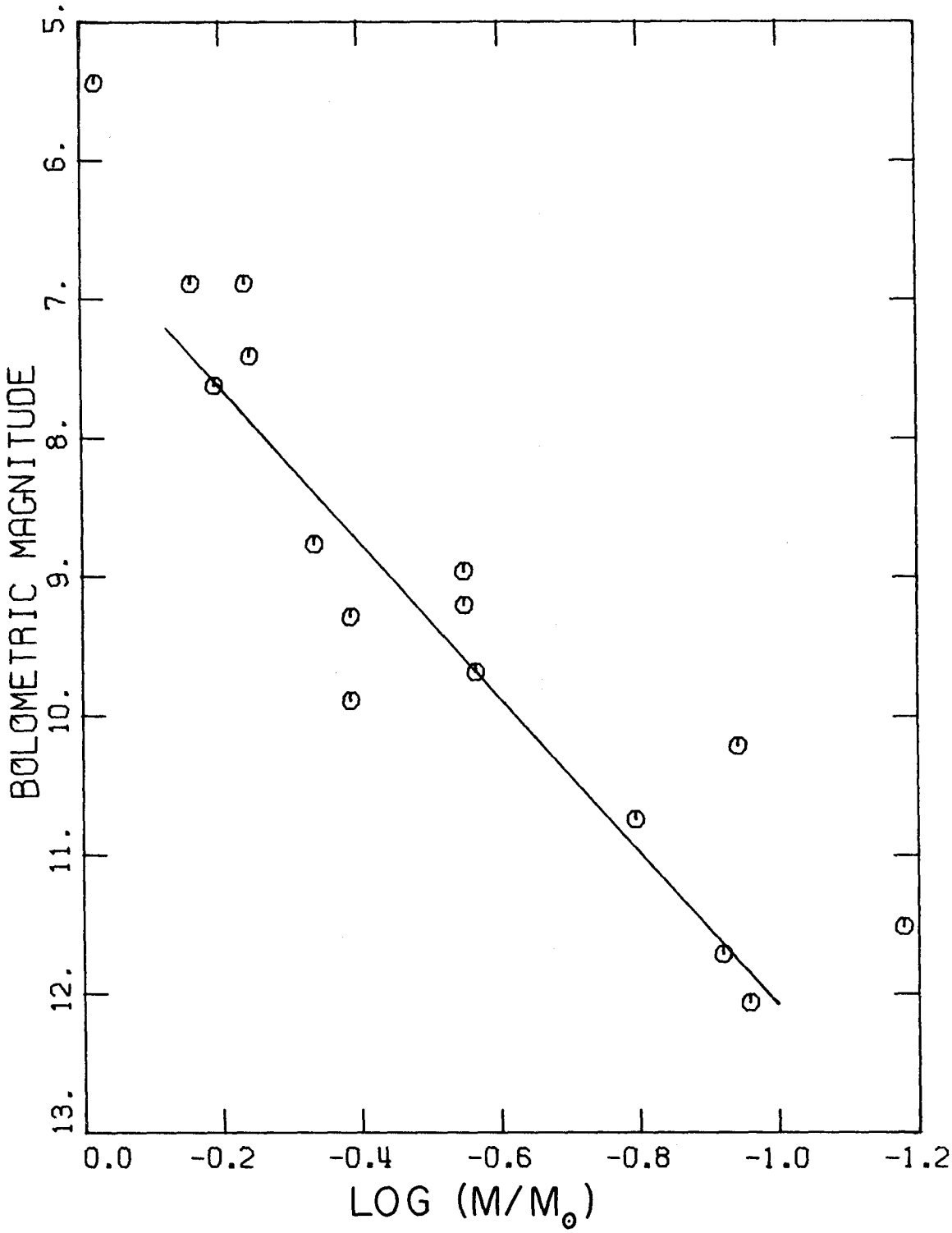

Fig.3-19.--Absolute bolometric magnitude vs. mass for the binary program stars from table 3-7. The mean components of YY Gem (=GL278) and W424(=GL473) were taken to be one-half of the observed flux. The mean relation indicated is $M_b = -5.6 \log(M/M_\odot) + 6.5$.

Table 3-7

Binary Stars with Known Masses

GL	Name	$M/M_\odot$	$\log(M/M_\odot)$	$R/R_\odot$	$\log(T_e)$	M_b	Reference
65A	L726-8	.12	-.921	.19	3.431	11.7	Worley and Behall (1973)
65B	UV Ceti	.11	-.959	.17	3.423	12.1	" " " "
234A	R614A	.11	-.943	.28	3.484	10.4	Lippincott and Hershey (1972)
278*	YY Gem	.64	-.194	.62	3.573	7.6	Harris et al. (1963)
473*	W424	.07	-1.174	.18	3.447	11.5	Heintz (1972)
644*	W630	.46	-.337	.43	3.538	8.8	Harris et al. (1963)
661A	+45°2505	.28	-.552	.39	3.538	9.0	" " " "
661B	"	.28	-.552	.36	3.532	9.2	" " " "
702A	70 Oph	.95	-.022	.83	3.728	5.4	van de Kamp (1971)
702B	" "	.69	-.161	.57	3.663	6.9	" " " "
725A	Σ2398	.41	-.387	.34	3.538	9.3	" " " "
725B	"	.41	-.387	.28	3.519	9.9	" " " "
820A	61 Cyg	.58	-.236	.65	3.633	6.9	" " " "

Table 3-7 (Continued)

GL	Name	$M/M_\odot$	$\log(M/M_\odot)$	$R/R_\odot$	$\log(T_e)$	M_b	Reference
820B	61 Cyg	.57	-.244	.62	3.591	7.4	van de Kamp (1971)
860A	Kruger-60	.27	-.568	.30	3.525	9.7	" " " "
860B	"	.16	-.796	.21	3.498	10.7	" " " "

* mean component

represents the empirical mean relation:

$$M_b = (-5.6 \pm 0.5) \cdot \log(M/M_\odot) + (6.5 \pm 0.3) \qquad (3\text{-}4)$$

which was derived from least-squares fit to the data omitting the systems 70 Oph, R614, and W424. The estimates of the probable errors in the coefficients of equation (3-4) are largely the result of the uncertainty in the value of the mass of the system L726-8. (Note that half the systems listed in table 3-7 have hydrogen emission lines and may be expected to be 0.2 to 0.3 magnitudes brighter than comparable stars without emission lines.) Equation (3-4) directly implies:

$$L/L_\odot \propto (M/M_\odot)^{2.2 \pm 0.2}$$

The system 70 Oph was omitted because it lies on the mass-luminosity relation for brighter stars where:

$$L/L_\odot \propto (M/M_\odot)^{3.5}$$

which Harris et al. (1963) state holds for M_b brighter than 7.5 magnitudes. R614 and W424 were omitted because they clearly lie above the trend of the other stars. In addition, the masses of R614B, W424A, and W424B are less than the published estimates of the lower mass limit of the hydrogen main sequence. This limit is $\sim 0.1\ M_\odot$. (see Kumar (1963) and Hoxie (1970)) These systems may still be

evolving downward in figure 3-19 and may never settle on the hydrogen burning sequence. The bolometric correction for R614B is very uncertain. I have estimated its bolometric magnitude to be $\sim$12 which results in a correction of 0.2 to the magnitude of R614A and yields its adopted value of $M_b = 10.4$. It is not clear why R614A is still above the average trend. Either its mass is seriously in error or it, too, must still be evolving downward. (Another possibility is that it might be a close binary.)

Hoxie (1970) calculates that a star of $0.1M_\odot$ should have a bolometric magnitude of $\sim$12.2. This means that stars such as W359, G158-27, and G51-15 are very close to the lower mass limit of the main sequence. They could be less massive than 0.1 $M_\odot$ and be evolving downward past the end of the main sequence and cooling toward a "black dwarf" configuration. But W359 and G158-27 in particular have old disk space motions which implies that they are relatively old objects and therefore must be massive enough to have ignited hydrogen and to have stabilized on the main sequence.

Greenstein et al. (1970) derive a bolometric magnitude of $\sim$13.1 for VB 10 which would imply that it has a mass of only $\sim$0.07 $M_\odot$ according to equation (3-4). This object also has an old disk type space motion which again implies that it is a relatively old object which has stabilized very near the end of the main sequence.

The theoretical mass-luminosity curves from Ezer and Cameron (1967) and Hoxie (1970) are plotted in figure 3-20 together with the stars from table 3-7. The slope of the theoretical curve changes at $M_b \sim 7.5$. Copeland et al. (1970) state that this break in the slope of the mass-luminosity relation may be due to the importance of H_2^- as a source of opacity in cooler stars with $M_b > 7.5$ magnitudes. This is also approximately where absorption bands of TiO begin to become important. The theoretical curves and the linear empirical relation (3-4) agree to within 0.4 magnitudes in the interval:

$$7.5 < M_b < 12.0$$

The effective temperatures in column 7 of table 3-7 were estimated by fitting blackbody curves through the data points for each star as described in the previous section (3-D). The radii given in column 4 were calculated directly from the observed luminosity and the assigned effective temperature. The resulting values of the radii are plotted against the values of the masses in figure 3-21. Theoretical curves from Ezer and Cameron (1967) and Hoxie (1970) are also plotted for comparison with the data. Hoxie has published diagrams similar to figures 3-20 and 3-21 for a slightly different set of stars. He assigned an effective temperature to his stars from Johnson's (1965, 1966) calibration of spectral types. The values adopted here, which

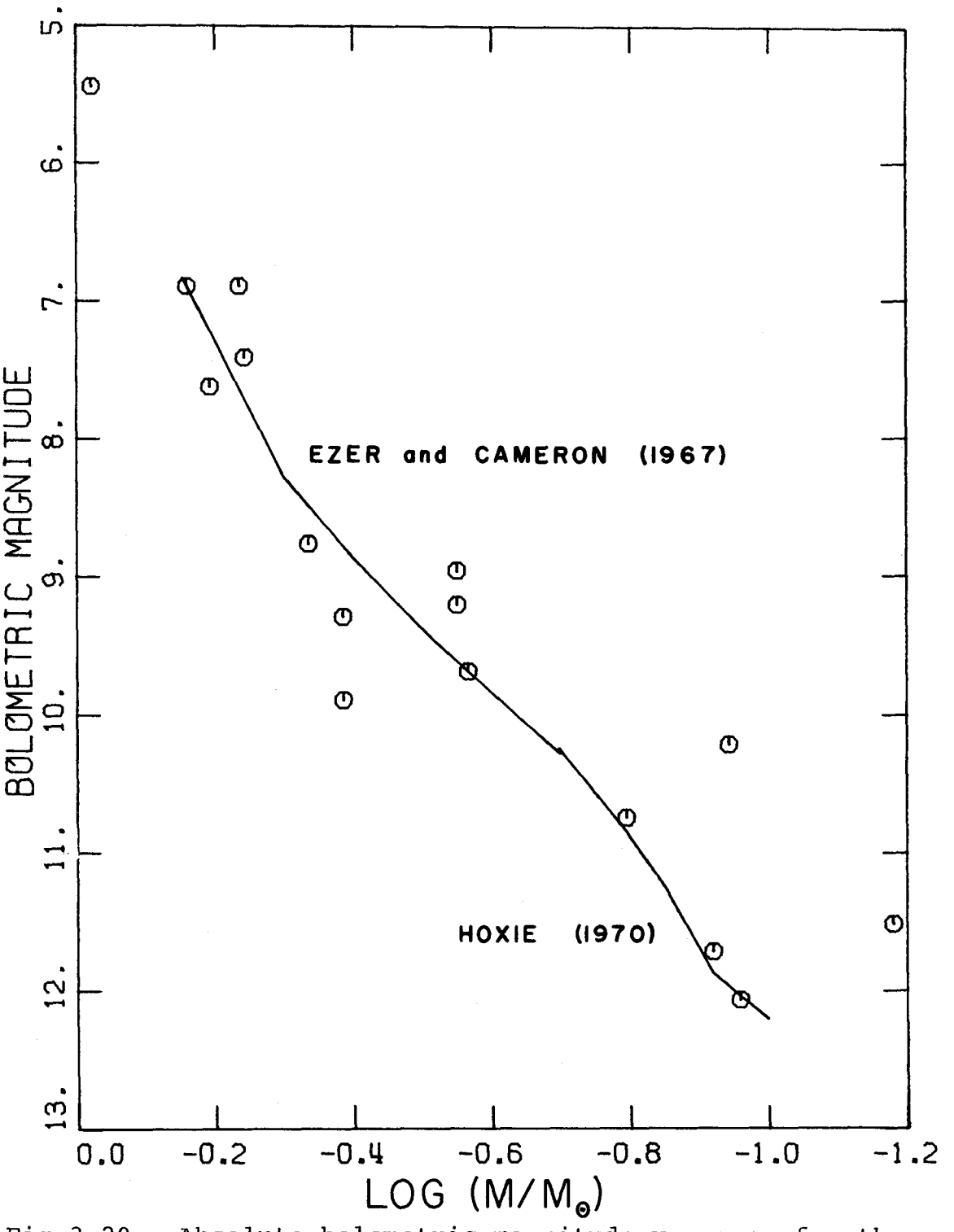

Fig.3-20.--Absolute bolometric magnitude vs. mass for the binary program stars from table 3-7. The mean components of YY Gem (=GL278) and W424 (=GL473) were taken to be one-half of the observed flux. Theoretical curves from Ezer and Cameron (1967) and Hoxie (1970) are indicated for comparison.

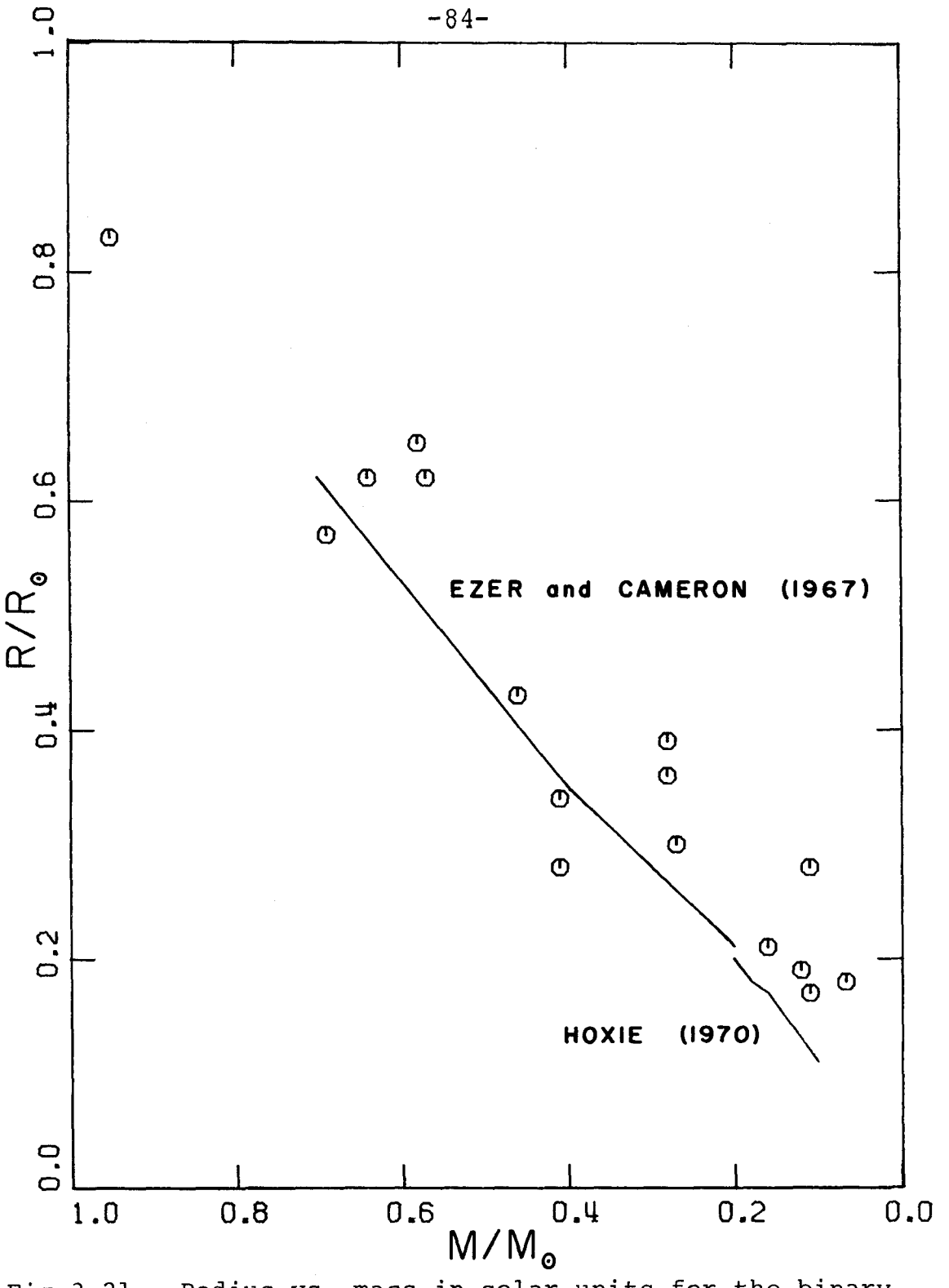

Fig.3-21.--Radius vs. mass in solar units for the binary program stars from table 3-7. The mean components for YY Gem (=GL278) and W424 (=GL473) are indicated. Theoretical curves from Ezer and Cameron (1967) and Hoxie (1970) are indicated for comparison.

are derived directly from photometric measurements, greatly reduce the systematic displacement of the stars from the theoretical curves mentioned by Hoxie. There still remains a tendency for the models to have radii which are too small for their masses. That is, the models seem to be systematically too hot (see also figure 3-18). Again, this systematic displacement of the theoretical curves is probably due to the difficulty of dealing with the effects of convection and molecular (TiO and H_2O) opacity in the outer layers of cool stars. The data stars still scatter badly, but the scatter will probably be further reduced by better values for their masses and more accurate photometry.

F. The Luminosity Function for Faint Dwarfs

It has been suggested recently that the numbers of stars at the faint end of the luminosity function, as given by van Rhijn (1936), should be increased by a substantial amount. Luyten (1968) calculated a luminosity function based on faint stars with large proper motions. He found a maximum in the number of faint stars at $M_{pg} = 15.7$ and derived a stellar mass density of:

$$\rho = 0.064\ M_{\odot} pc^{-3}$$

Sanduleak (1964), Pesch (1972), and Weistrop (1972), however, find many more faint stars which are presumably stars with small proper motions ignored by Luyten. Sanduleak

carried out an objective prism survey in a selected region for M dwarfs with $m_v < 17$. He found $\sim$1200 in 120 square degrees and Murray and Sanduleak (1972) conclude that these represent $\sim 0.23\ pc^{-3}$ which implies a contribution to the local mass density of:

$$\rho = 0.05\ M_\odot pc^{-3}$$

from stars with $M_v < 13$.

Weistrop took star counts in an area of 6 square degrees as a function of color and m_v for $12 < m_v < 18$. She found that the dwarfs redder than B-V = 1.4 are concentrated strongly toward the plane. By extrapolating her results from $M_v \leq 13$ to $M_v = 15$ she derived a stellar (i.e. red dwarf) mass density of :

$$\rho = 0.13\ M_\odot pc^{-3}$$

plus an additional estimate of $0.03\ M_\odot pc^{-3}$ due to white dwarfs and interstellar matter. In order to convert her number density into a mass density, Weistrop made use of a mass-luminosity relation given by Schmidt (1959). This relation is now much better known toward the faint end.

Table 3-8 lists the absolute visual magnitude, the corresponding absolute bolometric magnitude, the number density for each magnitude interval taken from Weistrop (1972), the mass calculated according to the relation

Table 3-8

The Luminosity Function

M_V	M_b	pc^{-3}	$M/M_\odot$	ρ
≤ 9	--	--	--	.018
10	8.3	.01	.47	.005
11	9.0	.03	.36	.010
12	9.6	.06	.30	.018
13	10.6	.13	.23	.030
14	10.9	.25*	.18	.045*
15	11.5	.40*	.14	.056*

* estimated

discussed in the previous section (3-E equation (3-4)), and the resulting contributions to the mass density in solar masses per cubic parsec. The total stellar mass density is increased to 0.18 $M_{\odot}pc^{-3}$ which implies a total mass density of:

$$\rho_{total} \sim 0.21\ M_{\odot}pc^{-3}$$

in the solar neighborhood. This is as large as the mass density required by Oort's (1965) dynamical analysis of stellar motions perpendicular to the galactic plane if the mass is concentrated in a narrow layer. Apparently, all the "missing mass" in the plane can be accounted for by faint M dwarfs. As Weistrop notes, there are some stars known with $M_V > 15$ and they may even be common enough to contribute further to the mass density.

In addition, a significant fraction of the stars counted by Weistrop may be expected to be binaries which would also tend to increase the total mass density. Approximately one-third of the M dwarfs that have hydrogen emission lines listed by Woolley et al. (1970) are known to be close doubles. (see also Worley (1969))

G. Old Disk Flare Stars

It has been suggested in the literature that some flare stars belong to the old disk population. Gershberg and Shakhovskaya (1971) and Lee and Hoxie (1972) among

others have suggested that Gr-34AB, SZ UMa, and W630 are old disk flare stars. These stars do have space motions that belong to the old disk population as defined by Eggen (1969)(see the Appendix). That is, in general the eccentricity of their galactic orbits is larger than is typical of earlier main sequence stars. Some of the other flare stars in the program also have old disk space motions. WX UMa, $+55^{o}$ 1823, W1130, and C1250 are definitely in this category. W359, VW Com, and BY Dra are borderline cases, but so is Gr-34 on the basis of its space motion alone. Greenstein et al. (1970) discuss the flare star VB 10. They list values of M_b = 13.1 and V-K = 8.7 magnitudes for it. Its space motion is also of the old disk population.

All of these stars which are in the program have been listed in table 3-9 with their bolometric magnitudes and V-K colors. In figure 3-22 these bolometric magnitudes are plotted against V-K for these flare stars together with the thirteen program flare stars that definitely have young disk space motions. (Three others have unknown radial velocities and an additional three flare stars are the fainter members of binary systems unresolved by the IR photometry.) Data for the young disk flare stars are listed in table 3-10. The line drawn in figure 3-22 indicates the average main sequence for low velocity stars which have no emission lines. There does not appear to be any

Table 3-9

Old Disk Flare Stars

GL	Type	Name	M_b	V-K
15A	M1	Gr-34	8.8	4.05
15B	M6	"	10.9	5.07
406	M8E	W359	12.2	7.46
412B	M8E	WX UMa	12.2	6.70
424	M1	SZ UMa	8.4	3.80
516	M4E	VW Com	9.1	4.60
616.2	M1E	+55°1823	6.7	4.23
644*	M4.5E	W630	8.8	4.58
719	M0E	BY Dra	6.2	3.43
781	M3E	W1130	9.4	4.04
815	M3E	CC1250	8.1	4.05

* mean component

Table 3-10

Young Disk Flare Stars

GL	Type	Name	M_b	V-K
65A	M5.5E	L726-8	11.7	6.58
278*	M0.5E	YY Gem	7.6	3.83
285	M4.5E	YZ CaMi	9.6	5.50
388	M4.5E	AD Leo	8.8	4.82
447	M5	R128	10.8	5.47
473*	M5.5E	W424	11.5	6.43
494	M2E	W462	7.4	4.19
551	M5E	Proxima	11.7	6.65
669B	M5E	R867	10.0	5.56
729	M4.5E	R154	10.9	5.19
735	M2E	--	7.8	4.60
867B	M4E	--	9.3	4.98
873	M4.5E	EV Lac	9.4	4.76

* mean component

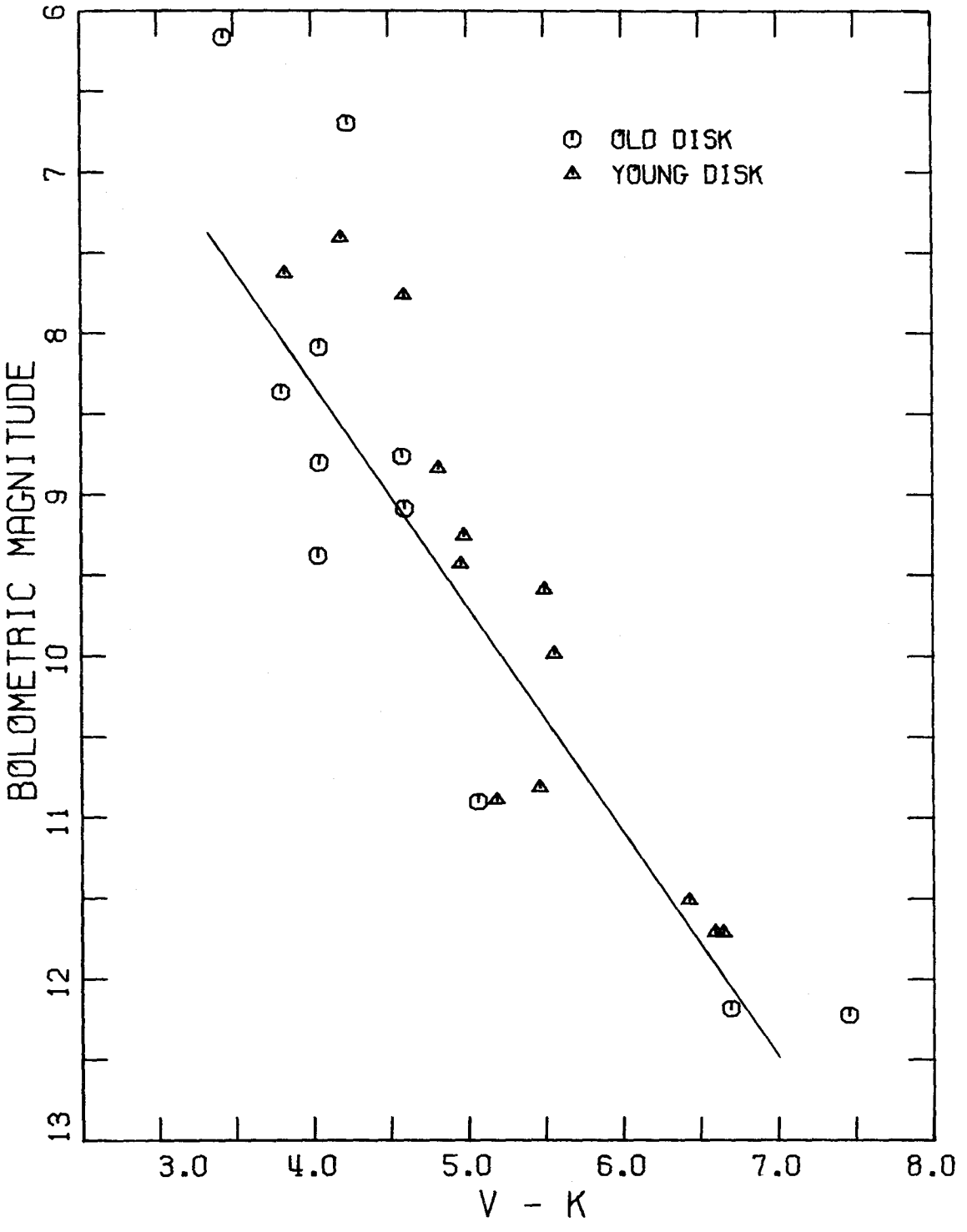

Fig.3-22.--Absolute bolometric magnitude vs. (V-2.2μ) color for the UV Ceti type flare stars from tables 3-9 and 3-10. Old disk and young disk populations are defined in the text. The mean relation indicated for the main sequence is $M_b = 1.39(V-K) + 2.74$.

significant difference between these two divisions of the flare stars, although the limited number of stars available for each group makes it difficult to draw any firm conclusions. (In a previous section (3-B) we have seen that the average sequence for all young disk stars does lie above the average sequence for all old disk stars (see figures 3-7a and 3-7b)). Gr-34B (= GL15B) has drawn attention ever since Joy (1947) misclassified it as a subdwarf (see Lippincott (1971)). It does appear to be subluminous in figure 3-22 and in fact lies very near to the position of Barnard's star (= GL699) in the M_b vs. V-K plane. But R154 (= GL729) lies right next to both of these stars in the figure and it has a young disk space motion. These stars have large parallaxes so that their distance moluli are well determined. Gr-34A and Gr-34B both have weak Ca II emission lines and no hydrogen emission lines except during flares. However, R128 (= GL447) also shows no hydrogen emission in the quiescent state and it has a young disk space motion.

An additional complication in trying to interpret the motions of the flare stars is that the available sample suffers from severe selection effects. The known flare stars in the solar neighborhood have been discovered haphazardly over a long period of time and in many different ways. Current surveys being carried out by Haro and others seem to be concentrating on young clusters and have passed

beyond the solar neighborhood. Thus, the list of known flare stars in the solar neighborhood must be incomplete to some unknown degree. There is a well known selection effect in current parallax catalogues for stars of high proper motions. This would favor old disk space motions over young disk motions and might lead us to suspect that the unbiased fraction of flare stars with old disk motions is less than the observed 11 out of 30.

The best survey for local M dwarfs without any bias with regards to their motions is the objective prism search carried out by Vyssotsky (1943, 1956) and Vyssotsky et al. (1946, 1952). He has estimated that this search is 5% incomplete for stars brighter than $m_V = 10$. Dyer (1956) has calculated the space motions of 305 of these stars from Vyssotsky's first three lists. Nineteen of these 305 stars have been found to show hydrogen emission lines. Of these, fourteen have young disk space motions and five have old disk space motions. Again, though, these numbers must still be incomplete in the sense that additional stars in Dyer's list may in fact have hydrogen emission lines. But if we make the assumption that, on the average, the space motions of flare stars are not too different from the space motions of all M dwarfs that show hydrogen emission, then the results from Dyer's list tends to indicate that we should not be surprised that about one-third of the flare stars in the solar neighborhood have old disk motions.

The important point here is that at least seven flare stars out of a total of about thirty known flare stars in the solar neighborhood do exist that have old disk space motions. This point is hard to explain because flare stars are traditionally believed to be young objects. Haro (1957) and Ambartsumian and Mirzoyan (1971) have suggested that flare stars are an intermediate evolutionary stage between very young T Tauri type stars and older main sequence stars without emission lines.

This picture of evolution implies that there is a decline in chromospheric activity with age in these stars. Such a decline is indicated by Wilson's (1963) correlation of H and K calcium emission line strength in G and K dwarfs with the age of clusters in the sense that the Pleiades show stronger emission then the Hyades, Praesepe, or Coma clusters which in turn have stronger emission than stars in the solar neighborhood. Furthermore, Haro and Chavira (1966) find that the younger clusters contain flare stars of earlier spectral types than the earliest type found in older clusters. That is, K2 flare stars can be found in Orion, K5 flare stars can be found in the Pleiades, but the earliest type of flare stars that has been found in the Hyades, Praesepe, and Coma clusters or the solar neighborhood is M0. This directly implies that the flare activity of early K stars must decay on a time scale of

less than the age of the Pleiades ($\sim 5 \times 10^7$ years) and the flare activity of late K flare stars must decay on a time scale of less than the age of the Hyades ($\sim 5 \times 10^8$ years). Presumably, M dwarf flare activity decays on a time scale which is greater than the age of the Hyades. However, this argument can only suggest that the M flare stars in the solar neighborhood are younger than the main sequence. An additional argument from stellar dynamics for a small age for flare stars is that, on the average, emission line M dwarfs have smaller peculiar space motions than M dwarfs without emission lines. So, on the average, flare stars may be young objects; but those individual flare stars that have old disk motions must be relatively old. It is difficult to understand why some old stars should still be in the flare stage while most have evolved through that stage to the main sequence, ceased their flare activity, and lost their emission lines. An unlikely possibility is that the chromospheric activity in these stars is a temporary phenomenon which may re-occur at some unknown interval. Although there appears to be no clear photometric difference between old and young disk flare stars in the quiescent state, the flare activity of the old disk objects should be examined more closely as a group to see if it is exactly equivalent to the UV Ceti type of activity.

Appendix

The data for the program stars are listed in table A-1. The entries in each column are as follows:

Col. 1: Number from Gliese's (1969) catalogue.

- G indicates Giclas number
- L indicates Luyten number
- * indicates mean component of binary taken to to be 1/2 of the measured flux
- AB indicates joint magnitudes for close binary

Col. 2: Spectral Type.

- sd indicates a Joy(1947) subdwarf
- E indicates hydrogen in emission

Col.3-10: UBVRIHKL magnitudes in Johnson's system.

Col. 5: P indicates photographic magnitude.

Col.11: Number of observations made at HKL.

Col.12: Adopted parallax.

Col.13: Absolute bolometric magnitude.

Col.14: Population type.

- OD indicates old disk space motion

YD indicates young disk space motion

HALO indicates halo space motion.

Col.15: Remarks.(see also Woolley et al.(1970) Table IIa for alternate names.)

W indicates Wolf number

R indicates Ross number

G indicates Giclas number

L indicates Luyten number

Ca II indicates H and K calcium lines in emission

Flare indicates UV Ceti type flare star

SB indicates spectroscopic binary

AB indicates astrometric binary

1 indicates R and I magnitudes were observed in Kron's system and converted into Johnson's system

2 indicates R and I magnitudes were derived from scanner observations

3 indicates |radial velocity| $\geq$ 65 km/sec

4 indicates Shakhovskaya (1971) lists as only suspected of UV Ceti type activity

* indicates additional notes follow the table

The following relations from Eggen (1972) were used to convert R and I magnitudes measured in Kron's system into Johnson's system:

$$R_j = R_k - 0.18 - 0.5 \cdot (R-I)_k \qquad (R-I)_k < 0.4$$

$$R_j = R_k - 0.38 \qquad (R-I)_k > 0.4$$

$$(R-I)_j = 1.25 \cdot (R-I)_k + 0.06$$

Those stars with known radial velocities were assigned to either the young disk (YD) population, the old disk (OD) population, or the halo population on the basis of their space motion. Following Eggen (1969) stars with small space velocities in the U-V plane were assigned to the young disk population. For U defined to be positive away from the galactic center, the approximate limits of young disk velocities are:

$$-20 \leq U \leq +50 \text{ km/sec}$$

$$-40 \leq V \leq +10 \text{ km/sec}$$

Eggen derived these limits from the small space velocities observed for young main sequence stars with early spectral types. Most of the asymmetry in these limits is due to the small peculiar motion of the sun. The remaining stars were assigned to the old disk if the eccentricity of their galactic orbits is less than 0.5 or to the halo population if the eccentricity is greater than 0.5. In addition, stars with a large space velocity component perpendicular to the galactic plane were assigned to the halo population, i.e. if $|W| > 75$ km/sec. These stars reach distances $\geq$ 1 kpc from the galactic plane. Stars with high radial

velocities ($|RV| \geq 65$ km/sec) that otherwise have been assigned to the old disk population are so indicated.

The magnitudes listed in table A-1 were taken from the following sources: Woolley et al. (1970), Gliese (1969), Riddle et al. (1970, 1971), Dahn et al. (1972), Dahn and Priser (1973), Frogel et al. (1972), Kron et al. (1957), Johnson (1965), and Eggen (1968, 1972b). The parallaxes listed in table A-1 were adopted from these sources and also from van Altena (1971, 1973), van Altena and Vilkki (1973), Appelbaum (1972), Chang (1972), Heintz (1972), Lippincott (1969, 1972, 1973), Lippincott and Hershey (1972), Routly (1972), Strand and Riddle (1969), van de Kamp and Worth (1972), Worley and Behall (1973), Grossenbacher et al. (1968), Mesrobian et al. (1969), Upgren et al. (1970), Kerridge et al. (1971), Upgren and Mesrobian (1971), Mesrobian and Upgren (1971), and Titter et al. (1972).

Table A-1

Data for 145 Nearby Stars

GL	TYPE	U	B	V	R	I	H	K	L	N	PI	M	POP	REMARKS
G158-27		16.91	15.61	13.76	11.65	9.68	7.71	7.38		2	224	12.0	OD	2
11AB	M6			12.00			8.02	7.74		6	059	-		
15A	M1	10.89	9.63	8.07	6.69	5.53	4.24	4.02	3.8	4	288	8.8	OD	GR-34,FLARE,CA II,SB
15B	M6	14.24	12.84	11.04	9.23	7.65	6.24	5.97	5.6	3	288	10.9	OD	FLARE,CA II
29.1	M0E		11.76	10.38			6.45	6.28	6.1	2	047	7.0	YD	FF AND,SB
40	M0		10.22	8.93			5.91	5.79		1	071	7.4	OD	CA II
48	M3.5E	12.68	11.53	10.06	8.40	6.96	5.63	5.44		2	114	8.3	OD	1
49	M2	12.28	11.07	9.57	8.10	6.90	5.59	5.41	5.2	2	109	8.1	YD	CA II,1
51	M7E	16.13	15.34	13.66	11.61	9.62	7.97	7.70		3	111	10.7		W47,FLARE,1,*
G 69-47		18.23	16.69	14.81	12.79	10.86	8.84	8.51		2	077	10.8		2
65AB	M5.5E			12.00	9.63	7.41	5.64	5.33	5.0	4	379	-	YD	L726-8,1,*
83.1	M8E	15.47	14.10	12.28	10.10	8.31	6.92	6.61		2	223	11.1		G3-33,FLARE
84.2	M0			11.10			6.73	6.51		2	063	8.0	OD	
96	M1.5	12.08	10.90	9.41	8.04	6.98	5.70	5.54		2	077	7.9	OD	CA II,1
102	M6			13.08	11.28	9.62	7.85	7.55		2	133	11.0		2,*
105.5	M0P	11.77	10.68	9.49			6.64	6.56		1	037	6.7	OD	G75-34,3
109	M4		12.13	10.58	8.94	7.50	6.20	5.96		2	134	9.2	OD	CA II,1
129	SDM0	17.05	15.78	14.32			10.94	10.68		1	030	10.5	HALO	W134,SB,*
G 77-31		16.76	15.61	13.78	12.17	10.25	8.08	7.78		2	117	11.1		2
G 95-59	MP	16.87	15.47	13.90			10.58	10.41		4	020	9.3	HALO	*
157.1	M4			12.60			8.05	7.81		2	053	9.0	OD	W1322,3
169.1	M4	13.91	12.73	11.09			5.99	5.72		4	170	9.5		STEIN 2051,*
170	M7			13.70	11.90	9.99	8.53	8.21		9	099	11.0		1
176	M2.5	12.66	11.48	9.94	8.42	7.13	5.87	5.65	5.5	2	097	8.1	OD	CA II,1
184	M0	12.50	11.34	9.93	8.59	7.56	6.41	6.22		1	064	7.7	HALO	G191-19,1
185AB	M1		9.70	8.29	6.96	5.98	4.78	4.59		1	131	-	YD	1
192	M5			11.30			6.67	6.49		4	070	8.2		
205	M1	10.65	9.44	7.97	6.53	5.39	4.00	3.85	3.6	2	170	7.5	OD	CA II
207.1	M3E			11.68			7.02	6.81		2	067	8.4		V371 ORI,FLARE
213	SDM5.5	14.45	13.25	11.60	9.67	8.01	6.58	6.34		2	166	10.1	HALO	R47
228	M3	12.94	11.86	10.41	8.83	7.47	6.28	6.07		2	104	8.7	OD	1,*
229	M1	10.86	9.63	8.14	6.72	5.61	4.32	4.14	4.0	2	174	7.8	YD	CA II,1
232	M6			13.30	11.38	9.75	8.12	7.85		3	117	10.9		2
234AB	M7E	14.04	12.81	11.07	9.06	7.25	5.76	5.46	5.2	5	248	10.4	YD	R614,FLARE,1,*
239	M1	12.31	11.13	9.63	8.34	7.37	6.10	5.90		2	104	8.4	OD	

Table A-1 (Continued)

GL	TYPE	U	B	V	R	I	H	K	L	N	PI	M	POP	REMARKS
247	M0P	10.92	9.78	8.58	7.48	6.78	5.69	5.59	5.5	2	049	6.2	OD	1
251	M4	12.70	11.50	9.90	8.36	6.94	5.52	5.29	5.0	3	168	9.1	YD	
268	M5E	14.37	13.18	11.47	9.57	7.76	6.12	5.83	5.5	4	173	9.8	YD	SB
270	M2		11.39	10.03			6.54	6.39		1	051	7.3	OD	CA II
273	M5	12.50	11.38	9.82	8.04	6.49	5.12	4.86	4.5	2	270	9.7	OD	G89-19
277A	M3.5E	13.25	12.07	10.61	8.88	7.49	6.17	5.94		1	068	8.3	YD	SB,1
277B	M4.5E	14.54	13.37	11.75	9.90	8.28	6.95	6.76		1	068	9.1	YD	1
278*	M0.5E	12.34	11.32	9.83	8.44	7.42	6.17	6.00	5.9	3	068	7.6	YD	YY GEM,FLARE
285	M4.5E	13.79	12.79	11.20	9.39	7.55	5.95	5.70	5.4	2	167	9.6	YD	YZ CMI,FLARE,1
299	M5	15.94	14.54	12.77	10.89	9.18	7.89	7.59		2	151	11.2	HALO	R619,1
300	M			13.80P			6.87	6.59		2	171	10.5		
G 51-15			16.87	14.81	12.25	9.88	7.54	7.20		1	271	12.4		2
324B	M5	16.00	14.80	13.15	11.15	9.44	7.90	7.64		3	074	9.7	YD	1
326AB	M6			11.80			7.50	7.19		4	082	-		
338A	M0	10.22	9.02	7.62	6.39	5.46	4.25	4.09	4.0	2	163	7.6	YD	CA II,1
338B	M0	10.30	9.10	7.72	6.47	5.52	4.30	4.15	4.1	2	163	7.6	YD	CA II,1
347	M5			11.60	10.57	9.12	7.81	7.60		2	064	9.2		1
352*	M4	13.49	12.34	10.81	9.20	7.82	6.53	6.31		2	110	9.1	OD	
369	M2		11.42	10.00			6.30	6.17		4	081	8.2	HALO	G161-80
380	M0	9.25	7.97	6.59	5.36	4.56	3.37	3.23	3.1	2	222	7.3	YD	G196-9,CA II
382	M2	11.99	10.77	9.30	7.80	6.56	5.26	5.07	4.9	2	115	7.9	YD	1
388	M4.5E	12.05	10.97	9.43	7.72	6.25	4.83	4.61	4.5	2	204	8.8	YD	AD LEO,FLARE
390	M0			10.10			6.29	6.09		2	069	7.7		
393	M2	12.34	11.15	9.63	8.13	6.88	5.60	5.37		2	130	8.5	YD	
402	M5			(11.66)	9.84	8.17	6.70	6.42	6.1	3	142	9.9	YD	SB,*
406	M8E	17.08	15.54	13.53	10.87	8.41	6.47	6.07	5.7	3	426	12.2	OD	W359,FLARE,*
411	M2	10.13	9.00	7.49	5.98	4.76	3.58	3.35	3.2	2	396	8.9	HALO	LALANDE 21185,CA II
412A	M2	11.48	10.30	8.76	7.29	6.22	4.93	4.69	4.5	2	192	8.6	OD	CA II
412B	M8E			(14.53)	12.23	10.18	8.16	7.83		4	192	12.2	OD	WX UMA,FLARE,*
413	M0P	11.90	10.89	9.77	8.81	8.14	7.00	6.91		2	028	6.3	HALO	G56-16,1,*
424	M1	11.82	10.74	9.32	7.95	6.94	5.72	5.52	5.3	2	119	8.4	OD	SZ UMA,FLARE
445	SDM4			10.90	9.07	7.51	6.21	5.96		2	195	10.0	HALO	+79 3888,1
447	M5	14.26	12.86	11.10	9.19	7.50	5.95	5.63	5.3	2	299	10.8	YD	R128,FLARE
463	M4			11.50			7.35	7.14		2	070	8.9	OD	
465	M4			11.70	9.75	8.44	7.24	6.95		2	110	9.8	OD	1

Table A-1 (Continued)

GL	TYPE	U	B	V	R	I	H	K	L	N	PI	M	POP	REMARKS
473*	M5.5E	16.27	15.03	13.21	10.83	8.75	7.13	6.78	6.5	2	234	11.5	YD	W424,FLARE
487	M4			10.80	9.28	7.77	6.35	6.09		2	116	9.1	YD	CA II,1
488	M0.5	11.17	9.90	8.49	7.32	6.42	5.09	4.94	4.8	3	091	7.2	YD	CA II
494	M2E	12.34	11.22	9.79	8.31	7.15	5.77	5.60	5.4	2	071	7.4	YD	W462,R458,FLARE,1
512	M4		12.76	11.24	9.54	8.07	6.70	6.46		3	084	8.7	YD	1,*
513	M5			13.50P			7.79	7.53		2	054	9.0	OD	
514	M1	11.79	10.55	9.04	7.61	6.52	5.29	5.09	4.9	2	133	8.2	OD	
514.1	M6	17.45	15.97	14.34			8.94	8.68		2	047	9.7		
516AB	M4E	14.17	12.92	11.39	9.60	8.26	7.00	6.75		3	066	-	OD	VW COM,FLARE,1
526	M4	10.99	9.91	8.46	7.06	5.92	4.68	4.48	4.3	2	205	8.5	OD	W498,CA II
537AB	M3	11.79	10.63	9.15	7.68	6.56	5.41	5.21		2	087	-	OD	CA II,1
544B	M6			14.50			9.83	9.53		2	053	10.9	OD	
550.1	M0		12.18	10.91			8.00	7.88		4	050	8.9	OD	*
551	M5E	14.56	13.02	11.05	8.68	6.42	4.73	4.40	4.2	-	761	11.7	YD	V645 CEN,FLARE,*
553.1	M4			13.40P			7.21	7.00		2	083	9.2		
555	M4	14.19	12.99	11.36	9.43	7.74	6.27	6.01		2	160	9.7		
568AB	M5			11.10			6.89	6.61		2	096	-		
570B	M1	10.76	9.56	8.02	6.65	5.47	4.17	3.97	3.8	2	180	7.8	OD	
581	M5	13.39	12.18	10.58	8.89	7.46	6.17	5.92		2	153	9.4	YD	
585	M6	16.64	15.46	13.67			8.53	8.26		4	091	10.8		
595	M5			11.70			7.44	7.19		2	111	10.1		
616.2	M1E	12.50	11.42	9.96	8.50	7.29	5.90	5.73	5.5	3	048	6.7	OD	+55 1823,1,4
617	M0	11.29	10.03	8.62	7.29	6.40	5.12	4.99	4.8	4	089	7.1	YD	CA II
628	M5	12.90	11.72	10.12	8.36	6.78	5.32	5.08	4.8	5	249	9.8	YD	W1061,SB
642	M1.5			11.10			7.34	7.18		2	058	8.5	OD	
643	SDM4	14.75	13.40	11.70	9.98	8.37	7.08	6.80		2	169	10.6	OD	W629,SB,1
644*	M4.5E	12.47	11.38	9.76	8.13	6.73	5.41	5.18	5.0	4	156	8.8	OD	W630,FLARE
654	M3.5	17.34	15.90	14.02			8.74	8.44		2	077	10.6	OD	
G139-12		12.58	11.50	10.07	8.63	7.43	6.18	5.99	5.8	2	101	8.5		
661AB	M3	11.90	10.89	9.40	7.77	6.33	5.00	4.79	4.6	2	153	-	OD	+45 2505,1
669A	M4E	14.09	12.91	11.36	9.63	8.11	6.68	6.45		2	095	9.0	YD	R868,1
669B	M5E	15.23	14.50	12.92	10.93	9.09	7.64	7.36		2	095	10.0	YD	R867,FLARE,1,*
687	M3.5	11.73	10.65	9.15	7.53	6.07	4.76	4.53	4.3	2	214	8.8	OD	G240-63,AB,1
695BC	M4	12.30	11.27	9.78			5.23	4.99	4.8	2	128	-	OD	CA II
699	SDM5	12.57	11.28	9.54	7.71	6.03	4.81	4.56	4.2	2	559	10.9	HALO	BARNARD'S STAR

Table A-1 (Continued)

GL	TYPE	U	B	V	R	I	H	K	L	N	PI	M	POP	REMARKS
702AB	K0	5.40	4.89	4.03	3.26	2.80	2.04	1.96	1.8	3	195	-	YD	70 OPH,CA II,1
717	M0	12.48	11.29	10.01	8.89	8.16	6.97	6.85		5	054	7.8	OD	W1462,1,3
719	M0E			8.30			5.00	4.87	4.7	2	064	6.2	OD	BY DRA,FLARE,SB
720	M2	12.39	11.24	9.82	8.49	7.48	6.31	6.12		1	082	8.1	YD	1
725A	M4	11.55	10.44	8.90	7.31	5.89	4.71	4.48	4.2	5	284	9.3	YD	≤2398A,1
725B	M5	12.42	11.28	9.69	8.01	6.50	5.27	5.02	4.7	5	284	9.9	YD	≤2398B,1
729	M4.5E			10.60	9.06	7.35	5.68	5.41	5.0	4	345	10.9	YD	R154,V1216 SGR,FLARE,1
735	M2E		11.82	10.07			5.69	5.47	5.1	2	086	7.8	YD	+8 142-393,FLARE,*
740	M2	11.98	10.68	9.23	7.87	6.82	5.57	5.43	5.3	2	085	7.5	OD	1
745A	SDM2		12.33	10.77	9.24	7.95	6.73	6.50		4	119	9.4	OD	R730,1
745B	SDM2		12.32	10.76	9.25	7.98	6.75	6.52		3	119	9.4	OD	R731,1
747AB	M5			11.20	9.55	8.01	6.73	6.45		2	122	-	OD	1
L1283-23				11.80	10.18	8.66	7.38	7.10		3	122	10.2		
748	M4			11.20	9.07	7.64	6.93	6.72		1	098	9.0	HALO	W1062
752	M3.5	11.76	10.61	9.12	7.53	6.19	4.83	4.64		3	164	8.3	OD	CA II,1
766AB	M4.5E			12.33	10.55	8.84	7.42	7.15		2	097	-		1
777	M6	17.17	16.09	14.38	12.13	10.33	8.92	8.65		3	056	10.1		1
781	M3E			12.10	10.59	9.45	8.26	8.06		4	059	9.4	OD	W1130,SB,1.4
786	M0		10.25	8.89			5.73	5.63	5.4	2	072	7.3	YD	
806	M3			10.80			6.73	6.47		2	085	8.6	YD	
809	M2	11.23	9.99	8.50	7.16	6.05	4.80	4.64	4.4	4	146	7.9	OD	CA II,SB,1
811.1	M4			11.30			7.16	6.96		1	044	7.6	OD	
815AB	M3E		11.60	10.10	8.63	7.41	6.13	5.95	5.7	2	075	-	OD	CC1250,FLARE,1
820A	K5	7.50	6.40	5.22	4.20	3.56	2.48	2.38	2.3	2	296	6.9	OD	61 CYGA,CA II
820B	K7	8.66	7.41	6.03	4.87	4.07	2.86	2.72	2.6	2	296	7.4	OD	61 CYGB,CA II
G231-27	SDM1			13.00			9.64	9.47		3	042	10.3	HALO	W1106,SB,*
829	M4			10.40	8.58	7.03	5.70	5.44	5.1	2	154	9.0	YD	CA II,1
830	M0	11.62	10.37	9.10	7.98	7.17	6.02	5.93		2	061	7.1	OD	-13 5945,1,3
860AB	M3	12.49	11.25	9.59	7.80	6.28	4.93	4.68	4.4	2	251	-	OD	KRUGER-60,*
866	M7E	15.68	14.14	12.18	9.89	7.73	5.87	5.53	5.2	3	305	10.9	OD	G156-31,1
867A	M2E	11.66	10.58	9.10	7.69	6.43	4.95	4.77	4.6	2	109	7.6	YD	SB,1
867B	M4E	14.15	13.07	11.45			6.71	6.47		2	109	9.3	YD	-21 6267,FLARE,1,4
873	M4.5E	12.90	11.80	10.20	8.46	6.94	5.48	5.24	5.0	2	200	9.4	YD	EV LAC,FLARE,1,*
876	M5	12.86	11.72	10.13	8.39	6.78	5.32	5.05	4.7	2	209	9.4	YD	R780,1
880	M2	11.35	10.18	8.67	7.21	6.02	4.74	4.55	4.4	2	143	7.9	OD	CA II,SB,1

Table A-1 (Continued)

GL	TYPE	U	B	V	R	I	H	K	L	N	PI	M	POP	REMARKS
884	M1	10.52	9.28	7.89	6.65	5.79	4.55	4.44	4.4	2	130	7.4	OD	1
896AB	M4E	13.00	11.94	10.23	8.40	6.76	5.30	5.05	4.9	2	155	-	YD	+19 5116,1,*
897AB	M5			10.39			6.00	5.80		2	069	-		
905	M6E	15.69	14.21	12.29	10.04	8.00	6.21	5.90	5.5	5	314	11.3	OD	R248,1,3
908	M0E	11.55	10.46	8.98	7.58	6.41	5.22	5.01	4.9	2	174	8.7	OD	1

Notes for Table A-1

GL	Notes
51	U magnitude too bright
65B	flare star UV Ceti
102	visual magnitude derived from scanner observations
129	parallax uncertain
G95-59	Eggen mis-identified this star(see Dahn and Priser (1973))
169.1	faint companion, H and K are joint magnitudes
228	faint companion, H and K are joint magnitudes
234AB	the bolometric magnitude listed has been corrected by 0.2 and refers only to the A component
402	visual magnitude estimated by Johnson (1965) from its color
406	Eggen (1971) claims R and I magnitudes are variable
412B	R and I magnitudes are uncertain, visual magnitude estimated by Johnson (1965) from its color
413	parallax uncertain
512	faint companion, H and K are joint magnitudes
550.1	Gliese questions the parallax
551	Proxima Centauri. Values for UBVRIHKL taken from Frogel et al. (1972)
669B	U magnitude too bright
735	Gliese questions the parallax and the B-V color
G231-27	parallax uncertain
860B	flare star DO Cep

GL	Notes
873	blue visual companion. HKL are joint magnitudes
896B	flare star EQ Peg

Table A-2 lists the binary systems which have been corrected for the contribution of the secondary. The magnitudes given refer to the A component and are listed with the same format as in table A-1. The following relations were used to correct the magnitudes:

$$\Delta U = 1.06 \cdot \Delta V$$

$$\Delta B = 1.05 \cdot \Delta V$$

$$\Delta R = 0.89 \cdot \Delta V$$

$$\Delta I = 0.73 \cdot \Delta V$$

$$\Delta H = 0.72 \cdot \Delta V$$

$$\Delta K = 0.67 \cdot \Delta V$$

$$\Delta L = 0.60 \cdot \Delta V$$

where $\Delta V = (m_v)_A - (m_v)_B$

Table A-2

Data for 16 Binary Systems

GL	TYPE	U	B	V	R	I	H	K	L	N	PI	M	POP	REMARKS
11A	M6			12.60			8.67	8.39		6	059	9.9		
65A	M5.5E	15.46	14.37	12.52	10.18	8.00	6.23	5.92	5.6	4	379	11.7	YD	L726-8,1,*
185A	M1		9.82	8.45	7.12	6.20	5.00	4.82		1	125	7.8	YD	1
326A	M6			12.40			8.15	7.84		4	082	10.1		
516A	M4E	14.78	13.53	12.00	10.23	8.91	7.65	7.40		3	066	9.1	OD	VW COM,FLARE,1
537A	M3	12.47	11.31	9.85	8.37	7.26	6.11	5.91		2	087	8.0	OD	CA II,1
568A	M5			11.60			7.45	7.18		2	096	9.7		
661A	M3	12.49	11.48	9.96	8.38	6.97	5.64	5.43	5.3	2	153	9.0	OD	+45 2505,1
695B	M4	12.84	11.81	10.33	8.64	7.29	5.83	5.60	5.4	2	128	8.8	OD	CA II
702A	K0	5.58	5.07	4.22	3.49	3.09	2.33	2.26	2.2	3	195	5.4	YD	70 OPH,CA II,1
747A	M5	16.81	15.39	13.54			8.16	7.86		2	093	10.4	OD	1
766A	M4.5E			12.70	10.95	9.29	7.87	7.61		2	097	10.2		1
815A	M3E		11.74	10.26	8.82	7.66	6.38	6.21	6.0	2	075	8.1	OD	CC1250,FLARE,1
860A	M3	12.70	11.47	9.85	8.09	6.63	5.28	5.04	4.8	2	251	9.7	OD	KRUGER-60,*
896A	M4E	13.13	12.07	10.38	8.57	6.99	5.54	5.30	5.1	2	155	9.0	YD	+19 5116,1,*
897A	M5			10.98			6.61	6.42		2	087	8.7		

References

Ambartsumian, V.A.,and L.V. Mirozoyan 1971, IAU Coloquium No.15, Veröff. Remeis-Sternwarte Bamberg, 9, 98.

Appelbaum, L.T. 1972, A.J., 77, 518.

Auman, J.R. 1966, Colloquium on Late Type Stars, ed., M. Hack, p.313.

Becklin, E.E. 1972, private communication.

Becklin, E.E., and G. Neugebauer 1968, Ap.J., 151, 145.

Chang, K. 1972, A.J., 77, 759.

Copeland, H., J.O. Jensen, and H.E. Jorgensen 1970, Astr. and Ap., 5, 12.

Dahn, C.C., A.L. Behall, H.H. Guetter, J.B. Priser, R.S. Harrington, K.Aa. Strand, and R.K. Riddle 1972, Ap.J. (Letters), 174, L87.

Dahn, C.C., and J.B. Priser 1973, A.J., 78, 253.

Dyer, E.R. 1956, A.J., 61, 228.

Eggen, O.J. 1968, Ap.J. Suppl., 16, 49, (No.142).

Eggen, O.J. 1969a, Publ.A.S.P., 81, 553.

Eggen, O.J. 1969b, Ap.J., 158, 1109.

Eggen, O.J. 1971, Ap.J. Suppl., 22, 389, (No.191).

Eggen, O.J. 1972a, Ap.J., 177, 489.

Eggen, O.J. 1972b, private communication.

Eggen, O.J. 1973, Ap.J., 182, 821.

Eggen, O.J., D. Lynden-Bell, and A.R. Sandage 1962, Ap.J., 136, 748.

Eggen, O.J., and A.R. Sandage 1962, Ap.J., 136, 735.

Ezer, D., and A.G.W. Cameron 1967, Can. J. Phys., 45, 3429.

———.1967,ibid., 45, 3461.

Frogel, J.A., D.E. Kleinmann, W. Kunkel, E.P. Ney, and D.W. Strecker 1972, Publ.A.S.P., 84, 581.

Gershberg, R.E., and N.I. Shakhovskaya 1971, IAU Colloquium No.15, Veröff.Remeis-Sternwarte Bamberg, 9, 126.

Gliese, W. 1969, Catalogue of Nearby Stars, Veröff. Astr. Rechen-Inst. Heidelberg, No.22.

Greenstein, J.L. 1973, private communication.

Greenstein, J.L., G. Neugebauer, and E.E. Becklin 1970, Ap.J., 161, 519.

Grossenbacher, R., W.S. Mesrobian, and A.R. Upgren 1968, A.J., 73, 744.

Haro, G. 1957, IAU Symp. No.3, ed., G.H. Herbig, p.26.

Haro, G., and E. Chavira 1966, Vistas in Astronomy, ed., A. Beer, 8, 89.

Harris, D.L., K.Aa. Strand, and C.E. Worley 1963, Basic Astronomical Data, ed., K.Aa. Strand, (Chicago: U. of Chicago Press), p.273.

Heintz, W.D. 1972, A.J., 77, 160.

Hoxie, D.T. 1970, Ap.J., 161, 1083.

Iriarte, B. 1971, Bol. Obs. Ton. y Tac., 6, 143, (No.37).

Johnson, H.L. 1964, Bol. Obs. Ton. y Tac., 3, 305, (No.25).

Johnson, H.L. 1965, Ap.J., 141, 170.

Johnson, H.L. 1966, Ann. Rev. Astr. and Ap., 4, 193.

Johnson, H.L., and R.I. Mitchell 1958, Ap.J., 128, 31.

Johnson, H.L., R.I. Mitchell, B. Iriarte, and W.Z. Wisniewski 1966, Comm. Lunar and Planetary Lab., 4, 99, (No.63).

Joy, A.H. 1947, Ap.J., 105, 96.

Kerridge, S.J., R. Grossenbacher, and A.R. Upgren 1971, A.J., 76, 77.

Kron, G.E., S.C.B. Gascoigne, and H.S. White 1957, A.J., 62, 205.

Kumar, S.S. 1963, Ap.J., 137, 1121.

Lee, T.A., and D.T. Hoxie 1972, Comm. 27 of IAU Info. Bull. on Variable Stars, No.707.

Lippincott, S.L. 1969, A.J., 74, 224.

Lippincott, S.L. 1971, IAU Colloquium No.15, Veröff. Remeis-Sternwarte Bamberg, 9, 109.

Lippincott, S.L. 1972, A.J., 77, 165.

Lippincott, S.L. 1973, A.J., 78, 303.

Lippincott, S.L., and J.L. Hershey 1972, A.J., 77, 679.

Luyten, W.J. 1968, M.N.R.A.S., 139, 221.

Mesrobian, W.S., R.M. Nelson, A.R. Upgren, and R. Grossenbacher 1969, A.J., 74, 752.

Mesrobian, W.S., and A.R. Upgren 1971, A.J., 76, 1133.

Murray, C.A., and N.Sanduleak 1972, M.N.R.A.S., 157, 273.

Oke, J.B. 1969, Publ.A.S.P., 81, 11.

Oort, J.H. 1965, Galactic Structure, ed., A. Blaauw and M. Schmidt, (Chicago: U. of Chicago Press), p.455.

Pesch, P. 1972, Ap.J., 177, 519.

Riddle, R.K., A.L. Behall, H.H. Guetter, and J.W. Christy 1971, Publ.A.S.P., 83, 210.

Riddle, R.K., J.B. Priser, and K.Aa. Strand 1970, Publ. U.S.N.O., XX, part III.

Routly, P.M. 1972, Publ.U.S.N.O., XX, part VI.

Sanduleak, N. 1964, A.J., 69, 720.

Schmidt, M. 1959, Ap.J., 129, 243.

Shakhovskaya, N.I. 1971, IAU Colloquium No.15, Veröff. Remeis-Sternwarte Bamberg, 9, 138.

Spinrad, H. 1973, Ap.J., 183, 923.

Strand, K.Aa., and R.K. Riddle 1969, A.J., 74, 1038.

Taylor, B.J. 1970, Ap.J. Suppl., 22, 177, (No.186).

Titter, J.C., W.S. Mesrobian, and A.R. Upgren 1972, A.J., 77, 875.

Tsuji, T. 1971, Publ.A.S.J., 23, 553.

Upgren, A.R. 1973, A.J., in press.

Upgren, A.R., and W.S. Mesrobian 1971, A.J., 76, 78.

Upgren, A.R., W.S. Mesrobian, R.M. Nelson, R. Grossenbacher, and, S.J. Kerridge 1970, A.J., 75, 319.

van Altena, W.F. 1971, A.J., 76, 932.

van Altena, W.F. 1973, Ap.J., 179, 865.

van Altena, W.F., and E.U. Vilkki 1973, A.J., 78, 201.

van de Kamp, P. 1969, Publ.A.S.P., 81, 5.

van de Kamp, P. 1971, Ann. Rev. Astr. and Ap., 9, 103.

van de Kamp, P., and M.D. Worth 1972, A.J., 77, 762.

van Rhijn, P.J. 1936, Publ. Kapteyn Astr. Lab. Groningen, No.47.

Vyssotsky, A.N. 1943, Ap.J., 97, 381.

Vyssotsky, A.N. 1956, A.J., 61, 201.

Vyssotsky, A.N., E.M. Janssen, W.J. Miller, S.J., and M.E. Walther 1946, Ap.J., 104, 234.

Vyssotsky, A.N., and B.A. Mateer 1952, Ap.J., 116, 117.

Weistrop, D. 1972, A.J., 77, 366.

———.1972,ibid., 77, 849.

Wilson, O.C. 1963, Ap.J., 138, 833.

Wilson, W.J., P.R. Schwartz, G. Neugebauer, P.M. Harvey, and E.E. Becklin 1972, Ap.J., 177, 523.

Woolley, R., E.A. Epps, M.J. Penston, and S.B. Pocock 1970, Royal Obs. Annals, No.5.

Worley, C.E. 1969, Low Luminosity Stars, ed., S.S. Kumar, (New York: Gordon and Breach Science Publ. Inc.),p.117.

Worley, C.E., and A.L. Behall 1973, A.J., in press.